Terpene-based (meth)acrylate polymers as new class of functional materials

Sayrung Noppalit

Terpenes-based (Meth)Acrylic Polymers as new class of functional materials

Sayrung Noppalit

Supervised by: L. Billon and J.M. Asua

Equipe de Physique et de Chimie des Polymères

University of Pau and Pays de l'Adour

Chemical Engineering Group

University of the Basque Country UPV/EHU

Donostia-San Sebastián

(2019)

Acknowledgements

I would like to express my sincere gratitude to my supervisors Prof. José M. Asua, Prof. Laurent Billon and Dr. Alexandre Simula for their valuable guidance, support, encouragement and patience. It was a precious opportunity for me to work under their supervision.

I would like to extent my gratitude to the professors of the Chemical Engineering Group, Professors Jose R. Leiza, Maria Paulis, Maria J. Barandiaran, Alejandro J. Müller, David Mecerreyes and Dr. Nicholas Ballard, and the professors from the Equipe de Physique et de Chimie des Polymères" (EPCP) in France, Professors Stéphanie Reynaud, Maud Save and Christine Lartigau-Dagron for their insightful comments and encouragement in the seminars. I would like to show my gratitude to Inés Plaza for her endless help and support in every aspect.

I would like to thank former and current members of our research groups in Polymat and EPCP for creating a nice research environment full of joy, learning and scientific discussions.

I would like to acknowledge the Dérivés Résiniques Terpéniques (DRT, France) for kindly supplying the starting materials.

I would like to thank Dr. José Ignacio Miranda from SGIker and Abdel Khouh from EPCP for their assistance in the NMR measurements, Virginie Pellerin for AFM analysis, Dr. Mercedes Fernandez and Dr. Xavier Callies for the technical support and discussion in rheology analysis.

Me gustaría agradecer a mi familia española (Adrian, Floren, Damian y Merche) y tailandesa en San Sebastián, que siempre me ayudan cuando lo necesito, que me recordó a mi hogar y estuvo a mi lado, y gracias a Floren por su comida.

และที่ขาดไม่ได้ ขอขอบคุณครอบครัว พ่อ แม่ มุก เมย์ และยาย ที่คอยให้ความรัก ความช่วยเหลือ คำปรึกษา คำแนะนำ และคอยอยู่เคียงข้างตลอดเวลา ขอบคุณมากๆ รักเสมอ..

Contents

Chapter 1. Introduction

Chapter 2. Monomer synthesis

Chapter 3. Renewable terpene derivative as a bio-sourced elastomeric building block in the design of functional acrylic copolymers

Chapter 4. Paving the way to sustainable waterborne pressure-sensitive adhesives using terpene-based triblock copolymer

Chapter 5. Nitroxide mediated miniemulsion polymerization of using terpene methacrylates

Chapter 1. Introduction

1.1. Introduction

The reduction in the consumption of fossil fuels is one of the most significant social and economic challenges of the modern era. The chemical industry, among others, still relies heavily on materials derived from oil to develop novel products at the cost of a non-negligible carbon footprint. More specifically, the use of polymers for commodity products as well as high-performance materials accounts for 7% of the consumption of fossil fuel, a figure that keeps on increasing.[1-4] These products include specialty materials like thermoplastic elastomers (TPEs), pressure sensitive adhesives (PSAs) and coatings, which have become increasingly attractive, due to their unique mechanical properties and excellent processability.[5, 6] Therefore, in order to reduce the fossil fuel dependence and the associated carbon footprint, the use of waste products and renewable natural resources as feedstock for polymer materials is an attractive opportunity. However, renewable polymers only have a small share of the whole

polymer market. This is due to the high cost and limited range of properties compared to the synthetic polymers produced from the petroleum chemical.[7-9] Therefore, it remains a challenge to design polymers with similar performances and cost as petroleum-based polymers.[10-12]

According to the European Bioplastic Association,[13] the term of 'biobased' means that the material or product is (partly) derived from biomass (plants). According to the market data compiled by the European Bioplastic Association in collaboration with nova-Institute, global bioplastics production capacity is set to increase from around 2.11 million tonnes in 2018 to approximately 2.62 million tonnes in 2023 (Figure 1.1).

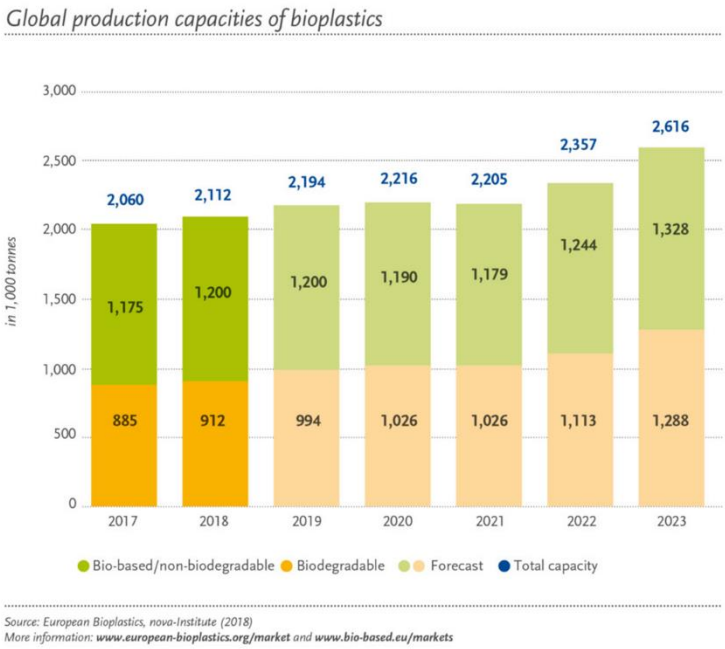

Figure 1.1. Global production capacities of bioplastics.

The renewable raw materials can be divided into three groups based on the origin; a) vegetable resources (cellulose, lignins, terpenes, starch, and vegetable oils), b) animal resources (chitosan, chitin and proteins), and c) bacteria polymers (bacteria cellulose and poly(hydroxyalkanoate)). Cramail *et al.* recently reviewed the use of lignin-based materials (prepared from vanillin, ferulic acid, guaiacol, syringaldehyde and 4-hydroxybenzoic acid) to produce thermoplastics and thermosets.[14] The

mechanical properties of the final polymers are affected by the substituents on the aromatic ring, and it was discovered that the presence of the methoxy groups led to an increase of impact strength. Among the plethora of reagents available, cardanol emerged as a valuable resource to modify the properties of epoxy-resins. Indeed, the mechanical properties were improved when the cardanol content was increased to 40%.[15] Another renewable resource worth mentioning is isosorbide, which can be used in the synthesis of polyesters and/or thermosets with high glass transition temperature (T_g = 130 ˚C) and good thermal stability.[16] In addition, the chain extension of isosorbide with *n*-butyl acrylate was also performed to yield soft/hard diblock copolymers, in which the two phase separation was observed with the detection of two T_gs.

1.2 Terpenes

One class of abundant vegetal materials that can be exploited is the terpene family. Terpenes are obtained by using steam distillation or by extraction of pine stumps. It is also one of the main byproducts of the Kraft process (Black liqueur), which is used in the paper industry to extract lignin from wood in the production of pulp.[17] The main components are α- and β-pinene. Terpenes are commonly utilized in fragrance and flavor formulations (*e.g.* limonene, camphor). Most of the terpenes are

either branched or cyclic molecules that contain one or more carbon-carbon double bond. Representative structures of some common terpenes are shown in Figure 1.2.

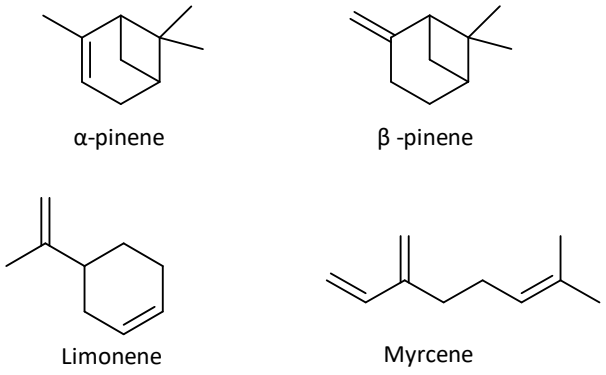

Figure 1.2. Chemical structure of some common terpenes.

When terpenes are chemically modified, for example by oxidation or rearrangement of the carbon skeleton, the resulting compounds are generally referred as terpenoids. The main terpenoid compounds found in some essential oils can be seen in Table 1.

Table 1.1. Main terpenoid compound of some essential oils.

Essential oil	**Botanical Name**	**Main Constituents**
Turpentine	Pinus spp.	Terpenes (pinenes, camphene)
Coriander	Coriandrum sativum	Linalool (65/80%)

Otto of rose	Rosa spp.	Geraniol, citronellol (>70%)
Geranium	Pelargonium spp.	Geraniol, citronellol
Lemon	Citrus limon	Limonene (90%)
Lemon grass	Cymbopogon spp.	Citral, citronellal (75/85%)
Citron scented	Eucalyptus citriodora	Citronellal (~70%)
Spearmint	Mentha spicata and Menta cardiac	Carvone (55/70%)
Peppermint	Mentha piperita	Menthol (45%)
Continental lavender	Lavandula officinalis	Linalool, linalyl acetate (much), ethyl penthyl ketone
Cinnamon bark	Cinnamomum verum Presl.	Cinnamic aldehyde (60/75%)
Cassia	Cinnamomum cassia	Cinnamic aldehyde (80%)
Cinnamon leaf	Cinnamomum verum Presl.	Eugenol (up to 80%)

The main terpenes and terpenoids, which can be considered as possible renewable platform chemicals, are pinene, limonene, careen, geraniol/nerol, citronellol, citral and citronellal. Valuable products can be obtained from terpenes *via* various chemical processes such as isomerization/rearrangement, hydrogenation, oxidation, hydration, hydroformylation, condensation, cyclization, ring opening, etc.[18] As an example, Scheme 1.1 presents some possible products that can be obtained from pinene. Terpenes can also be polymerized through the alkene moieties. Pinene, limonene and myrcene have also been extensively studied.[19]

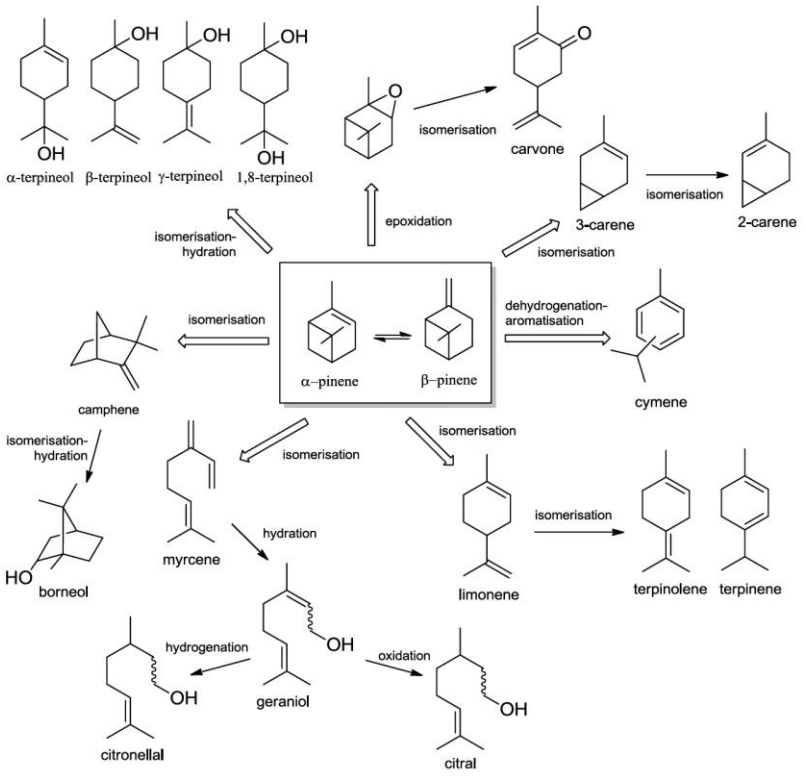

Scheme 1.1. Some of the possible products that can be obtained from pinene.[18]

1.2.1. Polymers derived from Pinenes

Pinenes are the most abundant class of terpene and they can be obtained from steam-distillation of resinous sap from pine or conifer trees. The two major components obtained are α-pinene and β-pinene. Cationic polymerization has been used to polymerize these monomers. The earliest work on the polymerization of α-pinene was reported in 1937.[20] The reaction was carried out in different solvents using $AlCl_3$ as a catalyst. A series of metal halides such as $AlCl_3$, $AlBr_3$, $AlEtCl_2$, $BF_3{\cdot}OEt_2$, $SnCl_4$, $TiCl_4$, and WCl_6 in conjunction with antimony trichloride ($SbCl_3$) were investigated as initiators for the cationic polymerization of α- pinene.[21, 22] It was found that $AlCl_3$ was the best suited to initiate the cationic polymerization. Considering the cationic polymerization mechanism, it should be noted that, even though α-pinene is readily protonated to form a tertiary carbocation, which can then rearrange to an unsaturated *p*-menthane isomer (Scheme 1.2), the attack of the endocyclic double bond to the isopropenyl cationic site is limited by steric hindrance.[23]

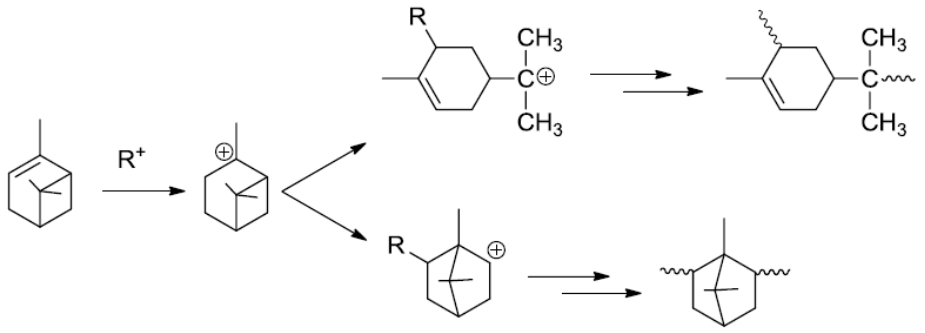

Scheme 1.2. An alternative mechanism of *α*-pinene cationic polymerization.

Thus, only oligomers of *α*-pinene can be obtained. Therefore, the vast majority of pinene polymerization involves the utilization of *β*-pinene. The earliest work on cationic polymerization of *β*-pinene employed Lewis acid metal halides like aluminium chloride, or ethyl aluminium dichloride as catalysts.[24-26] The general polymerization mechanism of cationic polymerization of *β*-pinene is presented in Scheme 1.3. Later, other Lewis acid initiators such as $SnCl_4$, $TiCl_4$, BF_3 and Et_2AlCl in various solvents and temperatures were also investigated.[27] Moreover, the cationic polymerization of *β*-pinene was tested under microwave irradiation using $AlCl_3$ as the initiator, which was shown to proceed rather rapidly and smoothly.[28] However, only low molar masses (< 4000 $g.mol^{-1}$) were obtained.

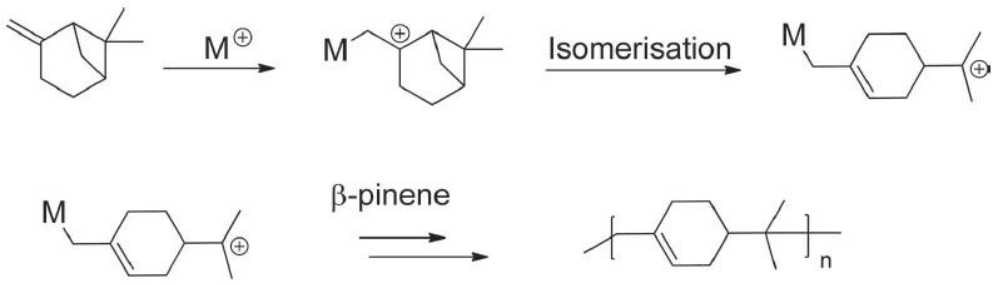

Scheme 1.3. Mechanism of the cationic polymerization of *β*-pinene.[29]

The living cationic polymerization of *β*-pinene was reported by Sawamoto *et al.* [29-31] The proposed polymerization mechanism is the attack of *β*-pinene on the cationic initiator form a tertiary carbocation, which then undergoes rearrangement of the pinene skeleton with the formation of a *p*-menthane type repeating unit.[29, 31] The main advantage of the living cationic polymerization is that it allows synthesizing block copolymers. The synthesis of block copolymers of *β*-pinene with styrene and *p*-methylstyrene (*p*MeSt),[31, 32] isobutylene [33] and other co-monomers[34, 35] using living cationic polymerization has been reported. Although most block copolymers prepared *via* living cationic polymerization had relatively low molecular weights, molecular weights up to 40,000 g.mol^{-1} could be achieved using $H_2O/EtAlCl_2$ co-catalyst system, at low temperature (-40 to -80 ℃).[36, 37] Recently, Kostjuk and co-workers[38] reported an effective initiating system for cationic polymerization of *β*-pinene using $AlCl_3$

($AlCl_3OPh_2$ or $AlCl_30.8EtOAc$) under industrially attractive experimental conditions (room temperature, low co-initiator concentration, and the possibility to use non-chlorinated solvents). Poly(*β*-pinene)s with relatively high molecular weight (M_n = 9,000-14,000 $g.mol^{-1}$) and good thermal properties were obtained. Free radical polymerization was also utilized to produce terpene containing copolymers. The copolymerization of *β*-pinene with conventional monomers such as methyl methacrylate (MMA),[39] styrene (S)[39] and acrylonitrile (AN)[40] resulted in limited incorporation of *β*-pinene monomer into the copolymer due to low reactivity ratios, and hence low yields that were obtained.

More recently, a more convenient approach to incorporate terpenes by free radical polymerization was introduced by Tang *et al.*, [19] in which rosin-based monomers bearing an acrylate moiety were prepared by esterification of pendant hydroxyl and acid groups. This allowed higher incorporation of the terpene-based materials into polymer matrices. Howdle *et al.*[41] utilized cyclic terpenes including *β*-pinene to prepare (meth)acrylate-based monomers *via* oxidation and subsequent esterification of the hydroxyl groups. The free radical polymerization of those monomers resulted in high monomer conversions (> 95 %), yielding polymers with $\overline{DP}_n$ up to about 100. The bio-based (meth)acrylic polymers displayed interesting

thermal properties, with T_gs ranging from room temperature to 120 °C. This was exploited to produce bio-based hard coatings after UV exposure in the presence of a thiol-based crosslinker. Lu and co-workers have reported the reversible addition-fragmentation chain-transfer (RAFT) polymerization copolymerization of β-pinene with acrylic monomers.[42] Although reasonable control was achieved, the reactivity ratios are not favorable for the efficient incorporation of β-pinene and the control over the polymer microstructure was therefore limited.

1.2.2. Polymers derived from Limonene/Myrcene

Another interesting terpene is limonene, which can be obtained from the isomerization of pinene or as a byproduct of the citrus industry.[43] Limonene is a chiral molecule. The (R)-enantiomer represents 90-96 % of citrus peel oil, and its world production exceeds 70,000 tons per year.[44] Limonene was copolymerized with monomers such as MMA,[45] AN,[46] and S[47, 48], but poor incorporation of limonene was achieved due to the unfavorable reactivity ratios. In contrast, the use of phenylmaleimide as comonomer yielded highly regulated polymers with efficient incorporation of limonene into the polymer.[49] Using a trithiocarbonate based RAFT agent, a reasonable control over the molecular weight could be obtained, although

dispersity of the polymers was greater than 1.5 in most cases. Limonene contains a C=C double bond, which can be converted to desirable functional groups by thiol-ene addition. Thiol-ene addition proceeds *via* a free radical chain mechanism and mainly produces anti-Markovnikov products.[50] The thiol-ene addition consist in the initially formation of thiyl radical which then attacks the unsaturated substrate forming a carbon radical. Then, the carbon radical reacts with the thiol molecule to give the final product and a new thiyl radical, thus propagating the radical chain (Scheme 1.4).[51]

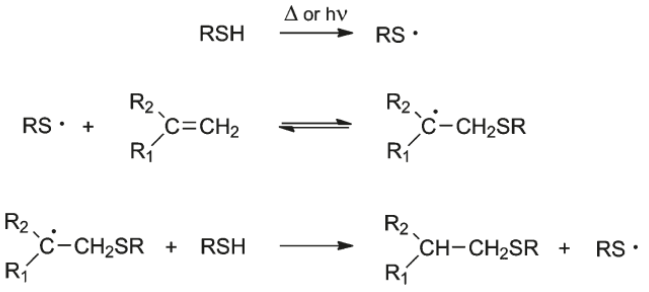

Scheme 1.4. Mechanism of Thiol-ene addition.

Jones *et al*[52] prepared terpene-based thiol by reacting hydrogen sulfide with various monoterpenes including limonene, terpinolene, car-3-ene and pulegone in the presence of aluminium trichloride or tribromide leading to a mixture of thiols and sometimes additionally bridged epi-sulphides. The main product from the reaction of

limonene with hydrogen sulphide was *p*-menth-1-en-8-thiol, characteristic of the grapefruit flavor. On the other hand, the main product from pulegone was 8-mercapto-trans-*p*-menth-3-one, an important component of Buchu leaf oil. Limonene-based homopolymers were also formed *via* thiol-ene addition technique,[51] displaying a relatively low molar mass and low T_g around -10 °C.

Myrcene is one terpene that has gained interest in recent years. Hillmyer e*t al.* prepared high molecular weight polymer of poly(3-methylenecyclopentene) using a combination of ring-closing metathesis and cationic polymerizations.[53] The final polymer exhibited a low glass transition temperature (T_g -28 °C). Moreover, an elastomer copolymer was obtained by copolymerization of myrcene and styrene *via* emulsion cationic polymerization. High molecular weight (from 60 to 120 kg.mol^{-1}) with relatively high dispersity (< 3.5) and single glass transition temperatures (from -40 to 15 °C) were obtained.[54,55] Recently, Sarkar and Bhowmick synthesized a series of elastomer copolymers of myrcene with styrene,[56] dibutyl itaconate[57] and methacrylates[58] *via* emulsion polymerization. However, low yields were obtained. Living anionic polymerization was utilized to design a hard/soft/hard triblock copolymer based on myrcene and *α*-methyl-*p*-methylstyrene (derived from limonene).[59] The resulting thermoplastic elastomer showed good microphase

separation and displayed better mechanical properties (tensile strengths up to 10 MPa and elongation at break of 1300 %) than those of a traditional petroleum-based poly(styrene)-*b*-poly(isoprene)-*b*-poly(styrene). Hilschmann and Kali have reported the RAFT homopolymerization of myrcene using a trithiocarbonate based RAFT agent.[60] Surprisingly, high regioselectivity was observed with > 96% of 1,4 addition. Metafiot *et al.* have reported the synthesis of myrcene homopolymers and elastomeric block copolymers with styrene by nitroxide mediated polymerization.[61] Reasonable control over the polymerization process was achieved, but the high entanglement molecular weight of the myrcene block resulted in brittle diblock copolymers.

1.2.3. Applications of terpene-based polymers

Available polyterpene resins are low molecular weight hydrocarbon like polymers used as adhesive components to impart tack (to both solvent-based and hot-melt systems), provide high gloss, good moisture vapor transmission resistance, good flexibility for wax coating and ensure viscosity control and increases the density to cast waxes.[23] Thakur and co-workers reported the application of poly(β-pinene) as semi-conductive material.[62] Upon doping poly(β-pinene) with iodine, the formed non-conjugated polymer became electrically conductive. The same authors also reported

that at high doping level of iodine, the non-conjugated polymer exhibited a large quadratic electro-optic effect that would be useful for non-linear optics application.[63]

1.3. Reversible deactivation radical polymerization (RDRP)

Free radical polymerization (FRP) is one of the major polymerization methods used for preparing high molecular weight polymers in both industrial and academic laboratories. Approximately 50 % of all commercial polymers are produced by radical polymerization.[64] This process exhibits tolerance to impurities and can be performed in bulk, solvent or dispersed system. Nevertheless, the major drawback of this process is that it is not possible to synthesize structurally advanced and well-defined macromolecular structures such as block copolymers or star polymers. In the free radical polymerization process, new chains are continually formed and terminated, with a lifetime of the active chain that spans from less than 1 second to 10 seconds. A consequence is that long chains are formed early in the process and in the absence of crosslinkers and chain transfer to polymer, the molecular weights decrease with monomer conversion due to the depletion of monomer (gel effect may lead to an increase of the molecular weight during the last stages of the process). In living ionic

polymerization, all chains are initiated at the beginning of the reaction and continue growing until all the monomer is consumed. From this, the molecular weight increases linearly with conversion and the molecular weight distribution is narrow. However, ionic polymerizations are restricted to a limited number of monomers and use very exigent reaction conditions. RDRP processes combine the robustness of the radical polymerization with the control and precision offered by living anionic polymerization. This has been achieved by using species that reversibly deactivate or terminate chains. These species control the concentration of active propagating species by maintaining a majority of chains in a dormant form. In radical polymerization, the rate of radical-radical termination is proportional to the square of radical concentration ($R_t \propto [P_n\bullet]^2$). Thus, the event of termination can be reduced relative to propagation ($R_p \propto [P_n\bullet]$) by reducing the radical concentration. Usually, the concentration of propagating radicals in reversible deactivation radical polymerization techniques (RDRP) is lower than in free radical polymerization. The RDRP techniques allow the facile production of well-defined polymers with good chain end fidelity and most importantly block copolymers. In these processes, the reaction ideally proceeds until all monomer is consumed and may continue if more monomer is added. The concentration of active species remains constant in living polymerization, the molecular weight increases linearly with the conversion and the molecular weight distribution is narrow, which is not observed in

the free radical polymerization system.[65] In practice, termination cannot be avoided and the ratio termination/propagation increases at high conversions. Nitroxide mediated polymerization (NMP),[66, 67] transition-metal mediated reversible deactivation polymerization (TMM-RDRP, ATRP)[32, 68, 69] and reversible addition-fragmentation chain transfer (RAFT) polymerization[70-72] are the most often used RDRP techniques.

Reversible deactivation radical polymerization (RDRP) was initially developed in homogeneous systems (bulk and solution). However, the advantages of the polymerization in aqueous dispersed media in terms of easiness of the process and environmental impact have pushed RDPR towards polymerization in dispersed media. One of the intrinsic features of polymerization in dispersed systems is the compartmentalization. There are two types of compartmentalization effects, which are the segregation effect and the confined effect. The segregation effect refers to two species located in separate particles being unable to react, and it is the reason that makes both the polymerization rate and molecular weights higher in the heterogeneous media than in homogeneous systems. The confined space effect refers to the fact that two species located in the same particle react at a higher rate in small particles than in large particles.

1.3.1. Nitroxide-Mediated Polymerization (NMP)

NMP is one of the RDRP technique based on the persistent radical effect (PRE). The exploitation of alkoxyamines as polymerization initiators and the use of NMP to produce block and end-functional polymers was first described in a patent application by Salomon *et al*. in 1985.[73] The activation-deactivation mechanism in NMP system is presented in Scheme 1.5, where k_{act} and k_{deact} denote the rate coefficients for thermal dissociation of alkoxyamine (activation) and coupling (deactivation), respectively. P-T, P• and T• denote alkoxyamine, propagating radicals and nitroxide, respectively. Ideally, T• only undergoes the reversible reaction with P•. On the other hand, P• is irreversibly consumed by termination. The net result is that after a very short initial time period when both [P•] and [T•] increase with time in similar fashion, the ratio [P•]/[T•] decreases and consequently, the rate of deactivation (P• + T•) is much higher than of termination (P• + P•). P• is gradually consumed by termination, and a true stationary state is never reached in the absence of an additional source of P• (such as the spontaneous thermal initiation of styrene).[74]

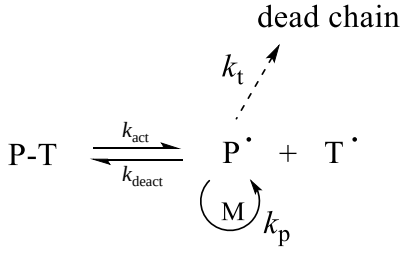

Scheme 1.5. The mechanism of NMP polymerization.

A wide range of nitroxides and derived alkoxyamines has been synthesized aiming at providing good control over the polymerization of a broad range of monomers. As the control is determined by the values of k_{act} and k_{deact}, and these coefficients depend on the structures of the nitroxide and the monomer, the development of the field has been largely driven by the search of nitroxide structures able to control a broad range of monomers. The investigation in the field has created a substantial body of knowledge about the effect of the substituents around the breakable C-ON bond.[75-78] It can be summarized that the stabilization of both propagating radical and the nitroxide favors the C-ON bond hemolysis (increase k_{deact}),[76, 79] steric strain on both nitroxide and alkyl fragment also increase the k_{deact},[80] high polar alkyl fragment of the alkoxyamine increase k_{deact} (k_{deact} decreases with increasing the polarity in the nitroxide fragment)[78] and the effect of the chain length depends on the nature of the propagating radical.[81]

Nitroxide/alkoxyamines usually used in NMP process include 2,2,6,6-tetramethyl-1-piperidinyloxy (TEMPO) ,[75, 82-84] 2,2,5-trimethyl-4-phenyl-3-azahexane-3-oxyl) (TIPNO),[85, 86] N-tert-butyl-N-[1-diethylphosphono-(2,2-dimethylpropyl)] (SG1),[87, 88] N-(1-methyl-(1-(4-nitrophenoxy)carbonyl)ethoxy)-N-(1-methyl-(1-(4-nitrophenoxy)carbonyl)ethyl) benzeneamine (DPAIO)[89, 90] and 3-(((2-cyanopropan-2-

yl)oxy)(cyclohexyl)amino)-2,2-dimethyl-3-phenylpropanenitrile (Dispolreg 007).[91-98] Monomers that can be polymerized in radical polymerization can be divided into two classes; (i) the more activated monomers (MAMs) include the vinyl group conjugated to neighboring functionality such as an aromatic ring (*e.g.* styrene) or a carbonyl group (*e.g.* (meth)acrylates, (meth)acrylamides and acrylonitrile); (ii) the less activated monomers (LAMs) include monomer where the vinylic group is adjacent to an electron rich atom (*e.g.* vinyl acetone, vinyl ester and vinyl amides). The choice of the regulator (*e.g.* nitroxide or alkoxyamine) is important to mediate the polymerization of MAMs and LAMs with good control and good retention of the chain ends. Simula *et al*[99] summarized the monomers that can be polymerized under controlled condition (Table 1.2.). TEMPO, TIPNO and BlocBuilder/SG1 can regulate the polymerization of LAMs, acrylate and styrene but good control cannot achieve with methacrylates, except if a slight amount of styrene is used as comonomer.[87, 100-102] The termination events via disproportionation were typically observed, due to the unfavorable rate constants of activation and deactivation and the enhanced penultimate effect of the poly(MMA) macroradical.[103] This issue can be minimized by addition of small amount of comonomer.[104, 105] The development of new nitroxide such as DPAIO could allowed the synthesis of polymethacrylates with good control and minimal undesired chains.[106, 107] Nevertheless, a limited versatility towards other monomers (*e.g.* acrylates and

styrene) is usually observed in this system. Recently, Ballard *et al* have introduced a new alkoxyamine which is 3-(((2-cyanopropan-2-yl)oxy)(cyclohexyl)amino)-2,2-dimethyl-3-phenylpropanenitrile or Dispolreg 007 to mediate the polymerization of methyl methacrylate and styrene with good control, both in solution and dispersed media.[91, 92, 94-96] Moreover, low fraction of disproportionation was obtained during the polymerization of methyl methacrylate, which is not the case of the SG1.[92] Some control over the polymerization of butyl acrylate was also achieved.[98] It can be seen that the nitroxide/alkoxyamines that control the polymerization of methacrylates cannot control the polymerization of all MAMs or LAMs (Table 1.2.). The good control of the polymerization depends on the stability of the nitroxide radical, the terminations and the k_{act} and k_{deact} values. As these parameters are different for each monomers, it is crucial to adapt the structure of the alkoxyamine to each monomers considered, which makes the existence of one universal alkoxyamine impossible.

Table 1.2. Nitroxides/alkoxyamines and monomer compatibility chart.[99]

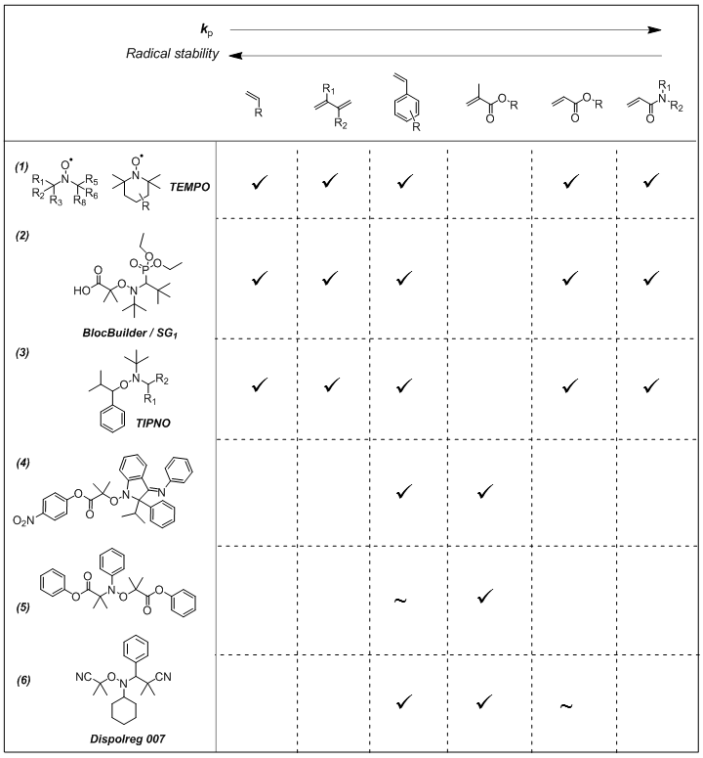

(1) TEMPO	✓	✓	✓		✓	✓
(2) BlocBuilder / SG1	✓	✓	✓		✓	✓
(3) TIPNO	✓	✓	✓		✓	✓
(4)			✓	✓		
(5)			~	✓		
(6) Dispolreg 007			✓	✓	~	

Emulsion polymerization has been used extensively to produce a wide range of speciality polymers. This process starts with a stirred mixture of water, initiator (usually water-soluble), monomer and emulsifier. Polymer particles are formed via micellar and/or homogeneous nucleation during interval I (0-10 % monomer conversion). During interval II (< 40 % monomer conversion), monomer droplets and monomer-swollen particles coexist, and monomer diffuses from droplet to particles as

the monomer is consumed in the particles by polymerization. In interval III (monomer conversion > 40 %), monomer droplets no longer exist, and the system consists of monomer-swollen particles in a continuous aqueous phase.[64, 108] The NMP was performed in emulsion polymerization, but only a few works were successful.[64, 109, 110] The reason was that the stable free radicals used were rather water-insoluble and they could not diffuse fast enough from the monomer droplets to the particles, which reduced the control of the polymerization. This problem also affects the other RDRP processes.

For this reason, the miniemulsion polymerization is commonly used with RDRP system. Droplet nucleation in miniemulsion polymerization avoids the diffusional limitations found in conventional emulsion polymerization and allows the incorporation of the water-insoluble compounds to the reaction loci. In the miniemulsion polymerization process, the surfactant is dissolved in water, the costabilizer is dissolved in the monomers and mixed with the aqueous solution of surfactant under stirring. Then the mixture is subjected to high efficient homogenization, resulting in stable small monomer droplets. Once the initiator is added to the system, the radicals enter into the monomer droplets and become polymer particles.[111, 112] The main alkoxyamine/nitroxides utilized in miniemulsion polymerization are TEMPO, SG1 and Dispolreg 007. TEMPO-based miniemulsion

NMP of styrene has been carried out successfully for a number of different systems such as TEMPO/BPO,[113, 114] KPS/TEMPO[114, 115] and PS-TEMPO.[116, 117] Due to the low equilibrium constant of TEMPO/styrene, the polymerization is generally conducted at high temperature (> 120 °C). In the case of the initiator/TEMPO system, their ratio is an essential parameter as if the initiator ratio is too high, the TEMPO is not present in enough quantity to ensure control/livingness. In addition, the hydrophobicity of the initiator is also important because the termination in the aqueous phase increases with increasing the concentration of water-soluble initiator.[115] Miniemulsion polymerization of styrene (120 °C) and acrylates (112 °C) controlled with an SG1-based alkoxyamines such as BlocBuilder,[118, 119] or combination of SG1 with the radical source like AIBN or KPS at 90 °C have been reported.[118, 120] However, in the case of any initiator, the molecular weight distributions are typically broad. Ballard *et al*[96] have reported the NMP miniemulsion polymerization of butyl methacrylate at moderate temperatures (T = 90 °C) using Dispolreg 007 as alkoxyamine. It was shown that high conversion and high solids content (52 %) with a reasonable control over the molecular weight could be obtained. More recently, the Dispolreg 007 was also utilized to polymerize methacrylic monomers via suspension polymerization.[95] High conversion with high molecular weights (100,000 $g.mol^{-1}$) were obtained. It also observed that under the same conditions the polymerization rate in suspension polymerization was faster than

bulk polymerization. This was related to the aqueous phase decomposition of nitroxide. Moreover, the versatility of this alkoxyamine was tested to form a diblock copolymer with methyl methacrylate and benzyl methacrylate.[95, 96]

1.3.2 Reversible addition-fragmentation chain transfer (RAFT) polymerization

RAFT polymerization has been extensively used to synthesize polymers with narrow molar mass distributions and block copolymers. This technique exhibits good tolerance to a wide range of monomers, solvent and initiators. In addition, it offers control over a wide range of monomers with different classes of chain transfer agent. The mechanism of RAFT polymerization is summarized in Scheme 1.6. The initiation and radical-radical termination occur as in free radical polymerization. Propagating radicals (P_n•) are formed from the initiator. The addition of P_n• to the thiocarbonylthio compound (A) followed by fragmentation of intermediate radical (B) results in a polymeric thiocarbonylthio compound (Aa) and a new radical (R•). Reaction of R• with monomer forms new propagating radicals (P_m•). A rapid equilibrium between the active propagating radicals (P_n• and P_m•) and the dormant polymeric thiocarbonylthio compound (Aa) provides an equal probability for all the chains to grow and allows the

production of narrow dispersity polymers. When the polymerization is completed, most of the polymer chains will retain the thiocarbonylthio end group.

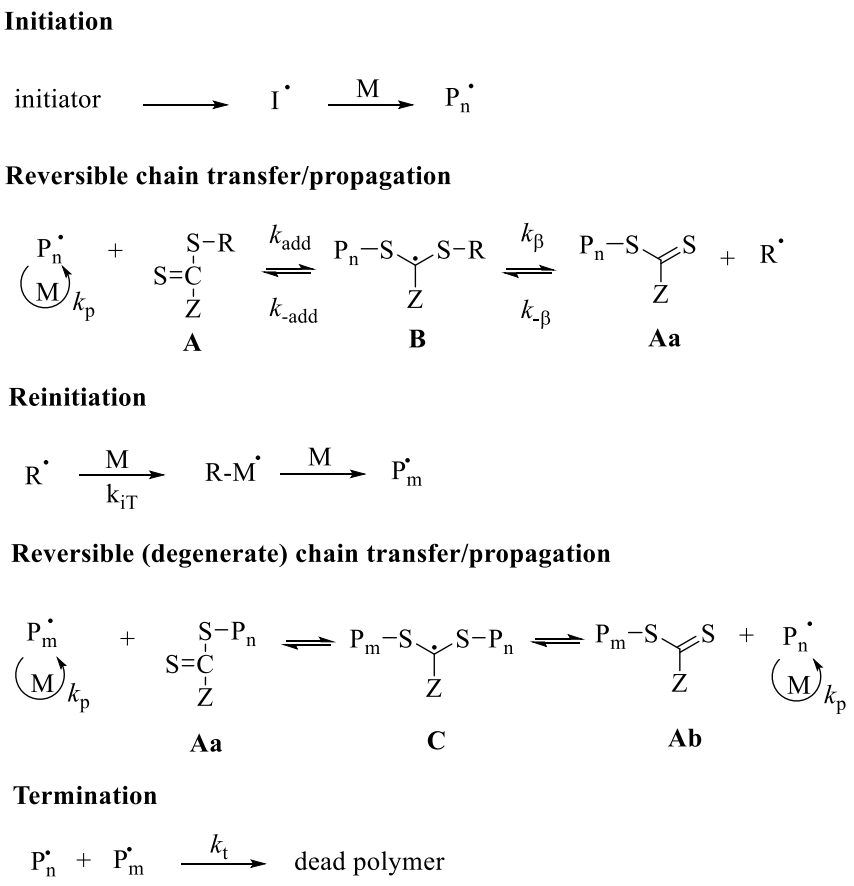

Scheme 1.6. The mechanism of RAFT polymerization.

The key of the degenerative chain transfer in RAFT polymerization is the chemical structure of the RAFT agent (Figure 1.3.). The substituents around the C=S are labelled as Z and R and the effectiveness of the RAFT agent depends on the monomer being polymerized and the transfer constant (C_{tr}) which is determined by the nature of the Z and R groups. Careful choice of RAFT agent, reactions conditions and monomer being polymerized is necessary to achieve good control over the polymerization and therefore well-defined polymeric products. Depending on the substituent group next to the C=S functionality, thiocarbonylthio can be divided into four groups; namely dithioesters, dithiocarbonates, trithiocarbonates and xanthates. The most effective RAFT agents are the dithioesters and trithiocarbonates which have carbon or sulfur atoms adjacent to the thiocarbonylthio group. For an efficient RAFT polymerization a) both the initial (A) and polymeric RAFT agent (Aa) should have a reactive C=S double bond (high k_{add}), b) the intermediate radicals B and C should fragment rapidly (high k_{β}, weak S-R bond) and give no side reactions, c) the intermediate B should partition in favor of the products ($k_{\beta} \geq k_{add}$) and d) the eliminated radicals (R') should efficiently re-initiate the polymerization.[121, 122]

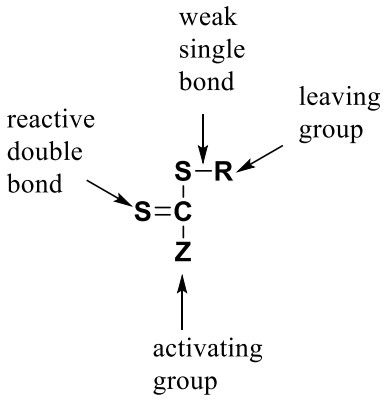

Figure 1.3. The structure of RAFT agent

The effectiveness of the RAFT agent depends on the monomer being polymerized and is determined by the properties of the free radical leaving group R and the group Z. Due to the fact that MAMs (more activated monomers) produce relatively more stabilized radicals, the Z-group has to be designed to help with the stabilization of the intermediate radical to favor radical addition on the C=S. Therefore, RAFT agents such as trithiocarbonates (Z = *S*-alkyl) or dithiocarbonates (Z = Ph) are commonly selected to control MAMs (MMA, St, MA). On the other hand, the high reactivity of LAMs (less activated monomers) make them poor homolytic groups, and they require intermediate radicals less stable, such as xanthates (Z = *O*-alkyl) or dithiocarbonates (Z = *N*-alkyl), in order to favor fragmentation of the propagating

radical, as a more stable intermediate acts as radical sink and limits the polymerization.[122] The guidelines for the proper RAFT agent for various monomers polymerization is presented in Figure 1.3.[122, 123]

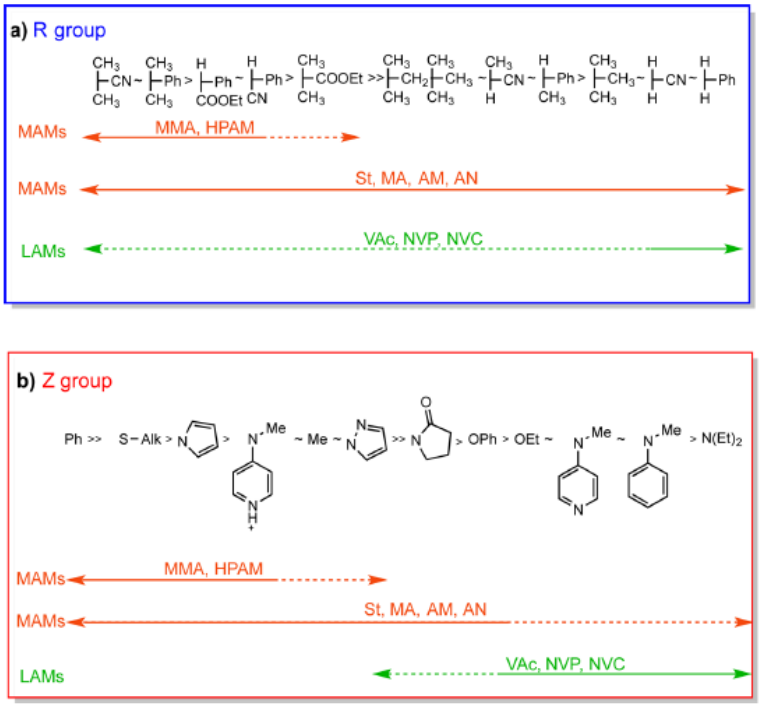

Figure 1.3. Guidelines for selection of RAFT agents [Z–C(=S)S–R] for various polymerizations. [122, 123]

RAFT polymerization is perhaps the most versatile RDPR, and numerous researches have extensively applied this technique in aqueous media. Monteiro *et al*[124]

reported the seed polymerization of styrene in emulsion polymerization using cumyl dithiobenzene as a RAFT agent, finding that due to the limited transport of the RAFT agent from monomer droplets to polymer particles, a broad molecular weight distribution was obtained. Miniemulsion polymerization avoids transport issues and has been utilized with a wide range of monomers such as styrene,[125-128] *n*-butyl acrylate,[129-131] methyl methacrylate,[132-134] *n*-butyl methacrylate,[125, 129, 133] as well as to synthesize di/tri-block copolymers.[130, 132, 135] A problem that often appeared in the early literature was the lack of the colloidal stability of the system during the miniemulsion polymerization.[125, 133] In an attempt to shed light on this issue, Luo *et al*[136] used the theory developed by Ugelstad *et al*[137] on the effect of low molecular weight water insoluble compounds on the swelling of the particles with monomer. Ugelstad *et al*[137] theoretically and experimentally demonstrated that those low molecular weight compounds tremendously increased the swelling of the particles by monomers. The oligomers formed at low conversion in RAFT miniemulsion polymerization can act as swelling agents. Luo *et al*[136] proposed that the statistical distribution of these oligomer at the beginning of the RAFT polymerization led to their uneven distribution amount the monomer droplets and monomer diffused from the droplets devoid of oligomers to those containing oligomer. This would increase the size of the droplets with oligomer and decrease that of the droplets without oligomer, which in turn would accelerate the

transport of monomer to the droplets containing oligomers. The word super-swelling has been coined to describe this system. The idea is appealing and it has been widely accepted as the cause of the stability problems in RAFT miniemulsion polymerization. However, a close look into the calculations presented by Luo *et al*[136] shows that what this article really shows is that super-swelling cannot occur in most of the real cases. In order to super-swelling to occur both small droplets size and high droplet water interfacial tensions are needed. For a droplet as small as 60 nm in diameter super-swelling does not occur if the interfacial tension is less or equal than 20 mN/m (Figure 2 in reference 136). On the other hand, for an interfacial tension as high as 25 mN/m, super-swelling does not occur for the particles sizes of 100 nm or larger (Figure 3 in reference 136). Considering that in the presence of surfactants the interfacial tensions are in the range of 5-10 mN/m and that the particles size of most miniemulsion above 100 nm, what Luo et al showed is that superswelling cannot be the case of the lack of colloidal stability of early works on the RAFT miniemulsion polymerization. Actually, no problems of the stability were found in this Thesis for the RAFT (Chapter 4) and nitroxide mediated (Chapter 5) polymerization and high solids content (52 wt%) polymer dispersion have been obtained by NMP.[96]

1.4. Block copolymers

Block copolymers (BCPs) are macromolecules formed by segments (blocks) of different composition. Methods to synthesize block copolymer include anionic polymerization, cationic polymerization and reversible deactivation radical polymerization. In addition, to linear multiblock copolymer, these methods can be utilized to create complex polymer architectures such as comb and star copolymers.[138]

Because of the interaction between the different blocks, block copolymers self-assemble into organized microdomain structures. AB diblock copolymers can form a variety of morphologies in the melt as well as in solution (Figure 1.5).[139]

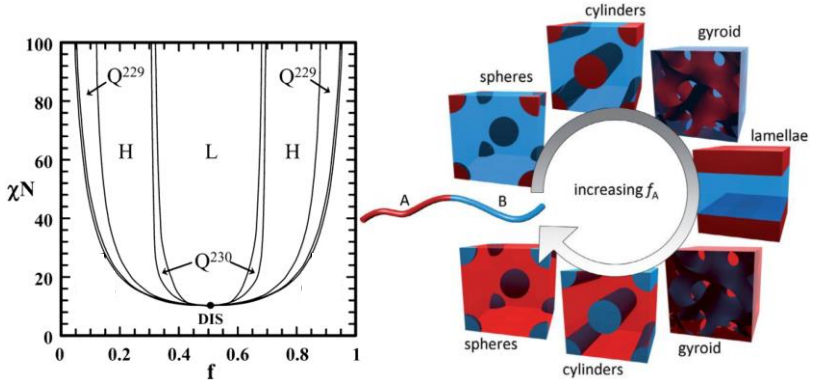

Figure 1.5. Scheme of microphase separated morphologies in block copolymer system.[140]

At high volume fractions of the B block, spheres of A are formed within the matrix of B typically arranged in body centered cubic lattice. Increasing the volume fraction of the A block results in the formation of hexagonally packed A cylinders within the matrix of B. In the case of similar volume fraction of both polymers, a lamellae structure is formed. In the composition range between cylinders and lamellae structures, a complex bi-continuous cubic double gyroid is formed.

The parameters controlling the block copolymer segregation are the interaction parameter between polymer A and B (χ_{AB} that provides the driving force for the phase separation) and the total degree of polymerization (N). A strong segregation between the blocks occur when $\chi N >> 10$ (strong segregation limit, SSL), whereas separation is only partial when $\chi N < 10$ (weak segregation limit, WSL).[141-143]

1.5. Pressure sensitive adhesive (PSA)

Pressure-sensitive adhesives (PSAs) are viscoelastic materials that firmly adhere to various surfaces upon applying a gentle pressure. PSAs should have both liquid-like viscosity and solid-like elasticity in order to obtain the sticky contact and the resistance to flow during the separation, respectively.[144-147] Acrylates dominate the waterborne PSAs market. Typically, acrylic based PSAs are random copolymers that contain

relatively long chain acrylates (e.g. 2-ethylhexyl acrylate, *n*-butyl acrylate) as soft monomers, whereas styrene or methyl methacrylate are often utilized as hard monomers.[148-150] These are petroleum-based monomers. To alleviate the dependency on petroleum, attempts to use materials from renewable resources have been reported. Renewable materials can be introduced into the adhesive in several ways. The most evident route is to use natural products that already have an adhesive characteristic such as proteins. The second way is to use building blocks or monomers that can be derived from renewable sources. Biobased acrylated methyl oleate was copolymerized with commercial methyl methacrylate and ethylene glycol dimethacrylate (EGDMA) to produce PSAs.[151, 152] Moreno *et al*.[153] reported the synthesis of PSAs based on biobased methacrylate oleic acid (MOA) and α-methylen-γ-butyrolactone in disperse media. Badía *et al*.[154] carried out the copolymerization of 2-octyl acrylate and isobornyl methacrylate to produce the waterborne PSAs.

Block copolymers are an interesting alternative to random copolymers because their mechanical properties can be tailor-made by modifying the functionality and the length of the blocks.[155-158] In addition, the synthesis of this type of copolymers is readily available by controlled radical polymerization.[156] In PSAs, block copolymers are AB and ABA types, where A is a glassy and B is a rubbery segment. The most studied of PSAs block copolymers are styrene-based linear ABA triblock copolymers, such as

poly(styrene-*b*-butadiene-*b*-styrene) (SBS)[159] and poly(styrene-*b*-isoprene-*b*-styrene).[5, 160] The synthesis of PSAs using bio-based monomers has been made and PSAs with good mechanical and adhesion properties have been reported.[161-166] Thus, triblock PSAs were prepared using bio-based acrylic isosorbide (AAI) and glucose acrylate tetraacetate as hard monomers and 2-ethylhexyl acrylate (2-EHA) or *n*-butyl acrylate (BA) as the "soft" monomers.[165, 167] Acrylic monomers obtained from depolymerization of lignocellolic biomass have also been used as hard monomers in combination to conventional soft acrylic monomers to produce partially bio-based PSAs.[31]

1.6. Objective of the thesis

Most synthetic plastics are derived from fossil fuel and their production increases every year. As a consequence, fossil resources are being exploited faster than they are being replenished. Therefore, the objective of the project is to contribute to the reduction of the petroleum dependences by using monomer based on bio-sourced terpenes. The bio-based terpenes are side products of the local paper industry of the "Landes" pine forest in the South West of France. Tetrahydrogeraniol (THG) and Cyclademol (CDM) were chosen as a terpene derivative to prepare (meth)acrylic

monomers, to replace its petroleum-based homologues *n*-butyl acrylate, 2-ethylhexyl acrylate, methyl methacrylate and styrene. Then, the synthesized bio-based monomers are polymerized in bulk, solution and aqueous dispersed systems by free radical polymerization, RAFT polymerization and NMP.

Waterborne PSAs formed by block copolymers are obtained by miniemulsion copolymerization of the terpene-based monomers. Hard/soft/hard, soft/hard/soft and soft/hard structures are synthesized. The effect of the polymer architecture and molecular weight on the adhesive properties are examined. The adhesive performance of full terpene di/tri block copolymers is compared with that of block copolymers containing some petroleum-based monomer.

1.7. Outline of the thesis

In Chapter 2, the presence of the hydroxyl group on the renewable starting material THG and CDM is utilized to incorporate a (meth)acrylic functionality. A commercially available linear terpene derivative, tetrahydrogeraniol, is utilized to prepare acrylic monomer, tetrahydrogeraniol acrylate (THGA) and tetrahydrogeraniol methacrylate (THGMA). Cyclademol utilized to prepare the cyclademol acrylate (CDMA) and cyclademol methacrylate (CDMMA) is also commercially available.

In Chapter 3, the synthesized bio-sourced based monomer THGA is polymerized by free radical and reversible-addition fragmentation chain transfer (RAFT) polymerization in bulk and solution. The effects of monomer concentration and the degree of polymerization (DP_n) are investigated. Finally, the retention of reactive chain ends is exploited to yield a soft/hard/soft and hard/soft/hard triblock copolymers poly(THGA-*b*-styrene-*b*-THGA). Thermal analysis and AFM imaging are used to further analyse this ABA triblock copolymer.

In Chapter 4, the THGA monomer based on linear terpene derivative is polymerized by RAFT miniemulsion polymerization. Different types of initiators and the degree of polymerization are studied. The poly(THGA) and poly(CDMA) are used to prepare the poly(THGA)-*b*-poly(CDMA)-*b*-poly(THGA) soft/hard/soft and poly(CDMA)-*b*-poly(THGA)-*b*-poly(CDMA) hard/soft/hard triblock copolymers. Furthermore, the adhesive properties of full terpene triblock copolymers between THGA and CDMA are compared with those of a triblock copolymer based on styrene.

In Chapter 5, nitroxide-mediated polymerization (NMP) is utilized to polymerize the THGMA monomer in solution and miniemulsion in the presence of 3-(((2-cyanopropan-2-yl)oxy)(cyclohexyl)amino)-2,2-dimethyl-3-phenylpropanenitrile (Dispolreg 007). The effects of temperature of polymerization and the degree of

polymerization are studied for the NMP in solution. In NMP miniemulsion polymerization, the stability and the degree of polymerization of poly(THGMA) are investigated. Furthermore, the poly(THGMA) is extended with a hard monomer (CDMMA) to form the soft/hard diblock copolymer, and the adhesive performance is compared with the block copolymers based on styrene.

In Chapter 6, the most relevant conclusions of this Thesis are presented.

A detailed description of the main experimental procedures and characterization techniques is presented in **Appendices I** and **II**.

1.8. References

(1). Gandini, A. The irruption of polymers from renewable resources on the scene of macromolecular science and technology. *Green Chem.* **2011,** 13, 1061-1083.

(2). Ragauskas, A. J.; Williams, C. K.; Davison, B. H.; Britovsek, G.; Cairney, J.; Eckert, C. A.; Jr, W. J. F.; Hallett, J. P.; Leak, D. J.; Liotta, C. L.; Mielenz, J. R.; Murphy, R.; Templer, R.; Tschaplinski, T. The Path Forward for Biofuels and Biomaterials. *Science* **2006,** 311, 484-489.

(3). Huber, G. W.; Iborra, S.; Corma, A. Synthesis of Transportation Fuels from Biomass: Chemistry, Catalysts, and Engineering. *Chem. Rev.* **2006,** 106, 4044-4098.

(4). Okada, M. Chemical syntheses of biodegradable polymers. *Prog. Polym. Sci.* **2002,** 27, 87-133.

(5). Pedemonte, E.; Turturro, A.; Bianchi, U.; Devetta, P. The cubic structure of a SIS three block copolymer. *Polymer* **1973,** 14, 145-150.

(6). Ruzette, A.-V.; Leibler, L. Block copolymers in tomorrow's plastics. *Nat. Mater.* **2005,** 4, 19.

(7). Beach, E. S.; Cui, Z.; Anastas, P. T. Green Chemistry: A design framework for sustainability. *Energy Environ. Sci.* **2009,** 2, 1038-1049.

(8). Anastas, P.; Eghbali, N. Green Chemistry: Principles and Practice. *Chem. Soc. Rev.* **2010,** 39, 301-312.

(9). Anastas, P. T.; Kirchhoff, M. M. Origins, Current Status, and Future Challenges of Green Chemistry. *Acc. Chem. Res.* **2002,** 35, 686-694.

(10). Averous, L. Biodegradable Polymer Blends and Composites from Renewable Resources. *Macromol. Chem. Phys.* **2009,** 210, 890-890.

(11). Gandini, A. Polymers from Renewable Resources: A Challenge for the Future of Macromolecular Materials. *Macromolecules* **2008,** 41, 9491-9504.

(12). Williams, C. K.; Hillmyer, M. A. Polymers from Renewable Resources: A Perspective for a Special Issue of Polymer Reviews. *Polym. Rev.* **2008,** 48, 1-10.

(13). https://www.european-bioplastics.org/

(14). Llevot, A.; Grau, E.; Carlotti, S.; Grelier, S.; Cramail, H. From Lignin-derived Aromatic Compounds to Novel Biobased Polymers. *Macromol. Rapid Commun.* **2016,** 37, 9-28.

(15). Unnikrishnan, K. P.; Thachil, E. T. Studies on the Modification of Commercial Epoxy Resin using Cardanol-based Phenolic Resins. *J. Elastomers Plast* **2008,** 40, 271-286.

(16). Gallagher, J. J.; Hillmyer, M. A.; Reineke, T. M. Isosorbide-based Polymethacrylates. *ACS Sustainable Chem. Eng.* **2015,** 3, 662-667.

(17). Schwab, W.; Fuchs, C.; Huang, F. C. Transformation of terpenes into fine chemicals. *Eur. J. Lipid Sci. Technol.* **2013,** 115, 3-8.

(18). Corma, A.; Iborra, S.; Velty, A. Chemical Routes for the Transformation of Biomass into Chemicals. *Chem. Rev.* **2007,** 107, 2411-2502.

(19). Wilbon, P. A.; Chu, F.; Tang, C. Progress in Renewable Polymers from Natural Terpenes, Terpenoids, and Rosin. *Macromol. Rapid Commun.* **2013,** 34, 8-37.

(20). Carmody, M. O.; Carmody, W. H. Polymerization of Terpenes. *J. Am. Chem. Soc.* **1937,** 59, 1312-1312.

(21). Lu, J.; Kamigaito, M.; Sawamoto, M.; Higashimura, T.; Deng, Y. X. Cationic polymerization of β-pinene with the AlCl3/SbCl3 binary catalyst: Comparison with α-pinene polymerization. *J. Appl. Polym. Sci.* **1996,** 61, 1011-1016.

(22). Higashimura, T.; Lu, J.; Kamigaito, M.; Sawamoto, M.; Deng, Y. X. Cationic polymerization of α-pinene with the binary catalyst AlCl3/SbCl3. *Makromol. Chem.* **1992,** 193, 2311-2321.

(23). Silvestre, A. J. D.; Gandini, A., In *Monomers, Polymers and Composites from Renewable Resources*, Belgacem, M. N., Gandini, A., Eds. Elsevier: Amsterdam, 2008; pp 1-16.

(24). Jiang, L.; Masami, K.; Mitsuo, S.; Toshinobu, H.; Yun-Xiang, D. Cationic polymerization of β-pinene with the AlCl3/SbCl3 binary catalyst: Comparison with α-pinene polymerization. *J. Appl. Polym. Sci.* **1996,** 61, 1011-1016.

(25). Roberts, W. J.; Day, A. R. A Study of the Polymerization of α- and β-Pinene with Friedel—Crafts Type Catalysts. *J. Am. Chem. Soc.* **1950,** 72, 1226-1230.

(26). Guiné, R. P. F.; Castro, J. A. A. M. Polymerization of β-pinene with ethylaluminum dichloride (C2H5AlCl2). *J. Appl. Polym. Sci.* **2001,** 82, 2558-2565.

(27). Martinez, F. Cationic polymerization of β-pinene. *J Polym Sci A Polym Chem* **1984,** 22, 673-677.

(28). Barros, M. T.; Petrova, K. T.; Ramos, A. M. Potentially Biodegradable Polymers Based on α- or β-Pinene and Sugar Derivatives or Styrene, Obtained under Normal Conditions and on Microwave Irradiation. *Eur. J. Org. Chem.* **2007,** 2007, 1357-1363.

(29). Lu, J.; Kamigaito, M.; Sawamoto, M.; Higashimura, T.; Deng, Y.-X. Living Cationic Isomerization Polymerization of β-Pinene. 1. Initiation with HCl−2-Chloroethyl Vinyl Ether Adduct/TiCl3(OiPr) in Conjunction with nBu4NCl. *Macromolecules* **1997,** 30, 22-26.

(30). Lu, J.; Kamigaito, M.; Sawamoto, M.; Higashimura, T.; Deng, Y. X. Living cationic isomerization polymerization of β-pinene. III. Synthesis of end-functionalized polymers and graft copolymers. *J. Polym. Sci. A Polym. Chem.* **1997,** 35, 1423-1430.

(31). Lu, J.; Kamigaito, M.; Sawamoto, M.; Higashimura, T.; Deng, Y.-X. Living Cationic Isomerization Polymerization of β-Pinene. 2. Synthesis of Block and Random Copolymers with Styrene or p-Methylstyrene. *Macromolecules* **1997,** 30, 27-31.

(32). Lu, J.; Liang, H.; Li, A.; Cheng, Q. Synthesis of block and graft copolymers of β-pinene and styrene by transformation of living cationic polymerization to atom transfer radical polymerization. *Eur. Polym. J.* **2004,** 40, 397-402.

(33). Li, A.-L.; Zhang, W.; Liang, H.; Lu, J. Living cationic random copolymerization of β-pinene and isobutylene with 1-phenylethyl chloride/TiCl4/Ti(OiPr)4/nBu4NCl. *Polymer* **2004,** 45, 6533-6537.

(34). Lu, J.; Liang, H.; Zhang, R.; Li, B. Synthesis of poly(β-pinene)-b-polytetrahydrofuran from β-pinene-based macroinitiator. *Polymer* **2001,** 42, 4549-4553.

(35). Lu, J.; Liang, H.; Zhang, W.; Cheng, Q. Synthesis of poly(β-pinene)-g-poly(meth)acrylate by the combination of living cationic polymerization and atom transfer radical polymerization. *J. Polym. Sci. A Polym. Chem.* **2003,** 41, 1237-1242.

(36). Keszler, B.; Kennedy, J. P., Synthesis of high molecular weight poly (β-pinene). In *Macromolecules: Synthesis, Order and Advanced Properties*, Springer Berlin, Heidelberg, 1992; pp 1-9.

(37). Satoh, K.; Sugiyama, H.; Kamigaito, M. Biomass-derived heat-resistant alicyclic hydrocarbon polymers: poly(terpenes) and their hydrogenated derivatives. *Green Chem.* **2006,** 8, 878-882.

(38). Kukhta, N. A.; Vasilenko, I. V.; Kostjuk, S. V. Room temperature cationic polymerization of β-pinene using modified AlCl3 catalyst: toward sustainable plastics from renewable biomass resources. *Green Chem.* **2011,** 13, 2362-2364.

(39). Ramos, A. M.; Lobo, L. S.; Bordado, J. M. Polymers from pine gum components: Radical and coordination homo and copolymerization of pinenes. *Macromol. Symp.* **1998,** 127, 43-50.

(40). Li, A. L.; Wang, Y.; Liang, H.; Lu, J. Controlled radical copolymerization of β-pinene and acrylonitrile. *J Polym Sci Part A: Polym Chem.* **2006,** 44, 2376-2387.

(41). Sainz, M. F.; Souto, J. A.; Regentova, D.; Johansson, M. K. G.; Timhagen, S. T.; Irvine, D. J.; Buijsen, P.; Koning, C. E.; Stockman, R. A.; Howdle, S. M. A facile and green route to terpene derived acrylate and methacrylate monomers and simple free radical polymerisation to yield new renewable polymers and coatings. *Polym. Chem.* **2016,** 7, 2882-2887.

(42). Li, A.-L.; Wang, X.-Y.; Liang, H.; Lu, J. Controlled radical copolymerization of β-pinene and n-butyl acrylate. *React. Funct. Polym.* **2007,** 67, 481-488.

(43). Burdock, G. A., *Fenaroli's Handbook of Flavor Ingredients*. 3 ed.; CRC Press: Boca Raton, FL, 1995.

(44). Kerton, F. M., *Alternative Solvents for Green Chemistry*. Royal Society of Chemistry Publishing: Cambridge, UK, 2009.

(45). Sharma, S.; Srivastava, A. K. Alternating Copolymers of Limonene with Methyl Methacrylate: Kinetics and Mechanism. *Polymer Chemistry. J. Polym.* **2003,** 40, 593-603.

(46). Sharma, S.; Srivastava, A. K. Radical Copolymerization of Limonene with Acrylonitrile: Kinetics and Mechanism. *Polym Plast Technol Eng.* **2003,** 42, 485-502.

(47). Sharma, S.; Srivastava, A. K. Synthesis and characterization of copolymers of limonene with styrene initiated by azobisisobutyronitrile. *Eur. Polym. J.* **2004,** 40, 2235-2240.

(48). Sharma, S.; Srivastava, A. K. Synthesis and characterization of a terpolymer of limonene, styrene, and methyl methacrylate via a free-radical route. *J. Appl. Polym. Sci.* **2004,** 91, 2343-2347.

(49). Satoh, K.; Matsuda, M.; Nagai, K.; Kamigaito, M. AAB-Sequence Living Radical Chain Copolymerization of Naturally Occurring Limonene with Maleimide: An End-to-End Sequence-Regulated Copolymer. *J. Am. Chem. Soc.* **2010,** 132, 10003-10005.

(50). Griesbaum, K. Probleme und Möglichkeiten der radikalischen Addition von Thiolen an ungesättigte Verbindungen. *Angew. Chem.* **1970,** 82, 276-290.

(51). Firdaus, M.; Espinosa, L. M. d.; Meier, M. A. R. Terpene-Based Renewable Monomers and Polymers via Thiol–Ene Additions. *Macromolecules* **2011,** 44, 7253-7262.

(52). Janes, J. F.; Marr, I. M.; Unwin, N.; Banthorpe, D. V.; Yusuf, A. Reaction of monoterpenoids with hydrogen sulphide to form thiols and epi-sulphides of potential organoleptic significance. *Flavour Fragr. J.* **1993,** 8, 289-294.

(53). Kobayashi, S.; Lu, C.; Hoye, T. R.; Hillmyer, M. A. Controlled Polymerization of a Cyclic Diene Prepared from the Ring-Closing Metathesis of a Naturally Occurring Monoterpene. *J. Am. Chem. Soc.* **2009,** 131, 7960-7961.

(54). Trumbo, D. L. Free radical copolymerization behavior of myrcene. *Polym. Bull.* **1993,** 31, 629-636.

(55). Hulnik, M. I.; Vasilenko, I. V.; Radchenko, A. V.; Peruch, F.; Ganachaud, F.; Kostjuk, S. V. Aqueous cationic homo- and co-polymerizations of β-myrcene and

styrene: a green route toward terpene-based rubbery polymers. *Polym. Chem.* **2018,** 9, 5690-5700.

(56). Sarkar, P.; Bhowmick, A. K. Terpene Based Sustainable Elastomer for Low Rolling Resistance and Improved Wet Grip Application: Synthesis, Characterization and Properties of Poly(styrene-co-myrcene). *ACS Sustainable Chem. Eng.* **2016,** 4, 5462-5474.

(57). Sarkar, P.; Bhowmick, A. K. Green Approach toward Sustainable Polymer: Synthesis and Characterization of Poly(myrcene-co-dibutyl itaconate). *ACS Sustainable Chemistry & Engineering* **2016,** 4, 2129-2141.

(58). Sarkar, P.; Bhowmick, A. K. Terpene based sustainable methacrylate copolymer series by emulsion polymerization: Synthesis and structure-property relationship. *J. Polym. Sci. A.* **2017,** 55, 2639-2649.

(59). Bolton, J. M.; Hillmyer, M. A.; Hoye, T. R. Sustainable Thermoplastic Elastomers from Terpene-Derived Monomers. *ACS Macro Lett.* **2014,** 3, 717-720.

(60). Hilschmann, J.; Kali, G. Bio-based polymyrcene with highly ordered structure via solvent free controlled radical polymerization. *Eur. Polym. J.* **2015,** 73, 363-373.

(61). Metáfiot, A.; Kanawati, Y.; Gerard, J.-F.; Defoort, B.; Maric, M. Synthesis of β-Myrcene-Based Polymers and Styrene Block and Statistical Copolymers by SG1

Nitroxide-Mediated Controlled Radical Polymerization. *Macromolecules* **2017,** 50, 3101-3120.

(62). Vippa, P.; Rajagopalan, H.; Thakur, M. Electrical and optical properties of a novel nonconjugated conductive polymer, poly(β-pinene). *J. Polym. Sci. B Polym. Phys.* **2005,** 43, 3695-3698.

(63). Rajagopalan, H.; Vippa, P.; Thakur, M. Quadratic electro-optic effect in a nano-optical material based on the nonconjugated conductive polymer, poly(β-pinene). *Appl. Phys. Lett.* **2006,** 88, 033109.

(64). Zetterlund, P. B.; Kagawa, Y.; Okubo, M. Controlled/Living Radical Polymerization in Dispersed Systems. *Chem. Rev.* **2008,** 108, 3747-3794.

(65). Moad, G.; Solomon, D. H., 9 - Living Radical Polymerization. In *The Chemistry of Radical Polymerization (Second Edition)*, Moad, G., Solomon, D. H., Eds. Elsevier Science Ltd: Amsterdam, 2005; pp 451-585.

(66). Hawker, C. J.; Bosman, A. W.; Harth, E. New Polymer Synthesis by Nitroxide Mediated Living Radical Polymerizations. *Chem. Rev.* **2001,** 101, 3661-3688.

(67). Nicolas, J.; Guillaneuf, Y.; Lefay, C.; Bertin, D.; Gigmes, D.; Charleux, B. Nitroxide-mediated polymerization. *Prog. Polym. Sci.* **2013,** 38, 63-235.

(68). Ouchi, M.; Terashima, T.; Sawamoto, M. Transition Metal-Catalyzed Living Radical Polymerization: Toward Perfection in Catalysis and Precision Polymer Synthesis. *Chem. Rev.* **2009,** 109, 4963-5050.

(69). Matyjaszewski, K. Atom Transfer Radical Polymerization (ATRP): Current Status and Future Perspectives. *Macromolecules* **2012,** 45, 4015-4039.

(70). Moad, G.; Rizzardo, E.; Thang, S. H. Living Radical Polymerization by the RAFT Process – A Third Update. *Aust. J. Chem.* **2012,** 65, 985-1076.

(71). Gody, G.; Maschmeyer, T.; Zetterlund, P. B.; Perrier, S. Pushing the Limit of the RAFT Process: Multiblock Copolymers by One-Pot Rapid Multiple Chain Extensions at Full Monomer Conversion. *Macromolecules* **2014,** 47, 3451-3460.

(72). Barner-Kowollik, C.; Davis, T. P.; Heuts, J. P. A.; Stenzel, M. H.; Vana, P.; Whittaker, M. RAFTing down under: Tales of missing radicals, fancy architectures, and mysterious holes. *J. Polym. Sci., Part A: Polym. Chem.* **2003,** 41, 365-375.

(73). Solomon, D. H.; Rizzardo, E.; Cacioli, P. Polymerization process and polymers produced thereby. 1986.

(74). Zetterlund, P. B.; Okubo, M. Compartmentalization in Nitroxide-Mediated Radical Polymerization in Dispersed Systems. *Macromolecules* **2006,** 39, 8959-8967.

(75). Moad, G.; Rizzardo, E. Alkoxyamine-Initiated Living Radical Polymerization: Factors Affecting Alkoxyamine Homolysis Rates. *Macromolecules* **1995,** 28, 8722-8728.

(76). Marque, S.; Mercier, C. L.; Tordo, P.; Fischer, H. Factors Influencing the C−O−Bond Homolysis of Trialkylhydroxylamines. *Macromolecules* **2000,** 33, 4403-4410.

(77). Marque, S.; Fischer, H.; Baier, E.; Studer, A. Factors Influencing the C−O Bond Homolysis of Alkoxyamines: Effects of H−Bonding and Polar Substituents. *J. Org. Chem.* **2001,** 66, 1146-1156.

(78). Fischer, H.; Kramer, A.; Marque, S. R. A.; Nesvadba, P. Steric and Polar Effects of the Cyclic Nitroxyl Fragment on the C−ON Bond Homolysis Rate Constant. *Macromolecules* **2005,** 38, 9974-9984.

(79). Beaudoin, E.; Bertin, D.; Gigmes, D.; Marque, S. R. A.; Siri, D.; Tordo, P. Alkoxyamine C–ON Bond Homolysis: Stereoelectronic Effects. *European Journal of Organic Chemistry* **2006,** 2006, 1755-1768.

(80). Bertin, D.; Gigmes, D.; Marque, S. R. A.; Tordo, P. Polar, Steric, and Stabilization Effects in Alkoxyamines C−ON Bond Homolysis: A Multiparameter Analysis. *Macromolecules* **2005,** 38, 2638-2650.

(81). Guerret, O.; Couturier, J.-L.; Chauvin, F.; El-Bouazzy, H.; Bertin, D.; Gigmes, D.; Marque, S.; Fischer, H.; Tordo, P., Influence of Solvent and Polymer Chain Length on the Hemolysis of SG1-Based Alkoxyamines. In *Advances in Controlled/Living Radical Polymerization*, American Chemical Society: 2003; Vol. 854, pp 412-423.

(82). Burguière, C.; Dourges, M.-A.; Charleux, B.; Vairon, J.-P. Synthesis and Characterization of ω-Unsaturated Poly(styrene-b-n-butyl methacrylate) Block Copolymers Using TEMPO-Mediated Controlled Radical Polymerization. *Macromolecules* **1999,** 32, 3883-3890.

(83). Georges, M. K.; Veregin, R. P. N.; Kazmaier, P. M.; Hamer, G. K. Narrow molecular weight resins by a free-radical polymerization process. *Macromolecules* **1993,** 26, 2987-2988.

(84). Listigovers, N. A.; Georges, M. K.; Odell, P. G.; Keoshkerian, B. Narrow-Polydispersity Diblock and Triblock Copolymers of Alkyl Acrylates by a "Living" Stable Free Radical Polymerization. *Macromolecules* **1996,** 29, 8992-8993.

(85). Nicolaÿ, R.; Marx, L.; Hémery, P.; Matyjaszewski, K. Synthesis and Evaluation of a Functional, Water- and Organo-Soluble Nitroxide for "Living" Free Radical Polymerization. *Macromolecules* **2007,** 40, 6067-6075.

(86). Marx, L.; Hemery, P. Synthesis and evaluation of a new polar, TIPNO type nitroxide for "living" free radical polymerization. *Polymer* **2009,** 50, 2752-2761.

(87). Benoit, D.; Grimaldi, S.; Robin, S.; Finet, J.-P.; Tordo, P.; Gnanou, Y. Kinetics and Mechanism of Controlled Free-Radical Polymerization of Styrene and n-Butyl Acrylate in the Presence of an Acyclic β-Phosphonylated Nitroxide. *J. Am. Chem. Soc.* **2000,** 122, 5929-5939.

(88). Benoit, D.; Chaplinski, V.; Braslau, R.; Hawker, C. J. Development of a Universal Alkoxyamine for "Living" Free Radical Polymerizations. *J. Am. Chem. Soc.* **1999,** 121, 3904-3920.

(89). Berti, C.; Colonna, M.; Greci, L.; Marchetti, L. Stable nitroxide radicals from phenylisatogen and arylimino-derivatives with organo-metallic compounds. *Tetrahedron* **1975,** 31, 1745-1753.

(90). Edeleva, M.; Marque, S. R. A.; Bertin, D.; Gigmes, D.; Guillaneuf, Y.; Morozov, S. V.; Bagryanskaya, E. G. Hydrogen-transfer reaction in nitroxide mediated polymerization of methyl methacrylate: 2,2-Diphenyl-3-phenylimino-2,3-dihydroindol-1-yloxyl nitroxide (DPAIO) vs. TEMPO. *J. Polym. Sci. A Polym. Chem.* **2008,** 46, 6828-6842.

(91). Simula, A.; Aguirre, M.; Ballard, N.; Veloso, A.; Leiza, J. R.; Es, S. v.; Asua, J. M. Novel alkoxyamines for the successful controlled polymerization of styrene and methacrylates. *Polym. Chem.* **2017,** 8, 1728-1736.

(92). Simula, A.; Ruipérez, F.; Ballard, N.; Leiza, J. R.; Es, S. v.; Asua, J. M. Why can Dispolreg 007 control the nitroxide mediated polymerization of methacrylates? *Polym. Chem.* **2019,** 10, 106-113.

(93). Ballard, N.; Aguirre, M.; Simula, A.; Agirre, A.; Leiza, J. R.; Asua, J. M.; Es, S. v. New Class of Alkoxyamines for Efficient Controlled Homopolymerization of Methacrylates. *ACS Macro Lett.* **2016,** 5, 1019-1022.

(94). Ballard, N.; Simula, A.; Aguirre, M.; Leiza, J. R.; Es, S. v.; M.Asua, J. Synthesis of poly(methyl methacrylate) and block copolymers by semi-batch nitroxide mediated polymerization. *Polym. Chem.* **2016,** 7, 6964-6972.

(95). Ballard, N.; Aguirre, M.; Simula, A.; Leiza, J. R.; Es, S. v.; M.Asua, J. Nitroxide mediated suspension polymerization of methacrylic monomers. *Chem Eng J* **2017,** 316, 655-662.

(96). Ballard, N.; Aguirre, M.; Simula, A.; Leiza, J. R.; Es, S. v.; Asua, J. M. High solids content nitroxide mediated miniemulsion polymerization of n-butyl methacrylate. *Polym. Chem.* **2017,** 8, 1628-1635.

(97). Mehravar, E.; Agirre, A.; Ballard, N.; Es, S. v.; Arbe, A.; Leiza, J. R.; Asua, J. M. Insights into the Network Structure of Cross-Linked Polymers Synthesized via Miniemulsion Nitroxide-Mediated Radical Polymerization. *Macromolecules* **2018,** 51, 9740-9748.

(98). Simula, A.; Ballard, N.; Aguirre, M.; Leiza, J. R.; Es, S. v.; M.Asua, J. Nitroxide mediated copolymerization of acrylates, methacrylates and styrene: The importance of side reactions in the polymerization of acrylates. *Eur. Polym. J.* **2019,** 110, 319-329.

(99). Simula, A.; Ballard, N.; Asua, J. M., Nitroxide Mediated Polymerization. In *In Nitroxides Synthesis, Properties and Applications*, Gigmes, D., Ed. 2019.

(100). Harrisson, S.; Couvreur, P.; Nicolas, J. SG1 Nitroxide-Mediated Polymerization of Isoprene: Alkoxyamine Structure/Control Relationship and α,ω–Chain-End Functionalization. *Macromolecules* **2011,** 44, 9230-9238.

(101). Abreu, C. M. R.; Fonseca, A. C.; Rocha, N. M. P.; Guthrie, J. T.; Serra, A. C.; Coelho, J. F. J. Poly(vinyl chloride): current status and future perspectives via reversible deactivation radical polymerization methods. *Progress in Polymer Science* **2018,** 87, 34-69.

(102). Guégain, E.; Guillaneuf, Y.; Nicolas, J. Nitroxide-Mediated Polymerization of Methacrylic Esters: Insights and Solutions to a Long-Standing Problem. *Macromol. Rapid Commun.* **2015,** 36, 1227-1247.

(103). Guillaneuf, Y.; Gigmes, D.; Marque, S. R. A.; Tordo, P.; Bertin, D. Nitroxide-Mediated Polymerization of Methyl Methacrylate Using an SG1-Based Alkoxyamine: How the Penultimate Effect Could Lead to Uncontrolled and Unliving Polymerization. *Macromol. Chem. Phys.* **2006,** 207, 1278-1288.

(104). Charleux, B.; Nicolas, J.; Guerret, O. Theoretical Expression of the Average Activation−Deactivation Equilibrium Constant in Controlled/Living Free-Radical Copolymerization Operating via Reversible Termination. Application to a Strongly Improved Control in Nitroxide-Mediated Polymerization of Methyl Methacrylate. *Macromolecules* **2005,** 38, 5485-5492.

(105). Mei, W.; Maric, M. Nitroxide-Mediated Polymerization of 2-Hydroxyethyl Methacrylate (HEMA) Controlled with Low Concentrations of Acrylonitrile and Styrene. *Macromol. React. Eng.* **2017,** 11, 1600067.

(106). Guillaneuf, Y.; Gigmes, D.; Marque, S. R. A.; Astolfi, P.; Greci, L.; Tordo, P.; Bertin, D. First Effective Nitroxide-Mediated Polymerization of Methyl Methacrylate. *Macromolecules* **2007,** 40, 3108-3114.

(107). Greene, A. C.; Grubbs, R. B. Nitroxide-Mediated Polymerization of Methyl Methacrylate and Styrene with New Alkoxyamines from 4-Nitrophenyl 2-Methylpropionat-2-yl Radicals. *Macromolecules* **2010,** 43, 10320-10325.

(108). Asua, J. M., *Polymer Reaction Engineering*. Blackwell Oxford: 2007.

(109). F.Cunningham, M. Controlled/living radical polymerization in aqueous dispersed systems. *Prog. Polym. Sci.* **2008,** 33, 365-398.

(110). Zetterlund, P. B.; Thickett, S. C.; Perrier, S.; Bourgeat-Lami, E.; Lansalot, M. Controlled/Living Radical Polymerization in Dispersed Systems: An Update. *Chem. Rev.* **2015,** 115, 9745-9800.

(111). M.Asua, J. Miniemulsion polymerization. *Prog. Polym. Sci.* **2002,** 27, 1283-1346.

(112). Asua, J. M. Challenges for industrialization of miniemulsion polymerization. *Prog. Polym. Sci.* **2014,** 39, 1797-1826.

(113). Prodpran, T.; Dimonie, V. L.; Sudol, E. D.; El-Aasser, M. S. Nitroxide-mediated living free radical miniemulsion polymerization of styrene. *Macromol. Symp.* **2000,** 155, 1-14.

(114). Lin, M.; Cunningham, M. F.; Keoshkerian, B. Achieving high conversions in nitroxide-mediated living styrene miniemulsion polymerization. *Macromol. Symp.* **2004,** 206, 263-274.

(115). Cunningham, M. F.; Xie, M.; McAuley, K. B.; Keoshkerian, B.; Georges, M. K. Nitroxide-Mediated Styrene Miniemulsion Polymerization. *Macromolecules* **2002,** 35, 59-66.

(116). Nakamura, T.; Zetterlund, P. B.; Okubo, M. Particle Size Effects in TEMPO-Mediated Radical Polymerization of Styrene in Aqueous Miniemulsion. *Macromol. Rapid Commun.* **2006,** 27, 2014-2018.

(117). Pan, G.; Sudol, E. D.; Dimonie, V. L.; El-Aasser, M. S. Nitroxide-Mediated Living Free Radical Miniemulsion Polymerization of Styrene. *Macromolecules* **2001,** 34, 481-488.

(118). Charleux, B.; Nicolas, J. Water-soluble SG1-based alkoxyamines: A breakthrough in controlled/living free-radical polymerization in aqueous dispersed media. *Polymer* **2007,** 48, 5813-5833.

(119). Farcet, C.; Lansalot, M.; Charleux, B.; Pirri, R.; Vairon, J. P. Mechanistic Aspects of Nitroxide-Mediated Controlled Radical Polymerization of Styrene in Miniemulsion, Using a Water-Soluble Radical Initiator. *Macromolecules* **2000,** 33, 8559-8570.

(120). Nicolas, J.; Charleux, B.; Guerret, O.; Magnet, S. Novel SG1-Based Water-Soluble Alkoxyamine for Nitroxide-Mediated Controlled Free-Radical Polymerization of Styrene and n-Butyl Acrylate in Miniemulsion. *Macromolecules* **2004,** 37, 4453-4463.

(121). Moad, G.; Thang, S. H., *Living Radical Polymerization by the RAFT Process – A Second Update*. 2009; Vol. 62.

(122). Perrier, S. 50th Anniversary Perspective: RAFT Polymerization—A User Guide. *Macromolecules* **2017,** 50, 7433-7447.

(123). Keddie, D. J.; Moad, G.; Rizzardo, E.; Thang, S. H. RAFT Agent Design and Synthesis. *Macromolecules* **2012,** 45, 5321-5342.

(124). Monteiro, M. J.; Hodgson, M.; Brouwer, H. D. The influence of RAFT on the rates and molecular weight distributions of styrene in seeded emulsion polymerizations. *J. Polym. Sci. A Polym. Chem.* **2000,** 38, 3864-3874.

(125). Tsavalas, J. G.; Schork, F. J.; Brouwer, H. d.; Monteiro, M. J. Living Radical Polymerization by Reversible Addition−Fragmentation Chain Transfer in Ionically Stabilized Miniemulsions. *Macromolecules* **2001,** 34, 3938-3946.

(126). Huang, X.; Sudol, E. D.; Dimonie, V. L.; Anderson, C. D.; El-Aasser, M. S. Stability in Styrene/HD Miniemulsions Containing a RAFT Agent. *Macromolecules* **2006,** 39, 6944-6950.

(127). Yang, L.; Luo, Y.; Li, B. The influence of surfactant coverage of the minidroplets on RAFT miniemulsion polymerization. *J. Polym. Sci. A Polym. Chem.* **2006,** 44, 2293-2306.

(128). Lansalot, M.; Davis, T. P.; Heuts, J. P. A. RAFT Miniemulsion Polymerization: Influence of the Structure of the RAFT Agent. *Macromolecules* **2002,** 35, 7582-7591.

(129). Russum, J. P.; Jones, C. W.; Schork, F. J. Continuous Living Polymerization in Miniemulsion Using Reversible Addition Fragmentation Chain Transfer (RAFT) in a Tubular Reactor. *Ind. Eng. Chem. Res.* **2005,** 44, 2484-2493.

(130). Smulders, W. W.; Jones, C. W.; Schork, F. J. Synthesis of Block Copolymers Using RAFT Miniemulsion Polymerization in a Train of CSTRs. *Macromolecules* **2004,** 37, 9345-9354.

(131). Luo, Y.; Liu, B.; Wang, Z.; Gao, J.; Li, B. Butyl acrylate RAFT polymerization in miniemulsion. *J. Polym. Sci. A Polym. Chem.* **2007,** 45, 2304-2315.

(132). Butté, A.; Storti, G.; Morbidelli, M. Miniemulsion Living Free Radical Polymerization by RAFT. *Macromolecules* **2001,** 34, 5885-5896.

(133). Brouwer, H. d.; Tsavalas, J. G.; Schork, F. J. Living Radical Polymerization in Miniemulsion Using Reversible Addition−Fragmentation Chain Transfer. *Macromolecules* **2000,** 33, 9239-9246.

(134). McLeary, J. B.; Tonge, M. P.; Roos, D. d. W.; Sanderson, R. D.; Klumperman, B. Controlled, radical reversible addition–fragmentation chain-transfer polymerization in high-surfactant-concentration ionic miniemulsions. *J. Polym. Sci. A Polym. Chem.* **2004,** 42, 960-974.

(135). Bowes, A.; Mcleary, J. B.; Sanderson, R. D. AB and ABA type butyl acrylate and styrene block copolymers via RAFT-mediated miniemulsion polymerization. *J. Polym. Sci. A Polym. Chem.* **2007,** 45, 588-604.

(136). Luo, Y.; Tsavalas, J.; Schork, F. J. Theoretical Aspects of Particle Swelling in Living Free Radical Miniemulsion Polymerization. *Macromolecules* **2001,** 34, 5501-5507.

(137). Ugelstad, J.; Mórk, P. C.; Kaggerud, K. H.; Ellingsen, T.; Berge, A. Swelling of oligomer-polymer particles. New methods of preparation. *Advances in Colloid and Interface Science* **1980,** 13, 101-140.

(138). Matyjaszewski, K.; Spanswick, J. Controlled/living radical polymerization. *Materials Today* **2005,** 8, 26-33.

(139). Matsen, M. W.; Bates, F. S. Unifying Weak- and Strong-Segregation Block Copolymer Theories. *Macromolecules* **1996,** 29, 1091-1098.

(140). Tseng, Y.-C.; Darling, S. B. Block Copolymer Nanostructures for Technology. *Polymers* **2010,** 2, 470-489.

(141). Helfand, E.; Wasserman, Z. R. Block Copolymer Theory. 5. Spherical Domains. *Macromolecules* **1978,** 11, 960-966.

(142). Leibler, L. Theory of Microphase Separation in Block Copolymers. *Macromolecules* **1980,** 13, 1602-1617.

(143). Matsen, M. W.; Schick, M. Stable and unstable phases of a diblock copolymer melt. *Physical review letters* **1994,** 72, 2660-2663.

(144). Chu, S. G., *Viscoelastic Properties of Pressure Sensitive Adhesive*. 2nd ed ed.; Satas, D., Ed: Van Nostrand Reinhold: New York, 1989.

(145). CHANG, E. P. Viscoelastic Properties of Pressure-Sensitive Adhesives. *J. Adhesion* **1997,** 60, 233-248.

(146). Benedek, I.; Feldstein, M. M., Taylor & Francis Group: Boca Raton, FL, 2009; Vol. 1, p 1-2.

(147). Creton, C. 50th Anniversary Perspective: Networks and Gels: Soft but Dynamic and Tough. *Macromolecules* **2017,** 50, 8297-8316.

(148). Benedek, I., *Pressure-sensitive adhesives and applications*. CRC Press: 2004.

(149). Ebnesajjad, S.; Landrock, A. H., Chapter 5 - Characteristics of Adhesive Materials. In *Adhesives Technology Handbook (Third Edition)*, Ebnesajjad, S., Landrock, A. H., Eds. William Andrew Publishing: Boston, 2015; pp 84-159.

(150). Agirre, A.; Nase, J.; Degrandi, E.; Creton, C.; Asua, J. M. Miniemulsion Polymerization of 2-Ethylhexyl Acrylate. Polymer Architecture Control and Adhesion Properties. *Macromolecules* **2010,** 43, 8924-8932.

(151). Bunker, S. P.; Wool, R. P. Synthesis and characterization of monomers and polymers for adhesives from methyl oleate. *J. Polym. Sci. A Polym. Chem.* **2002,** 40, 451-458.

(152). Bunker, S.; Staller, C.; Willenbacher, N.; Wool, R. Miniemulsion polymerization of acrylated methyl oleate for pressure sensitive adhesives. *Int J Adhes Adhes* **2003,** 23, 29-38.

(153). Moreno, M.; Goikoetxea, M.; Cal, J. C. d. l.; Barandiaran, M. J. From fatty acid and lactone biobased monomers toward fully renewable polymer latexes. *J. Polym. Sci. A.* **2014,** 52, 3543-3549.

(154). Badía, A.; Movellan, J.; Barandiaran, M. J.; Leiza, J. R. High Biobased Content Latexes for Development of Sustainable Pressure Sensitive Adhesives. *Ind. Eng. Chem. Res.* **2018,** 57, 14509-14516.

(155). Boutillier, J.-M.; Disson, J.-P.; Havel, M.; Inoubli, R.; Magnet, S., Self-assembling acrylic block copolymers for enhanced adhesives properties. Adhesives & Sealants Industry Magazine, 2013

(156). Jennings, J.; He, G.; Howdle, S. M.; Zetterlund, P. B. Block copolymer synthesis by controlled/living radical polymerisation in heterogeneous systems. *Chemical Society reviews* **2016,** 45, 5055-5084.

(157). Creton, C. Block Copolymers for Adhesive Applications. *Macromolecular Engineering* **2011**, 1731-1751.

(158). Holmberg, A. L.; Reno, K. H.; Wool, R. P.; Epps, I. I. I. T. H. Biobased building blocks for the rational design of renewable block polymers. *Soft Matter* **2014,** 10, 7405-7424.

(159). Kraus, G.; Rollmann, K. W.; Gruver, J. T. Dynamic Properties of a Model Reinforced Elastomer. Styrene-Butadiene Reinforced with Polystyrene. *Macromolecules* **1970,** 3, 92-96.

(160). Tse, M. F. Studies of triblock copolymer-tackifying resin interactions by viscoelasticity and adhesive performance. *J ADHES SCI TECHNOL* **1989,** 3, 551-570.

(161). Badía, A.; Movellan, J.; Barandiaran, M. J.; Leiza, J. R. High Biobased Content Latexes for Development of Sustainable Pressure Sensitive Adhesives. *Industrial & Engineering Chemistry Research* **2018,** 57, 14509-14516.

(162). Wanamaker, C. L.; O'Leary, L. E.; Lynd, N. A.; Hillmyer, M. A.; Tolman, W. B. Renewable-Resource Thermoplastic Elastomers Based on Polylactide and Polymenthide. *Biomacromolecules* **2007,** 8, 3634-3640.

(163). Shin, J.; Martello, M. T.; Shrestha, M.; Wissinger, J. E.; Tolman, W. B.; Hillmyer, M. A. Pressure-Sensitive Adhesives from Renewable Triblock Copolymers. *Macromolecules* **2011,** 44, 87-94.

(164). Ding, K.; John, A.; Shin, J.; Lee, Y.; Quinn, T.; Tolman, W. B.; Hillmyer, M. A. High-Performance Pressure-Sensitive Adhesives from Renewable Triblock Copolymers. *Biomacromolecules* **2015,** 16, 2537-2539.

(165). Gallagher, J. J.; Hillmyer, M. A.; Reineke, T. M. Acrylic Triblock Copolymers Incorporating Isosorbide for Pressure Sensitive Adhesives. *ACS Sustainable Chemistry & Engineering* **2016,** 4, 3379-3387.

(166). Heinrich, L. A. Future opportunities for bio-based adhesives – advantages beyond renewability. *Green Chemistry* **2019,** 21, 1866-1888.

(167). Nasiri, M.; Saxon, D. J.; Reineke, T. M. Enhanced Mechanical and Adhesion Properties in Sustainable Triblock Copolymers via Non-covalent Interactions. *Macromolecules* **2018,** 51, 2456-2465.

Chapter 2. Monomer Synthesis

2.1. Introduction

Terpene is an abundant bio-based monomer that contains one or more unsaturated carbons. The most representative and viable source of terpenes are the turpentine resins extracted from coniferous trees and citric fruits. Terpenes are commonly utilized in fragrance and flavors formulations (*e.g*. limonene, camphor). Attempts to form polymers by direct polymerization of terpenes have been reported.[1] However, the results obtained show that the terpenes do not easily polymerize and only low molecular weight could be obtained working at low temperature *via* cationic polymerization.[2-7] Moreover, the copolymerization of the terpenes with several commercial monomers *via* free radical polymerization led to low incorporation of the terpene compound due to the low reactivity ratio.[8-12] A more convenient approach to incorporate terpenes by free radical polymerization was introduced by Tang *et al*.[13], in which rosin based monomers bearing an acrylate moiety were prepared by

esterification of pendant hydroxyl and acid groups. This yielded a higher incorporation of the terpene based materials into polymer matrices. More recently, Howdle *et al*.[14] utilized commercially available cyclic terpenes (e.g. α-pinene, β-pinene, limonene and carvone) to prepare (meth)acrylate based monomers *via* oxidation and subsequent esterification of the hydroxyl groups. The free radical polymerization of those monomers resulted in high monomer conversions (> 95 %), thus yielding polymers of a few thousands Daltons (up to $\bar{M}_n$ ~ 23,600 g.mol^{-1}). The bio-based (meth)acrylic polymers displayed interesting thermal properties, with T_g ranging from 12 to 142 °C.

In this work, we focus our attention to synthesize a new class of renewable bio-based monomers from side products of the local paper industry of the "Landes" forest in the South West of France. This is the biggest European farmed forest and produces thousands of tons of functional organic renewable molecules extracted from the black liquor, *i.e.* terpenes, especially. Tetrahydrogeraniol (THG) and cyclademol (CDM) (Figure 2.1) were selected. THG has a branched-linear structure that is expected to give a low T_g polymer as its synthetic homologue, *i.e.* EthylHexyl. On the other hand, the cyclic structure of CDM is expected to yield a hard polymer mimicking the chemical structure of the Norbornyl group. Combination of these monomers opens a wide range

of possibilities, although this PhD thesis focuses on the block copolymers for bio-based adhesives.

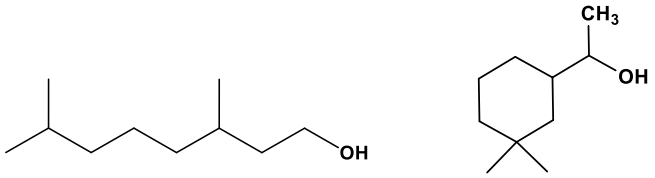

Tetrahydrogeraniol (THG) Cyclademol (CDM)

Figure 2.1. Structure of tetrahydrogeraniol (THG) and cyclademol (CDM).

2.2. Experimental

2.2.1. Materials

The materials are given in Appendix **I**

2.2.2. Synthesis procedures

2.2.2.1. Synthesis of tetrahydrogeraniol acrylate (THGA) and tetrahydrogeraniol methacrylate (THGMA)

Method A: Esterification with acryloyl chloride

THGA was first prepared by esterification of tetrahydrogeraniol with acryloyl chloride. Tetrahydrogeraniol (9.50 g, 0.06 mol), triethylamine (6.07 g, 0.06 mol) and dichloromethane (180 mL) were added to a three-neck 500 mL round-bottom flask (RBF) equipped with rubber seals, dropping funnel and a magnetic stirrer. The mixture was placed in an ice bath and left under stirring for 2 hours. Subsequently, acryloyl chloride (8.14 g, 0.09 mol) was added dropwise *via* the dropping funnel. Upon complete addition, the mixture was left under stirring for 30 minutes in the ice bath and for 24 hours at ambient temperature. Then, the mixture was filtered and the mixture was washed several times with brine and deionized water. The organic phase was passed through basic alumina column and the volatiles were removed by rotary evaporation to yield a transparent viscous liquid.

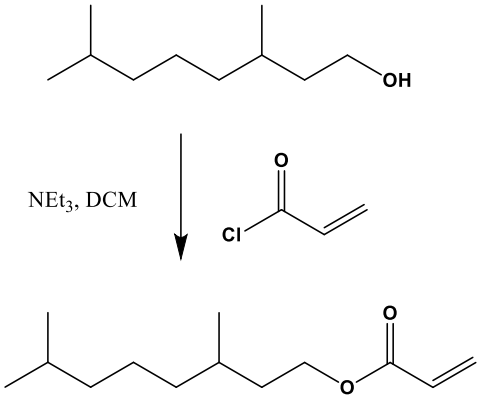

Scheme 2.1. Reaction scheme to synthesize the THGA by method A.

Method B: Esterification with acrylic acid or methacrylic acid.

Esterification of THG with acids was also tried aiming at both THGA and THGMA. Tetrahydrogeraniol (28.5 g, 0.18 mol), acrylic acid (21.84 g, 0.30 mol) or methacrylic acid (25.81 g, 0.30 mol), 2-methyltetrahydrofuran (250 mL), propylphosphonic anhydride (57 g, 0.18 mol) and triethylamine (16 g, 0.164 mol) were mixed in a 500 mL round bottom flask and stirred at room temperature for 24 hours. Then, water was added and the aqueous phase extracted with diethyl ether. Afterwards, the mixture was washed several times with brine and deionized water. The organic phase was passed through basic alumina column and the volatile solvent was removed by rotary evaporation to yield a transparent viscous liquid.

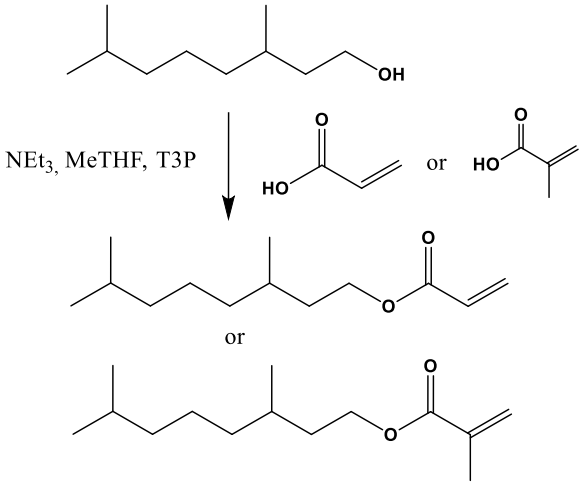

Scheme 2.2. Reaction scheme to synthesize THGA and THGMA by method B.

2.2.2.2. Synthesis of cyclademol acrylate (CDMA) and cyclademol methacrylate (CDMMA)

Method B: Esterification with acrylic acid or methacrylic acid.

A mixture of cyclademol (28.12 g, 0.18 mol), acrylic acid (21.84 g, 0.30 mol) or methacrylic acid (25.81 g, 0.30 mol), 2-methyltetrahydrofuran (250 mL), propylphosphonic anhydride (57 g, 0.18 mol) and triethylamine (16 g, 0.164 mol) were mixed in a 500 mL round bottom flask and stirred at room temperature for 24 hours. The water was added and the aqueous phase extracted with diethyl ether. Then, the

mixture was washed several times with brine and deionized water. The organic phase was passed through basic alumina and the volatile solvent was removed by rotary evaporation to yield a transparent viscous liquid.

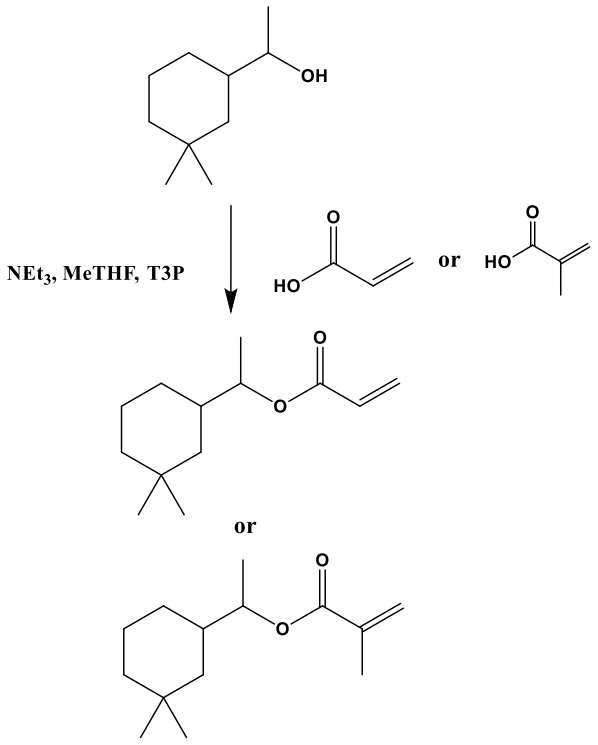

Scheme 2.3. Reaction scheme to synthesize the CDMA and CDMMA by method B.

2.2.3. Characterization

The monomer was characterized by ^{1}H NMR ($CDCl_3$, 400 MHz) and ^{13}C NMR ($CDCl_3$, 100 MHz).

2.3. Results and discussion

The presence of the hydroxyl group on the renewable starting material was utilized to incorporate a (meth)acrylate functionality. In this work, tetrahydrogeaniol acrylate (THGA), tetrahydrogeraniol methacrylate (THGMA), cyclademol acrylate (CDMA) and cyclademol methacrylate (CDMMA) were synthesized. The preparation of the tetrahydrogeraniol meth(acrylate) monomer was first carried out by (meth)acylation with (meth)acryloyl chloride (Scheme 2.1). The success of the reaction was confirmed by ^{1}H and ^{13}C NMRs. Figure 2.2 shows the ^{1}H and ^{13}C NMR spectra of the THGA monomer. It can be seen that, the NMR results provided the signal at 6.38, 6.12 and 5.80 ppm, which correspond to the protons of methylene and vinyl groups. The characteristic peaks are assigned, as follow: 6.38 (b) (dd, 1H, C$\boldsymbol{H}_2$=CH-C=O), 6.12 (c) (s, 1H, CH_2=C$\boldsymbol{H}$-C=O), 5.80 (a) (dd, 1H, C$\boldsymbol{H}_2$=CH-C=O), 4.18 (d) (s, O-C$\boldsymbol{H}_2$-CH_2-CH_2), 1.69 (k) (m, 1H, $(CH_3)_2$-C$\boldsymbol{H}$-CH_2), 1.50 (e) (m, 2H, CH-C$\boldsymbol{H}_2$-CH_2-O), 1.47 (f)

(m, 1H, CH_3-C***H***-CH_2-CH_2), 1.28 (i) (m, 2H, CH-CH_2-C***H***$_2$-CH_2-CH), 1.14 (h, j) (m, 4H, CH-C***H***$_2$-CH_2-C***H***$_2$-CH), 0.91 (g) (d, 3H, C***H***$_3$-CH-CH_2-CH_2), 0.89 (l) (d, 6H, (C***H***$_3$)$_2$-CH-CH_2-CH_2). The signal of ^{13}C NMR of monomer, as follow: Cc (166), Ca (130), Cb (129), Cd (63), Cj (39), Ch (37), Ce (35), Cf (30), Ck (28), Ci (25), Cl (23), Cg (19).

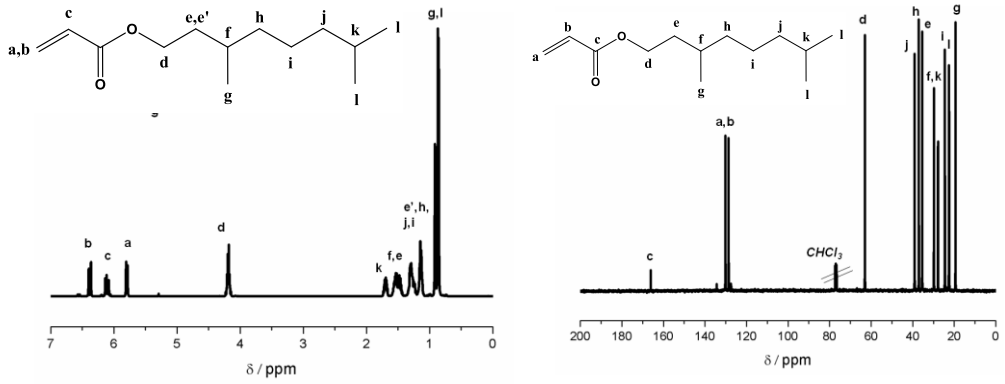

Figure 2.2. ^{1}H and ^{13}C NMR of THGA monomer by acryloyl chloride.

It should be noted that, this route provided high yield (~ 85%, Table 2.1) of the synthesized THGA monomer. However, we recognise that this synthetic route is not sustainable or green. Therefore, the hunt for a more sustainable system prompted us to explore new synthetic approaches which are more environmentally friendly. For this, we used (meth)acrylic acid and T3P® as catalyst, which avoids the use of chlorinated

reagents and thus reduces the environmental impact.[14] THGA, THGMA, CDMA and CDMMA were synthesized by using (meth)acrylic acid. The success of the reaction was confirmed by ^{1}H NMR (Figure 2.3), showing the presence of the reactive vinyl bonds. The ^{1}H NMR signals of these monomers show as follow,

THGA monomer; 6.37 (b) (dd, 1H, C***H***$_2$=CH-C=O), 6.11 (c) (s, 1H, CH$_2$=C***H***-C=O), 5.80 (a) (dd, 1H, C***H***$_2$=CH-C=O) 4.18 (d) (s, O-C***H***$_2$-CH$_2$-CH$_2$), 1.69 (k) (m, 1H, (CH$_3$)$_2$-C***H***-CH$_2$), 1.50 (e) (m, 2H, CH-C***H***$_2$-CH$_2$-O), 1.47 (f) (m, 1H, CH$_3$-C***H***-CH$_2$-CH$_2$), 1.28 (i) (m, 2H, CH-CH$_2$-C***H***$_2$-CH$_2$-CH), 1.14 (h, j) (m, 4H, CH-C***H***$_2$-CH$_2$-C***H***$_2$-CH), 0.91 (g) (d, 3H, C***H***$_3$-CH-CH$_2$-CH$_2$), 0.89 (l) (d, 6H, (C***H***$_3$)$_2$-CH-CH$_2$-CH$_2$).

THGMA monomer; 6.12 (a) (m, 1H, C***H***$_2$=CH-C=O), 5.56 (b) (p, 1H, C***H***$_2$=C-(CH$_3$)(C=O), 4.21 (d) (ddt, 2H, O=C-O-C***H***$_2$), 1.96 (c) (t, 3H, CH$_2$=C-C***H***$_3$), 1.73 (k) (ddt, 1H, (CH$_3$)$_2$-C***H***-CH$_2$), 1.55 (e) (m, 2H, CH-C***H***$_2$-CH$_2$-O), 1.54 (f) (m, 1H, CH$_3$-C***H***-CH$_2$), 1.31 (i) (m, 2H,CH$_2$-C***H***$_2$-CH$_2$-CH), 1.18 (h) (m, 2H, C***H***$_2$-CH$_2$-CH$_2$-CH), 1.18 (J) (m, 2H, CH$_2$-CH$_2$-C***H***$_2$-CH), 0.92 (g) (dd, 3H, C***H***$_3$-CH-CH$_2$-CH$_2$), 0.91 (l) (dd, 6H, (C***H***$_3$)$_2$-CH-CH$_2$-CH$_2$).

CDMA monomer; 6.36 (a) (dd, 1H, O=C-CH=C***H***$_2$), 6.09 (c) (ddd, 1H, O=C-C***H***=CH$_2$), 5.8 (b) (dd, 1H, O=C-CH=C***H***$_2$), 4.74 (d) (m, 1H, C***H***-O-C=O), 1.64 (f) (m,

1H, C***H***-CH-O-C=O), 1.44-1.33 (h,k,m) (m, 4H, C***H***$_2$-C***H***$_2$-C***H***$_2$-CH(C***H***$_2$-C)-CH-O-C=O), 1.18 (d, 4H (e,i), C***H***$_2$-CH$_2$-CH-CH(C***H***$_3$)-O-C=O), 1.05 (g,j) (m, 2H, C***H***2-CH$_2$-C***H***$_2$-CH-CH(CH$_3$)-O-C=O), 0.9 (l) (m, 1H, CH(C***H***$_2$-C)-CH-O-C=O), 0.85 (m, 6H (n), C(C***H***$_3$)$_2$)

CDMMA monomer; 6.1 (a) (s,1H, O=C-C(CH$_3$)=C***H***$_2$), 5.5 (b) (s,1H, O=C-C(CH$_3$)=C***H***$_2$), 4.7 (d) (m, 1H, C***H***-O-C=O), 1.95 (c,f) (s, 4H, C***H***-CH-O-C-C(C***H***$_3$)), 1.5 (h, k, m) (m, 4H, C***H***$_2$-C***H***$_2$-C***H***$_2$-CH(C***H***$_2$-C)-CH-O-C=O), 1.2 (e, i) (m, 4H, C***H***$_2$-CH$_2$-CH-CH(C***H***$_3$)-O-C=O), 1.05 (j, g) (m, 2H, C***H***$_2$-CH$_2$-C***H***$_2$-CH-CH(CH$_3$)-O-C=O), 0.95 (l) (s, 1H, CH(C***H***$_2$-C)-CH-O-C=O), 0.9 (n) (s, 6H, C(C***H***$_3$)$_2$).

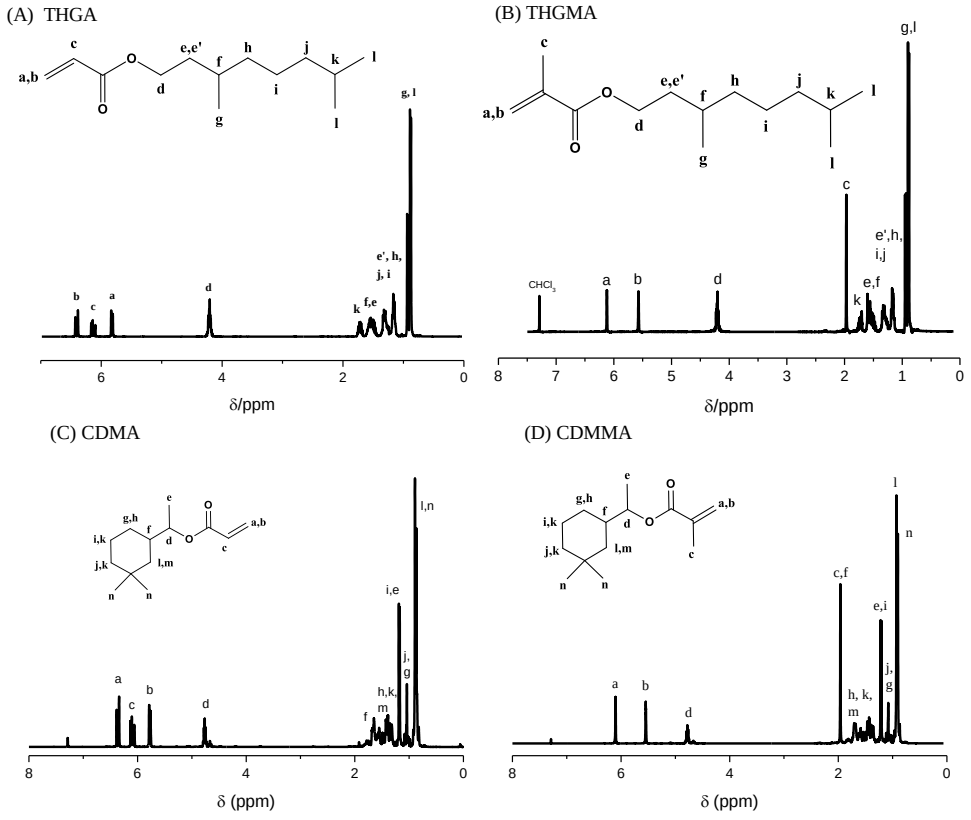

Figure 2.3. ^{1}H NMR of the synthesized terpene monomers by (meth)acrylic acid.

The yield of the final product is presented in Table 2.1. It can be seen that high yield of terpene methacrylates (THGMA and CDMA) was achieved, while moderate yield of terpene acrylates was obtained.

Table 2.1. The % yield of terpene monomers.

Monomer	Yield (%)
Tetrahydrogeraniol acrylate (by acryloyl chloride)	85
Tetrahydrogeraniol acrylate (by acrylic acid)	60
Tetrahydrogeranilol methacrylate (by methacrylic acid)	85
Cyclademol acrylate (by acrylic acid)	65
Cyclademol methacrylate (by methacrylic acid)	82

2.4. Conclusions

The (meth)acrylate moieties capable of undergoing by free radical polymerization were successfully incorporated into the terpene derivatives (tetrahydrogeraniol (THG) and cyclademol (CDM)) by following two different approaches, esterification with acryloyl chloride and with (meth)acrylic acids. THGA, THGMA, CDMA and CDMMA were successfully synthesized by esterification with (meth)acrylic acid, which is greener than the acryloyl method. Furthermore, the presence of the reactive vinyl bond was confirmed by ^{1}H NMR spectroscopy. High

yield for methacrylate terpenes (~ 82 %) and relatively moderate yields for acrylate functionality (~ 60 %) were obtained. The biosourced-based monomers synthesized in this chapter were utilized throughout this thesis.

2.5. References

(1). Ramos, A. M.; Lobo, L. S.; Bordado, J. M. Polymers from pine gum components: Radical and coordination homo and copolymerization of pinenes. *Macromol. Symp.* **1998,** 127, 43-50.

(2). Roberts, W. J.; Day, A. R. A Study of the Polymerization of α- and β-Pinene with Friedel—Crafts Type Catalysts. *J. Am. Chem. Soc.* **1950,** 72, 1226-1230.

(3). Jiang, L.; Masami, K.; Mitsuo, S.; Toshinobu, H.; Yun-Xiang, D. Cationic polymerization of β-pinene with the AlCl3/SbCl3 binary catalyst: Comparison with α-pinene polymerization. *J. Appl. Polym. Sci.* **1996,** 61, 1011-1016.

(4). Martinez, F. Cationic polymerization of β-pinene. *J Polym Sci A Polym Chem* **1984,** 22, 673-677.

(5). Keszler, B.; Kennedy, J. P., Synthesis of high molecular weight poly (β-pinene). In *Macromolecules: Synthesis, Order and Advanced Properties*, Springer Berlin, Heidelberg, 1992; pp 1-9.

(6). Yu, P.; Li, A. L.; Liang, H.; Lu, J. Polymerization of β-pinene with Schiff-base nickel complexes catalyst: Synthesis of relatively high molecular weight poly(β-pinene) at high temperature with high productivity. *J Polym Sci Part A: Polym Chem.* **2007,** 45, 3739-3746.

(7). Satoh, K.; Sugiyama, H.; Kamigaito, M. Biomass-derived heat-resistant alicyclic hydrocarbon polymers: poly(terpenes) and their hydrogenated derivatives. *Green Chem.* **2006,** 8, 878-882.

(8). Yadav, S.; Srivastava, A. K. Synthesis of Functional and Alternating Copolymer of α-Terpineol with Butylmethacrylate. *Polym Plast Technol Eng.* **2004,** 43, 1229-1243.

(9). Yadav, S.; Srivastava, A. K. Copolymerization of α-terpineol with styrene: Synthesis and characterization. *J Polym Sci Part A: Polym Chem.* **2003,** 41, 1700-1707.

(10). Li, A. L.; Wang, Y.; Liang, H.; Lu, J. Controlled radical copolymerization of β-pinene and acrylonitrile. *J Polym Sci Part A: Polym Chem.* **2006,** 44, 2376-2387.

(11). Trumbo, D. L. Free radical copolymerization behavior of myrcene. *Polym. Bull.* **1993,** 31, 629-636.

(12). Sharma, S.; Srivastava, A. K. Synthesis and characterization of a terpolymer of limonene, styrene, and methyl methacrylate via a free-radical route. *J. Appl. Polym. Sci.* **2004,** 91, 2343-2347.

(13). Wilbon, P. A.; Chu, F.; Tang, C. Progress in Renewable Polymers from Natural Terpenes, Terpenoids, and Rosin. *Macromol. Rapid Commun.* **2013,** 34, 8-37.

(14). Sainz, M. F.; Souto, J. A.; Regentova, D.; Johansson, M. K. G.; Timhagen, S. T.; Irvine, D. J.; Buijsen, P.; Koning, C. E.; Stockman, R. A.; Howdle, S. M. A facile and green route to terpene derived acrylate and methacrylate monomers and simple free radical polymerisation to yield new renewable polymers and coatings. *Polym. Chem.* **2016,** 7, 2882-2887.

Chapter 3. Renewable terpene derivative as a bio-sourced elastomeric building block in the design of functional acrylic copolymers

3.1. Introduction

The studies reported in literature aimed at obtaining polymers based on terpenes are discussed in Chapter 1 and the reader is referred to that chapter.

This chapter explores the possibility of synthesizing thermoplastic elastomers partially based on terpenes. The "soft" segment was formed by tetrahydrogeraniol acrylate (THGA) synthesized in Chapter 2. This monomer has a branched acyclic ten carbon structure that mimics petroleum-based soft monomer such as *n*-butyl acrylate and 2-ethylhexyl acrylate. The long branched structure promotes low glass transition temperatures (T_g ~ - 46 °C).

THGA was first polymerized by free radical polymerization in bulk and solution at 80 °C, yielding molar masses up to $\bar{M}_n$ = 278,000 g.mol^{-1} and monomer conversions up to 99 %. THGA was also polymerized in the presence of a bi-functional RAFT agent S,S´-dibenzyl trithiocarbonate (DBTTC). Degrees of polymerization ranging from *DP*n 25 to 500 were targeted. Finally, the retention of reactive chain ends was exploited to yield a soft/hard/soft triblock copolymer poly(THGA)-*b*-poly(styrene)-*b*-poly(THGA). This soft/hard/soft triblock copolymer was further analyzed by thermal analysis and AFM imaging, thus highlighting a phase separation between soft and hard phases.

3.2. Experimental

3.2.1. Materials

The materials are given in Appendix **I**

3.2.2. Synthesis procedures

3.2.2.1 Free radical polymerization of THGA

The free radical polymerization of THGA was performed at various monomer concentrations in toluene, $[M]_0$ = 0.6, 1.8, 3.6 mol.L^{-1} and in bulk (Table 3.1, entries 1-4). In the experiments, 2.50 g of THGA (1.18 x 10^{-2} mol) and the amount of toluene needed to obtain the desired monomer concentration were placed into a 25 mL RBF equipped with rubber seals and a magnetic stirring bar. The mixture was deoxygenated for 30 minutes with purging nitrogen and subsequently placed into an oil bath at 80 °C. Then, AIBN (AIBN/THGA about 1.94 x 10^{-3} mol/mol) dissolved in a small amount of toluene was added as a shot *via* a deoxygenated syringe to initiate the polymerization. Polymerization was carried out under stirring for 7 hours at 80 °C and samples were carefully taken via a deoxygenated syringe.

3.2.2.2. RAFT polymerization of THGA

The RAFT polymerization of THGA was also performed at various monomer concentrations in toluene, $[M]_0$ = 0.6, 1.8, 3.6 mol.L^{-1} and in bulk; using a ratio $[DBTTC]_0/[I]_0$ = 2 and maintaining constant the degree of polymerization targeted (DPn = 250) (Table 3.1 entries 5-8). In addition, for a degree of polymerization of 250, $[DBTTC]_0/[I]_0$ = 10 was used (entries 9 to 12). The $[M]_0/[DBTTC]_0$ ratios were varied to target DP_ns of 25, 50, 100, 250 and 500 (Table 3.1, entries 11 and 13 to 16).

$[DBTTC]_0/[I]_0$ = 10 was used in these experiments except for entry 15 aiming at *DP*n = 25, where $[DBTTC]_0/[I]_0$ = 20 was used to limit termination.

Typically, THGA (2.50 g, 1.18 x 10^{-2} mol), the required amount of DBTTC and toluene (16 g) were placed into a 25 mL round bottom flask equipped with rubber seals and a magnetic stirring bar. The mixture was deoxygenated for 30 minutes with purging nitrogen and subsequently placed in an oil bath at 80 °C. Then a solution of AIBN (0.75 mg, 4.56 x 10^{-6} mol) dissolved in a small amount of toluene was added as a shot to initiate the polymerization. The system was allowed to polymerize under stirring for 6 hours at 80 °C and samples were carefully taken via a deoxygenated syringe. The polymer solution was quenched by cooling and contact to air, precipitated three times in methanol and dried under vacuum to yield the purified polymer as a white powder.

Table 3.1. Reaction conditions for the polymerizations of THGA

Entry	$[M]_0$ ($mol.L^{-1}$)	$[DBTTC]_0$ ($mol.L^{-1}$)	$[I_2]_0$ ($mol.L^{-1}$)	$[DBTTC]_0/[I]_0$
1	0.6	-	1.23×10^{-3}	-
2	1.8	-	3.50×10^{-3}	-
3	3.6	-	6.88×10^{-3}	-
4	bulk	-	9.45×10^{-3}	-
5	0.6	2.47×10^{-3}	1.23×10^{-3}	2
6	1.8	7.03×10^{-3}	3.50×10^{-3}	2
7	3.6	1.38×10^{-2}	6.89×10^{-3}	2
8	Bulk	1.89×10^{-2}	9.45×10^{-3}	2
9	0.6	2.31×10^{-3}	4.56×10^{-6}	10
10	1.8	7.12×10^{-3}	4.56×10^{-6}	10
11	3.6	1.40×10^{-2}	4.56×10^{-6}	10
12	Bulk	1.88×10^{-2}	4.56×10^{-6}	10
13	3.6	3.62×10^{-2}	1.12×10^{-5}	10
14	3.6	7.03×10^{-2}	2.28×10^{-5}	10
15	3.6	1.42×10^{-1}	2.28×10^{-5}	20

16	3.6	7.17×10^{-3}	2.30×10^{-6}	10

3.2.2.3. Chain extension of poly(THGA) to yield a soft/hard/soft triblock copolymer

A poly(THGA) based macro-RAFT agent was previously prepared in solution [M]0 = 3.6 mol.L-1, $[DBTTC]_0/[AIBN]_0$ = 10, $[M]_0/[DBTTC]_0$ = 98 and the polymerization stopped at 95 % conversion. The mixture was purified by precipitation in methanol to yield a polymer with M_n = 19,000 g.mol^{-1}, $Đ$ = 1.07. The macro RAFT-agent was subsequently placed in a 25 mL RBF equipped with a rubber seal and a magnetic stirring bar in the presence of styrene (10 g, 1.9 x 10^{-2} mol, $[St]_0/[macro\text{-}CTA]_0$ = 500). The mixture was deoxygenated for 30 minutes with purging nitrogen and subsequently placed into an oil bath at 80 °C. Then, a solution of AIBN (2.8 mg, 1.7 x 10^{-5} mol) dissolved in a small amount of toluene was added as a shot via a deoxygenated syringe to initiate the polymerization. Polymerization was left to stir for 8 hours at 80 °C to reach 89 % conversion. The polymer solution was quenched by cooling and contact to air, precipitated three times in methanol and dried under vacuum to yield the purified triblock copolymer (M_n = 68 000 g.mol^{-1}, $Đ$ = 1.15).

3.2.2.4. Chain extension of poly(styrene) to yield an hard/soft/hard triblock copolymer

A poly(styrene) based macro-RAFT agent was prepared in solution $[M]_0$ = 3.6 mol.L-1, $[DBTTC]_0/[AIBN]_0$ = 10, $[M]_0/[DBTTC]_0$ = 97 and stopped at 92 % conversion. The mixture was purified by precipitation in methanol to yield a polymer with M_n = 8,600 g.mol^{-1}, $Đ$ = 1.15. The macro RAFT-agent was subsequently placed in a 25 mL RBF equipped with a rubber seal and a magnetic stirring bar in the presence of THGA (5 g, 2.3 x 10^{-2} mol, $[THGA]_0/[macro\text{-}CTA]_0$ = 503). The mixture was deoxygenated for 30 minutes with purging nitrogen and subsequently placed into an oil bath at 80 °C. Then, a solution of AIBN (0.76 mg, 4.6 x 10^{-6} mol) dissolved in a small amount of toluene was added as a shot *via* a deoxygenated syringe to initiate the polymerization. Polymerization was left to stir for 8 hours at 80 °C to reach 90 % conversion. The polymer solution was quenched by cooling and contact to air, precipitated three times in methanol and dried under vacuum to yield the purified triblock copolymer (M_n = 98,500 g.mol^{-1}, $Đ$ = 1.3)

3.2.3. Characterization

Monomer conversion was calculated from ^{1}H NMR ($CDCl_3$, 400 MHz), the information is given in Appendix **I**.

The theoretical molar masses were calculated using equations 1 and 2, the information is given in Appendix **I**.

3.3. Results and discussion

3.3.1. Free radical polymerization of THGA in bulk and solution

The bio-sourced based monomer THGA synthesized in Chapter 2 was first polymerized by radical polymerization in the presence of AIBN at 80 °C ($[M]_0/[I_2]_0$ = 516) (Scheme 1). Various monomer concentrations $[M]_0$ were tested, ranging from 0.6 $mol.L^{-1}$ in toluene to bulk. The results are presented in Table 3.2.

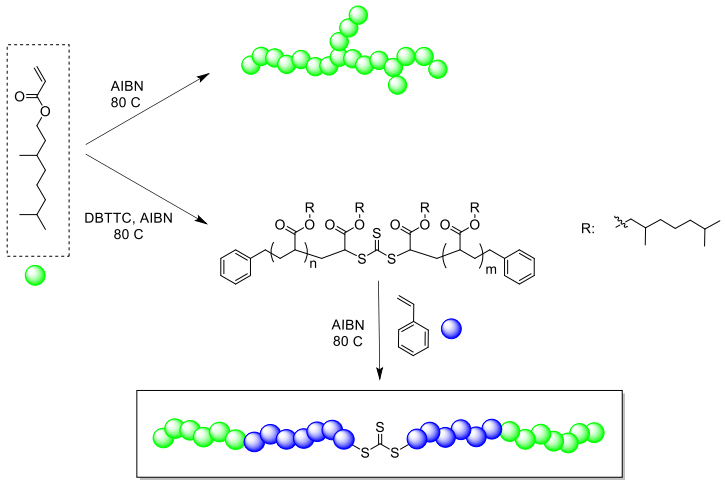

Scheme 3.1. Reaction scheme to yield poly(THGA) and ABA triblock copolymer poly(THGA)-*b*-poly(styrene)-*b*- poly(THGA) from tetrahydrogeraniol.

Table 3.2. Reaction conditions and resulting monomer conversion and molar masses for the free radical polymerization of THGA at 80 °C.

Entry	$[M]_0$ (mol.L^{-1})	$[I_2]_0$ (mol.L^{-1})	$[M]_0/[I_2]_0$	Conv. (%)[a]	$\bar{M}_n$ Exp (g.mol^{-1})[b]	$Đ$
1	0.6	1.23×10^{-3}	516	67	16 200	2.5
2	1.8	3.50×10^{-3}	516	80	47 100	2.5
3	3.6	6.88×10^{-3}	516	92	69 300	2.8
4	bulk	9.45×10^{-3}	516	99	278 000	2.4

[a] Calculated from ^{1}H NMR. [b] Extracted from SEC-MALS analysis using the measured *dn/dc* value for poly(THGA) (*dn/dc* = 0.0678 mL.g^{-1}).

Table 3.2 and Figure 3.1 show that high monomer conversions could be reached. As the monomer to initiator ratio was fixed, increasing the initial monomer concentration resulted in an increase in conversion with near complete monomer conversion achieved in 3 hours for the reaction in bulk. The molecular weight was observed to increase for increasing concentration of the monomer in the reaction medium. The increase in molecular weight with increased monomer concentration is likely an effect of the increased tendency for intermolecular chain transfer reactions at reduced monomer concentrations. It should be noted that unlike what is observed in the polymerization of most acrylic monomers no gel formation was observed for the reaction in bulk.[1]

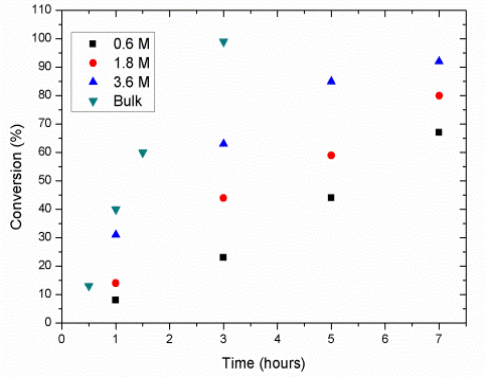

Figure 3.1. Evolution of the monomer conversion as a function of time during the free radical polymerization of terpene acrylate at 80 °C in toluene $[M]_0/[I_2]_0$ = 516. (Squares) $[M]_0$ = 0.6 mol.L^{-1}. (Circles) $[M]_0$ = 1.8 mol.L^{-1}. (Up triangles) $[M]_0$ = 3.6 mol.L^{-1}. (Down triangles) Bulk.

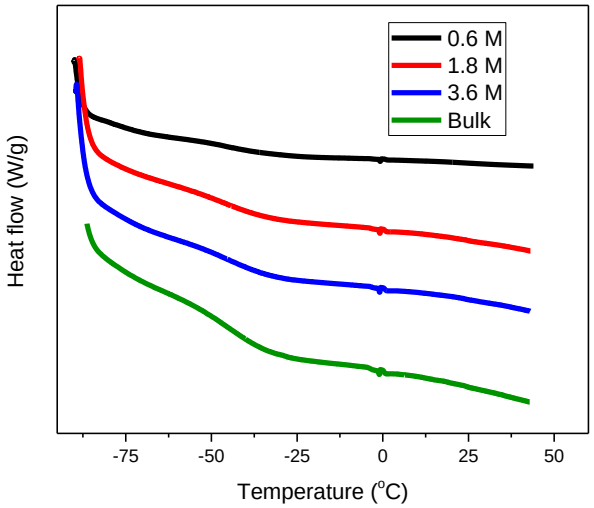

Figure 3.2. DSC thermogram of poly(THGA) homopolymers synthesized by free radical polymerization at different monomer concentrations.

Figure 3.2 presents the DSC thermograms of the homopolymers. All samples showed a glass transition temperature at T_g ~ - 46 °C. The changes in molar mass from $\bar{M}_n$ = 16,200 g.mol^{-1} to $\bar{M}_n$ = 278,000 g.mol^{-1} did not significantly influence the value of T_g. Hence, THGA could potentially be utilized as a substitute for other widely used petroleum based acrylics such as ethyl acrylate (T_g = -20 ˚C), butyl acrylate (T_g = -54 °C) or 2-ethylhexyl acrylate (T_g = -85 °C).[2]

3.3.2. RAFT polymerization of THGA in solution

3.3.2.1. The influence of the $[\text{RAFT agent}]_0/[I_2]_0$ ratio

The promising results obtained in free radical polymerization prompted us to aim for more functional polymer materials, such as block copolymers. In order to do so, RAFT polymerization was employed using the commercially available bi-functional S,S´-dibenzyl trithiocarbonate (DBTTC) to mediate the polymerization of THGA at 80 °C. Various monomer concentrations were tested, ranging from 0.6 $mol.L^{-1}$ to bulk, whilst keeping $[DBTTC]_0/[I_2]_0$ = 2 and 10 and targeting the same degree of polymerization $DP_n = [M]_0/[DBTTC]_0$ = 250. The reaction conditions and resulting monomer conversions and molar masses are summarized in Table 3.3, entries 5 to 12.

Table 3.3. Reaction conditions and resulting monomer conversion and molar masses for the RAFT polymerization of THGA at 80 °C.

Entry	$[M]_0$ (mol.L^{-1})	$[M]_0$/ $[DBTTC]_0$	$[DBTTC]_0$/ $[I_2]_0$	Conv. (%)[a]	$\bar{M}_n$ Theor (g.mol^{-1})[b]	$\bar{M}_n$ Exp (g.mol^{-1})[c]	$Đ$
5	0.6	250	2	33	16 800	18 300	1.9
6	1.8	250	2	75	37 800	27 300	1.9
7	3.6	250	2	92	46 400	36 000	1.2
8	Bulk	250	2	97	48 600	35 000	1.8
9	0.6	250	10	51	26 000	22 000	1.1
10	1.8	250	10	91	45 500	39 600	1.2
11	3.6	250	10	94	47 100	50 000	1.1
12	Bulk	250	10	95	47 600	46 200	1.1
13	3.6	100	10	96	19 200	22 300	1.1
14	3.6	50	10	94	9 700	12 000	1.1
15	3.6	25	20	94[d]	5 200	5 700	1.2
16	3.6	500	10	95[e]	93 200	96 500	1.2

[a] After 6 hours of polymerization, calculated from ^{1}H NMR. [b] Calculated using the monomer conversions; initial concentrations $[M]_0$, $[DBTTC]_0$, $[I_2]_0$; $f = 0.5$; $f_C = 1$ and the value of $k_{D\ AIBN}$ at 80 °C (see supporting information for details). [c] Extracted from SEC-MALS analysis using the measured *dn/dc* value for poly(THGA) (*dn/dc* = 0.0678 mL.g^{-1}). [d] After 8 hours of polymerization. [e] After 4 hours of polymerization

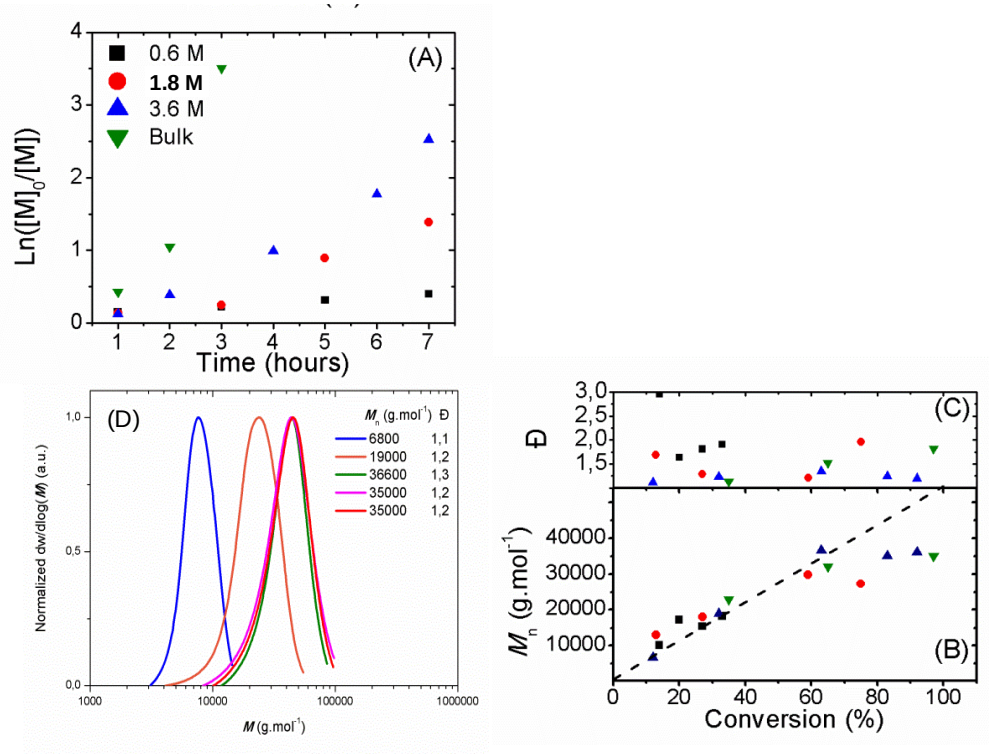

Figure 3.3 Kinetics of the RAFT polymerization of terpene acrylate at 80 °C in toluene at various monomer concentrations (Squares) $[M]_0$ = 0.6 mol.L^{-1}; (Circles) $[M]_0$ = 1.8 mol.L^{-1}; (Up triangles) $[M]_0$ = 3.6 mol.L^{-1}; (Down triangles) bulk (entries 5-8 in Table 3.3). The DP_n = $[M]_0/[CTA]_0$ ratio is kept at DP_n = 250. (A) Evolution of the ln($[M]_0/[M]$) as a function of time. (B) Evolution of the measured molar masses as a function of monomer conversions; the dash line is a guide for the eye. (C) Evolution of the dispersity values as a function of monomer conversion. (D) Molar mass distributions of poly(terpene acrylate) prepared by RAFT polymerization at 80 °C ($[M]_0$ = 3.6 mol.L^{-1}, DP_n = 250) at various monomer conversions.

Similar to the free radical polymerizations, higher initial monomer concentration $[M]_0$ resulted in higher rate of polymerization (see Table 3.2). In the case of $[DBTTC]_0/[I_2]_0 = 2$, the monomodal molar mass distribution (MMD) could be obtained with relatively high dispersity values at low monomer concentration. In addition, for high conversions the experimental molar masses were lower than the theoretical ones showing that the number of polymer chains was not determined by the RAFT agent. (Figure 3.3). This was attributed to the low $[DBTTC]_0/[I_2]_0$ ratio used in these experiments. Better control was achieved when the ratio was increased ($[DBTTC]_0/[I_2]_0 = 10$). At all monomer concentrations, relatively low dispersity values ($Đ \sim 1.2$) were obtained(see Table 3.3 and Figure 3.4). However, in the case of 0.6 and 1.8 $mol.L^{-1}$, the experimental molar masses were lower than the predicted values (Table 3.3 and Figure 3.4B). This discrepancy cannot be attributed to errors in the calculation of the theoretical molar masses, as the non-negligible presence of initiator-derived chains were taken into account due to the low $[DBTTC]_0/[I_2]_0$ ratio. Moreover, errors in the SEC measurement cannot be of fault, as the $\overline{M}_n$s were determined by a combination of refractive index and light scattering (MALS) detection using the measured *dn/dc* value for poly(terpene acrylate) (*dn/dc* = 0.0678 $mL.g^{-1}$). Consequently, it is important to look deeper into the unusual evolution of molecular weight displayed in Figure 3.4B.

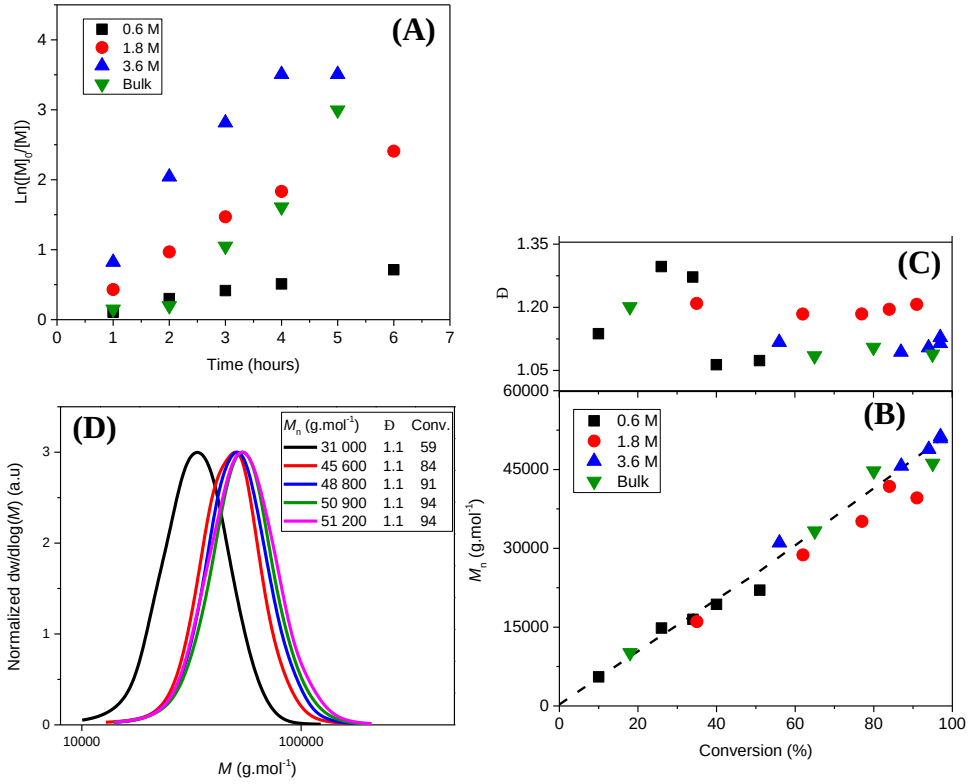

Figure 3.4. Kinetics of the RAFT polymerization of terpene acrylate at 80 °C in toluene at various monomer concentrations (Squares) $[M]_0$ = 0.6 mol.L^{-1}; (Circles) $[M]_0$ = 1.8 mol.L^{-1}; (Up triangles) $[M]_0$ = 3.6 mol.L^{-1}; (Down triangles) bulk (entries 9-12 in Table 3.3). The DP_n = $[M]_0/[DBTTC]_0$ ratio is kept at DP_n = 250. (A) Evolution of the ln($[M]_0/[M]$) as a function of time. (B) Evolution of the measured molar masses as a function of monomer conversions; the dash line is a guide for the eye. (C) Evolution of the dispersity values as a function of monomer conversion. (D) Molar mass distributions (from SEC-MALS) of poly(terpene acrylate) prepared by RAFT polymerization at 80 °C ($[M]_0$ = 3.6 mol.L^{-1}, DP_n = 250) at various monomer conversions.

In Figure 3.4B it can be seen that the evolution of $\bar{M}_n$ as a function of monomer conversion at low monomer concentration (0.6 and 1.8 mol.L^{-1}) deviates from linearity at higher conversions, while at higher monomer concentrations molar mass evolves linearly throughout the whole conversion range. This might be due to the occurrence of undesired chain transfer to solvent reactions, as well as chain transfer to polymer reactions which introduces the presence of mid-chain radical (MCRs). Both intramolecular (also referred to as backbiting) and intermolecular chain transfer reactions are relatively common in acrylic polymerization, with intramolecular transfer being the predominant pathway.[1, 3, 4] The presence of MCRs in the polymer chains can yield the formation of branches and/or the formation of macromonomers (bearing ω-vinyl functionalities) and initiating radicals through β-scission, although both reactions typically only begin to become significant at high temperatures.[1, 5-7] The presence of branching has relatively limited effect on the molecular weight distribution, but β-scission creates new chains leading to both a decrease in $\bar{M}_n$ as well as a broadening of the dispersity.[8, 9] It has previously been shown that this leads to a dramatic decrease in $\bar{M}_n$ at high conversions as it is observed for the reaction in Figure 3.4B.[8, 9]

In order to determine if this effect is indeed important in the polymerization of THGA at lower monomer concentrations, the presence of intramolecular transfer to

polymer reactions was checked by NMR though the presence of quartenary carbons (***C***$_q$) by ^{13}C NMR and the presence of macromonomer formation in ^{1}H NMR. An example for the reaction of THGA at 80 °C with $[M]_0$ = 1.8 mol.L^{-1} (entry 9) is shown in Figure 3.5. It can be observed that the branching content at 91 % conversion was around 2.70 %. It should be noted that this branching content is significantly higher than that expected for typical acrylic monomers at similar temperatures.[2, 10,58] For example at this reaction temperature and conversion, *n*-butyl acrylate would be expected to have a degree of branching of less than 1 %.[11]

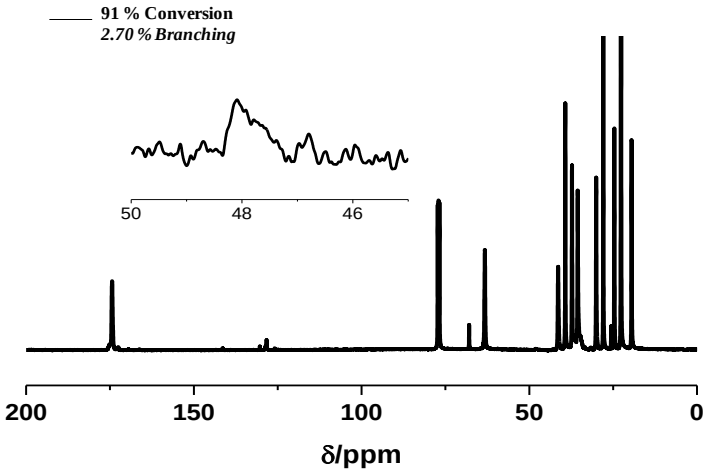

Figure 3.5. Quantitative ^{13}C NMR ($CDCl_3$, 125 MHz) of a poly(THGA) prepared by RAFT polymerization at 80 °C in toluene (entry 6 in Table 3.3). $[M]_0$ = 1.8 mol.L^{-1}, $[M]_0/[DBTTC]_0$ = 250 and $[DBTTC]_0/[I_2]_0$ = 10. Spectra recorded at 91 % monomer conversion.

Moreover, the presence of unsaturated carbon from the β-scission formation is confirmed by ^{1}H NMR (Figure 3.6), with a percentage of macromonomers of 0.12 % at 91 % conversion. The effect that this concentration of macromonomer can have on the evolution of $\overline{M}_n$ can be determined by estimating the number of chains generated by β-scission relative to that of the RAFT agent. In this way, the theoretical DP_n at 91% conversion based only of RAFT agent derived chains is 228 (≈48,000 g.mol^{-1}), but taking into account the effects of β-scission this decreases to 179 (≈38,000 g.mol^{-1}), which is in rough agreement with the experimentally determined molar mass (see Table 3.3). It should be noted that, in agreement with previous work which has suggested that under conditions of RDRP the amount of branching is significantly reduced,[12] in the absence of chain transfer agent, the % branching and β-scission are relatively higher (% branching = 3.06 and β-scission = 0.57) (Figure 3.7).

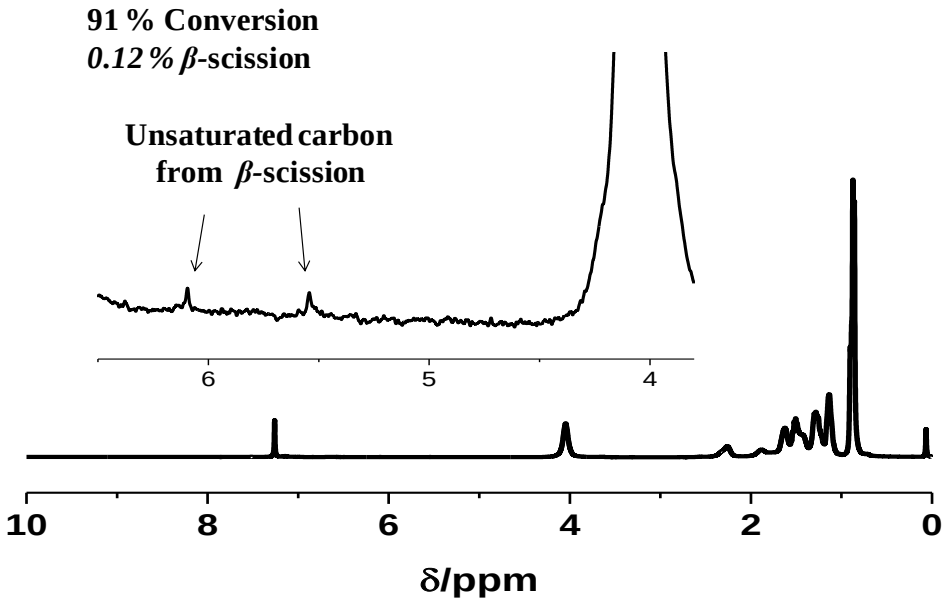

Figure 3.6. ^{1}H NMR ($CDCl_3$, 400 MHz) of poly(THGA) prepared by RAFT polymerization at 80 °C in toluene (entry 6 in Table 2), $[M]_0$ = 1.8 mol.L^{-1} at 91 % monomer conversion.

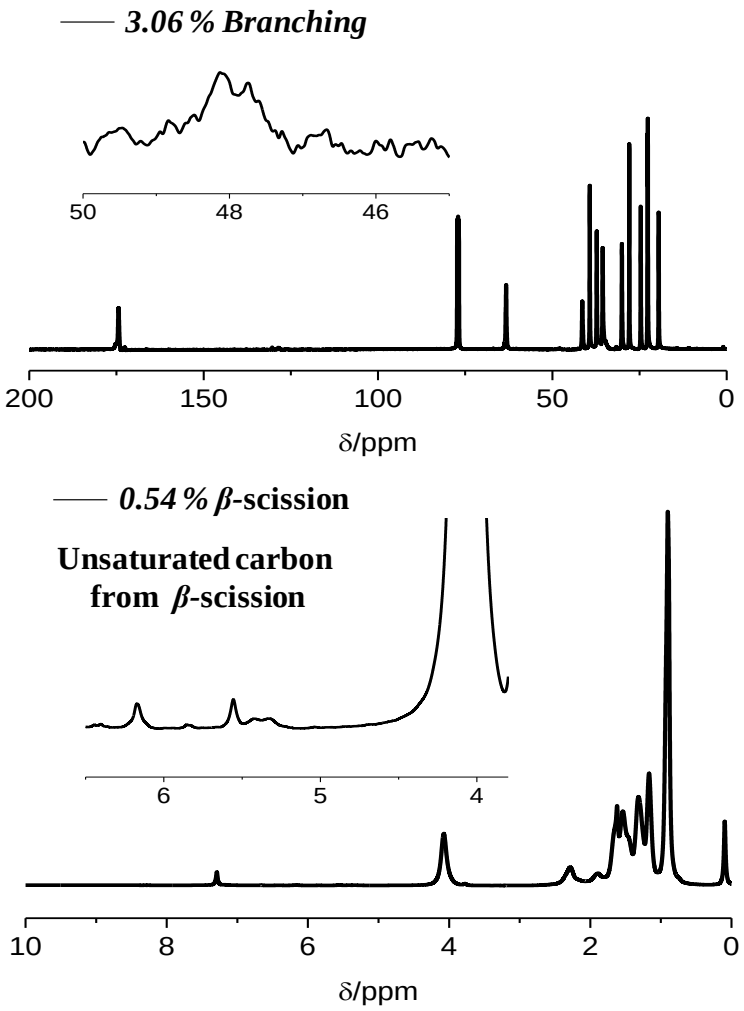

Figure 3.7. Quantitative ^{13}C (top) ($CDCl_3$, 125 MHz) and ^{1}H NMR (bottom) ($CDCl_3$, 400 MHz) of poly(THGA) prepared by free radical polymerization at 80 °C in toluene (entry 2 in Table 3.2), $[M]_0$ = 1.8 mol.L^{-1} at 80 % conversion.

3.3.2.2. The effect of targeted degree of polymerization

In order to determine the extent of control over the RAFT polymerization of the bio-sourced based monomer, polymerizations were conducted at various target DP_ns, $[M]_0/[DBTTC]_0$ = 25, 50, 100, 250 and 500. The reaction conditions, resulting monomer conversions and molar masses are summarized in Table 3.3 entries 11 and 13 to 16. In Figure 3.8A it can be observed that at lower target degree of polymerization, the rate of polymerization was significantly lower despite having high concentration of initiator. This may be attributed to some retardation caused by the RAFT process itself as has been extensively reported in literature.[13-18] More importantly, in Figures 3.8B and 3.8C, it can be seen that in all cases excellent agreement between the theoretical and experimental $\bar{M}_n$ was achieved and narrow molar mass distributions were obtained, even up to high conversion. This demonstrates that under the correct reaction conditions (high concentration of THGA), good control over the polymerization of THGA can be achieved at molar masses targeting the range 5,000-100,000 $g.mol^{-1}$.

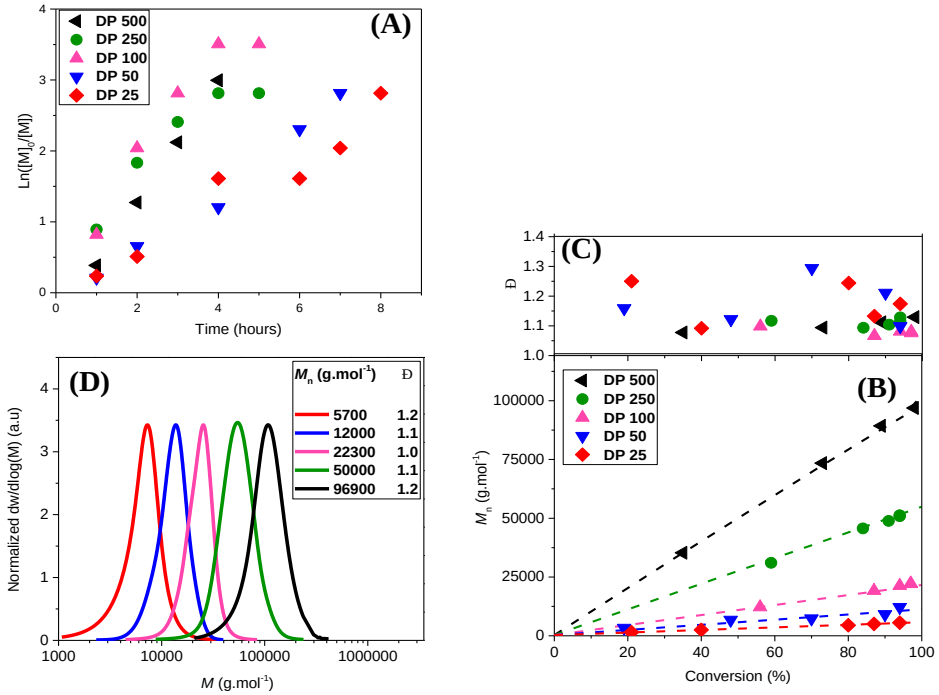

Figure 3.8. Kinetics of the RAFT polymerization of terpene acrylate at 80 °C in toluene at various DP_n = $[M]_0/[DBTTC]_0$ and $[M]_0$ = 3.6 mol.L^{-1}. (Left triangles) *DP* 500; (Circles) *DP* 250; (Up triangles) *DP* 100; (Down triangles) *DP* 50; (Diamonds) *DP* 25. (A) Evolution of the ln($[M]_0/[M]$) as a function of time. (B) Evolution of the measured molar masses as a function of monomer conversions; the dash lines are the theoretical evolution of molar masses calculated from equations 1 and 2. (C) Evolution of the dispersity values as a function of monomer conversion and (D) Molar mass distributions (from SEC-MALS) of the final sample of poly(terpene acrylate) prepared by RAFT polymerization at 80 °C ($[M]_0$ = 3.6 mol.L^{-1}) at various DP_ns (Entries 11 and 13 to 16 in Table 3.3).

3.3.2.3. Triblock copolymers

The main advantage of a RDRP process is that the retention of end group fidelity allows the preparation of block copolymers. We aimed to exploit the *"livingness"* of the RAFT polymerization of poly(THGA) to prepare a soft-hard-soft ABA triblock copolymer, using poly(styrene) as the "hard" phase (see Scheme 1 for details). To this end, a poly(THGA) macro-RAFT agent was prepared at 80 °C for 8 hours, using an initial $[M]_0$ = 3.6 mol.L^{-1}, a ratio $[DBTTC]_0/[I_2]_0$ = 10 and targeting a DP_n = $[M]_0/[DBTTC]_0$ of 98. Subsequently, a second monomer aliquot (styrene herein, [S]/[macro-RAFT] = 500) was added to the purified macro-RAFT agent in the presence of AIBN to re-initiate polymerization at 80 °C. In Figure 3.9, the success of the chain extension is evidenced by SEC, with the MMD clearly shifting to higher molar masses (89 % conversion, $\overline{M}_n$ = 68,000 g.mol^{-1}). A monomodal distribution is obtained for the ABA triblock copolymer with low dispersity value ($Đ$ = 1.15). The slight increase in dispersity value during the chain extension is primarily attributed to the polymerization of the less activated monomer styrene with an active macro-RAFT agent, which yielded to a non-optimum addition-fragmentation process.[19, 20] In addition, the broadening of the MMD might also be due to the small presence of dead chains (i.e. not bearing a trithiocarbonate group) during the formation of the macro-RAFT agent.

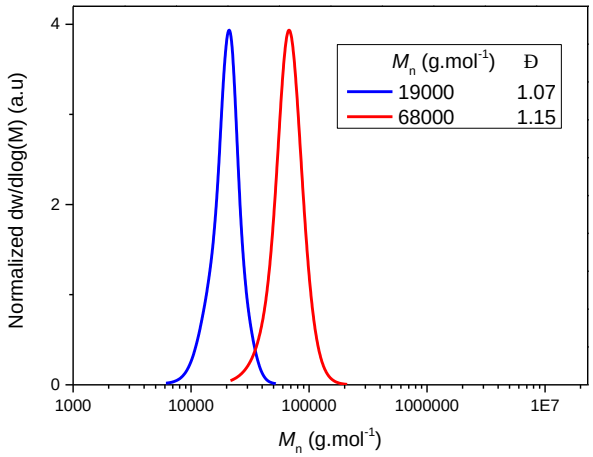

Figure 3.9. SEC traces of the chain extension of a poly(terpene acrylate) macro-RAFT agent with styrene at 80 °C.

The presence of "dead" chains in the formation of the macro-RAFT agent was investigated using a fluorescence detector in SEC. Fluorescence detection was preferred to a UV-vis detection due to the difference in *dn/dc* values between the poly(THGA) (*dn/dc* = 0.0678 mL.g^{-1}) and the poly(styrene) block (*dn/dc* = 0.19 mL.g^{-1}, λ_0 = 546 nm). A similar macro-RAFT agent was prepared through the copolymerization of fluorescein o-acrylate and with THGA at 80 ˚C for 3 h (95 % conversion, $\bar{M}_n$ = 25,600 g.mol^{-1}), with [THGA]$_0$/[fluorescein o-acrylate]$_0$ = 35, [DBTTC]$_0$/[I$_2$]$_0$ = 2 and DP_n [M]$_0$/[DBTTC]$_0$ = 100. The macro RAFT agent was then

utilized in the polymerization of styrene ($[S]_0/[\text{Macro-RAFT}]_0$ = 500, 82 % conversion, $\bar{M}_n$ = 92,000 g.mol^{-1}). In Figure 3.10, good shift towards lower retention time is evidenced with minimal termination using the fluorescence detector, thus confirming the formation of ABA triblock copolymer.

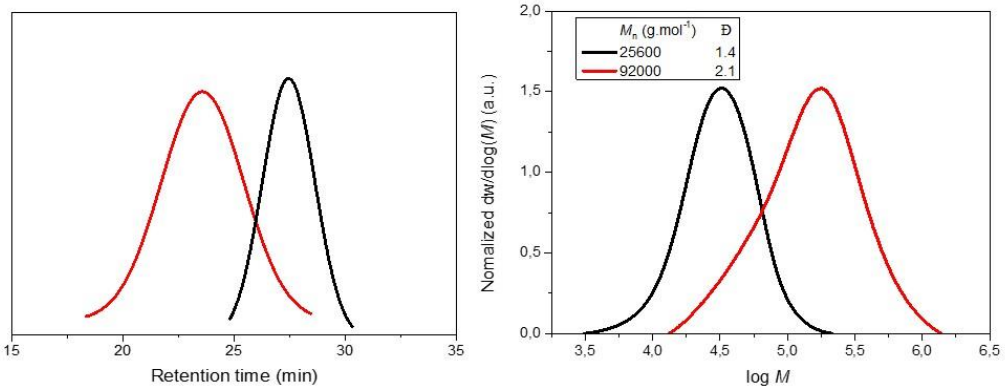

Figure 3.10. SEC traces of the chain extension of a poly(terpene acrylate)-*co*-poly(fluorescein o-acrylate) macro-RAFT agent with styrene at 80 °C. (Left) Fluorescence detection, λ = 350 nm. (Right) DRI detection.

Using the values of monomer conversions for each monomer (i.e. THGA and styrene) and the DP_n targeted, it is possible to calculate the composition of the triblock copolymer. Herein, the poly(THGA)-*b*-poly(styrene)-*b*-poly(THGA) is composed of 36 *wt*.% of poly(THGA) and 64 *wt*.% of poly(styrene). The segregation between the

soft and hard phases, poly(THGA) and poly(styrene) respectively, was evidenced by AFM. In Figure 3.11A, the phase separated morphology is shown for the soft-hard-soft triblock copolymer, with the darkest domains corresponding to the soft phase and the lighter domains to the hard phase. More specifically, the poly(THGA) phase is dispersed in poly(styrene) in a lamellae transition, in line with the theoretical predictions. The observation of the soft and hard phases is further highlighted through an analysis of the rheological behavior of the triblock copolymer. In Figure 3.11B, the presence of the two glass transition temperatures is observed (-22 °C and 110 °C for the soft and hard phase respectively).

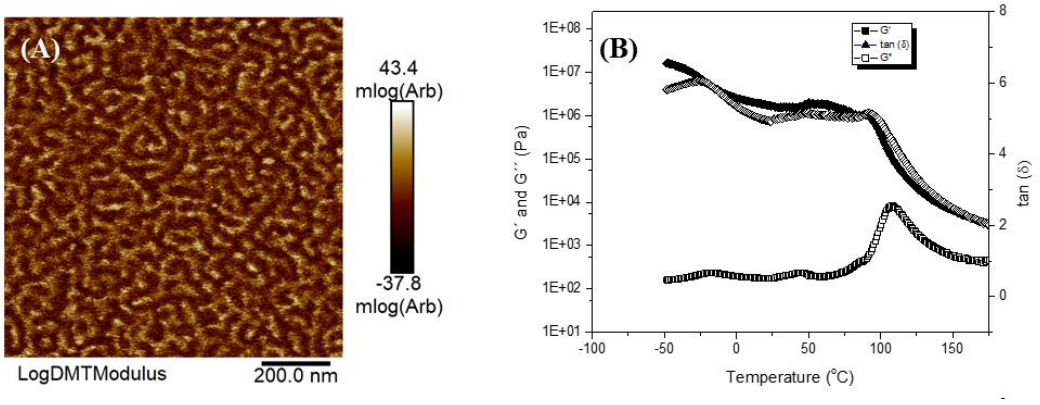

Figure 3.11. (A) AFM picture of a poly(THGA)-*b*-poly(styrene-*b*-poly(THGA) ABA triblock copolymer (LogDMT modulus with scale bar = 200 nm). (B) G´ (filled squares), G´´ (squares) and tan δ (filled triangles) as a function of the temperature of a PTHGA-*b*-PS-*b*-PTHGA ABA triblock copolymer.

However, the soft-hard-soft configuration of the triblock copolymer might not be desired for the formation of thermoplastic elastomers (TPEs). Hence, a hard-soft-hard triblock copolymer was prepared utilizing a poly(styrene) macro-RAFT agent ($[Styrene]_0$ / $[DBTTC]_0$ = 97, $[BBTTC]_0$ / $[AIBN]_0$ = 10 at 80 C; 92 % conversion, with M_n = 8,600 g.mol^{-1} and $Đ$ = 1.15). The good chain end fidelity was exploited to yield a well-defined poly(styrene)-*b*-poly(THGA)-*b*-poly(styrene) triblock copolymer ([THGA]/[macro-CTA] = 503, reaching 90 % monomer conversion), with M_n = 98,500 g.mol^{-1} and low dispersity value ($Đ$ = 1.3, Figure 3.12A). This copolymer was composed of 75 *wt.*% of the soft poly(THGA) phase and of 25 *wt.*% of the hard poly(styrene) phase. In Figure 3.12B, the separation of the two phases in a cylindrical transition is evidenced by AFM, which is in sharp contrast compared to that of the PTHGA-*b*-PS-*b*-PTHGA triblock copolymer. The presence of the two domains is confirmed through rheology, with the appearance of the T_gs of the soft and hard phases at –30 °C and 102 °C respectively (Figure 3.12D). The facile preparation of those well-defined soft-hard-soft and hard-soft-hard triblock copolymers ($Đ$ < 1.3) demonstrate that THGA could be a potential substitute to petroleum-based monomers (e.g. 2-EHA) for the formation of thermoplastic elastomers.

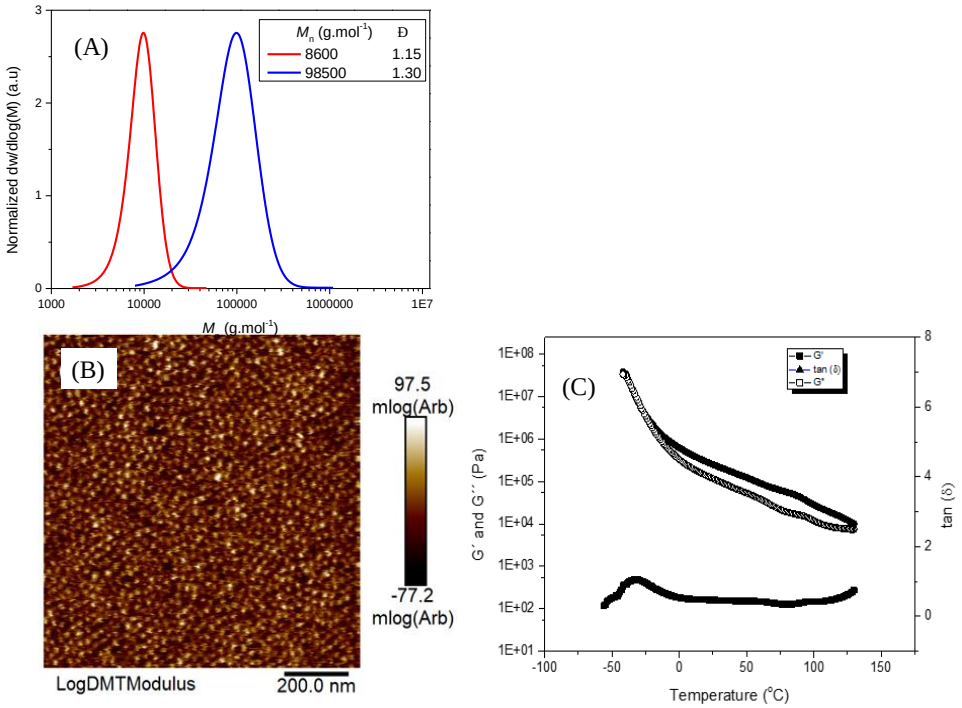

Figure 3.12. (A) SEC traces of the chain extension of a poly(styrene) macro-RAFT agent with THGA. (B) AFM picture of a poly(styrene)-*b*-poly(THGA)-*b*-poly(styrene) ABA triblock copolymer (LogDMT modulus with scale bar = 200 nm). (C) G´ (filled squares), G´´ (squares) and tan δ (filled triangles) as a function of the temperature of a PS-*b*-PTHGA-*b*-PS ABA triblock copolymer.

3.4. Conclusions

The bio-based tetrahydrogeraniol acrylates (THGA) synthesized in Chapter 2 was easily polymerized in both toluene solution and bulk *via* free radical polymerization, reaching almost complete monomer conversion and relatively high molar mass (up to $\bar{M}_n$ = 278,000 g.mol^{-1}) and displayed a relatively low T_g (-46 ˚C). Further control over the targeted molar mass of the poly(terpene acrylate) polymers was achieved *via* RAFT polymerization. The effects of monomer and RAFT agent concentrations were investigated. At high monomer concentrations, excellent control over the polymerization could be achieved with molar mass up to 100,000 g.mol^{-1} and narrow molecular weight distributions ($Đ$ ~ 1.2) at conversions in excess of 90 %. At low monomer concentrations, evidence of branching and β-scission side reactions were observed leading to a molar mass lower than the theoretical value. The "living" nature of the poly(THGA) chain end was tested through chain extension with a second monomer, styrene. Hence, tri-block copolymers of poly(THGA)-*b*-poly(styrene)-*b*-poly(THGA) and poly(styrene)-*b*-poly(THGA)-*b*-poly(styrene) were successfully prepared, as evidenced by SEC. The morphology of the tri-block copolymers was observed *via* AFM and revealed the formation of a phase-separation between soft

(poly(terpene acrylate)) and hard (poly(styrene)) phases. The complete phase separation was also highlighted by rheological measurement, detecting the two glass transition temperature at low and high temperature for the poly(terpene acrylate) and poly(styrene) blocks respectively.

3.5 References

(1). Ballard, N.; Asua, J. M. Radical polymerization of acrylic monomers: An overview. *Prog. Polym. Sci.* **2018,** 79, 40-60.

(2). Agirre, A.; Nase, J.; Degrandi, E.; Creton, C.; Asua, J. M. Miniemulsion Polymerization of 2-Ethylhexyl Acrylate. Polymer Architecture Control and Adhesion Properties. *Macromolecules* **2010,** 43, 8924-8932.

(3). Ahmad, N. M.; Heatley, F.; Lovell, P. A. Chain Transfer to Polymer in Free-Radical Solution Polymerization of n-Butyl Acrylate Studied by NMR Spectroscopy. *Macromolecules* **1998,** 31, 2822-2827.

(4). Odian, G., *Principles of Polymerization, Fourth Edition*. John Wiley & Sons: Hoboken,NJ, 2004.

(5). Ballard, N.; Hamzehlou, S.; Asua, J. M. Intermolecular Transfer to Polymer in the Radical Polymerization of n-Butyl Acrylate. *Macromolecules* **2016,** 49, 5418-5426.

(6). Heatley, F.; Lovell, P. A.; Yamashita, T. Chain Transfer to Polymer in Free-Radical Solution Polymerization of 2-Ethylhexyl Acrylate Studied by NMR Spectroscopy. *Macromolecules* **2001,** 34, 7636-7641.

(7). Chiefari, J.; Jeffery, J.; Mayadunne, R. T. A.; Moad, G.; Rizzardo, E.; Thang, S. H. Chain Transfer to Polymer: A Convenient Route to Macromonomers. *Macromolecules* **1999,** 32, 7700-7702.

(8). Guillaneuf, Y.; Gigmes, D.; Junkers, T. Investigation of the End Group Fidelity at High Conversion during Nitroxide-Mediated Acrylate Polymerizations. *Macromolecules* **2012,** 45, 5371-5378.

(9). Veloso, A.; García, W.; Agirre, A.; Ballard, N.; Ruipérez, F.; Cal, J. C. d. l.; Asua, J. M. Determining the effect of side reactions on product distributions in RAFT polymerization by MALDI-TOF MS. *Polym. Chem.* **2015,** 6, 5437-5450.

(10). Castignolles, P.; Graf, R.; Parkinson, M.; Wilhelm, M.; Gaborieau, M. Detection and quantification of branching in polyacrylates by size-exclusion chromatography (SEC) and melt-state 13C NMR spectroscopy. *Polymer* **2009,** 50, 2373-2383.

(11). Hamzehlou, S.; Ballard, N.; Reyes, Y.; Aguirre, A.; Asua, J. M.; Leiza, J. R. Analyzing the discrepancies in the activation energies of the backbiting and β-scission reactions in the radical polymerization of n-butyl acrylate. *Polym. Chem.* **2016,** 7, 2069-2077.

(12). Ballard, N.; Rusconi, S.; Akhmatskaya, E.; Sokolovski, D.; Cal, J. C. d. l.; Asua, J. M. Impact of Competitive Processes on Controlled Radical Polymerization. *Macromolecules* **2014,** 47, 6580-6590.

(13). Coote, M. L. Ab Initio Study of the Addition−Fragmentation Equilibrium in RAFT Polymerization: When Is Polymerization Retarded? *Macromolecules* **2004,** 37, 5023-5031.

(14). Kwak, Y.; Goto, A.; Fukuda, T. Rate Retardation in Reversible Addition−Fragmentation Chain Transfer (RAFT) Polymerization: Further Evidence for Cross-Termination Producing 3-Arm Star Chain. *Macromolecules* **2004,** 37, 1219-1225.

(15). Ting, S. R. S.; Davis, T. P.; Zetterlund, P. B. Retardation in RAFT Polymerization: Does Cross-Termination Occur with Short Radicals Only? *Macromolecules* **2011,** 44, 4187-4193.

(16). Kwak, Y.; Goto, A.; Tsujii, Y.; Murata, Y.; Komatsu, K.; Fukuda, T. A Kinetic Study on the Rate Retardation in Radical Polymerization of Styrene with Addition−Fragmentation Chain Transfer. *Macromolecules* **2002,** 35, 3026-3029.

(17). Bathfield, M.; D'Agosto, F.; Spitz, R.; Ladaviere, C.; Charreyre, M.-T.; Delair, T. Additional Retardation in RAFT Polymerization: Detection of Terminated Intermediate Radicals. *Macromol. Rapid Commun.* **2007,** 28, 856-862.

(18). Moad, G. Mechanism and Kinetics of Dithiobenzoate-Mediated RAFT Polymerization – Status of the Dilemma. *Macromol. Chem. Phys.* **2014,** 215, 9-26.

(19). Adamy, M.; Herk, A. M. v.; Destarac, M.; Monteiro, M. J. Influence of the Chemical Structure of MADIX Agents on the RAFT Polymerization of Styrene. *Macromolecules* **2003,** 36, 2293-2301.

(20). Dayter, L. A.; Murphy, K. A.; Shipp, D. A. RAFT Polymerization of Monomers with Highly Disparate Reactivities: Use of a Single RAFT Agent and the Synthesis of Poly(styrene-block-vinyl acetate). *Aust. J. Chem.* **2013,** 66, 1564-1569.

Chapter 4. Paving the way to sustainable waterborne pressure-sensitive adhesives using terpene-based triblock copolymer

4.1. Introduction

The successful syntheses of homopoly(THGA) and thermoplastic elastomers made out of soft/hard/soft and hard/soft/hard triblock copolymers of THGA and styrene were described in Chapter 3. However, the polymerization was carried out in solution, namely with an extensive use of solvent. In order to overcome this problem, miniemulsion polymerization is used in this chapter. In addition, as polyTHGA presents a low T_g, its use as pressure sensitive adhesive is explored.

Pressure sensitive adhesives (PSAs) are important polymer materials, with a global revenue estimated to USD 6 billion in 2017 (and a substantial growth is expected

in the next years).[1] Efforts to improve the sustainability of those materials by the substitution of some petroleum-based chemicals to bio-based alternatives have been reported.[2, 3] Thus, for polymers synthesized by step growth polymerization, diols and diacids derived from renewable precursors served as monomers for the synthesis of robust PSAs. [4, 3] Also, lactide and menthide have been used as building blocks for the synthesis of nanostructured PSAs *via* ring-opening polymerization.[5-9]

Although step growth polymers serve in some niche applications, polyacrylates produced by free radical polymerization dominate the PSA market.[1] Typically, acrylic based PSAs are random copolymers that contain relatively long chain acrylates (e.g. 2-ethylhexyl acrylate, *n*-butyl acrylate) as soft monomers, whereas styrene or methyl methacrylate are commonly utilized as hard monomers.[10] Therefore, search for renewable substitutes is an active field. [2, 3, 11]

Block copolymers are an interesting alternative to random copolymers because their mechanical properties can be tailor-made by modifying the functionality and the length of the blocks.[12-15] In addition, the synthesis of this type of copolymers is readily available by controlled radical polymerization.[13] It is then not surprising that attempts to synthesize PSAs using bio-based monomers have been made and PSAs with good

mechanical and adhesion properties have been reported.[2, 6-9, 11] Thus, triblock PSAs were prepared using bio-based acrylic isosorbide (AAI) and glucose acrylate tetraacetate as hard monomers and 2-ethylhexyl acrylate (2-EHA) or *n*-butyl acrylate (BA) as the "soft" monomer.[9, 16] Acrylic monomers obtained from depolymerization of lignocellusolic biomass have also used as hard monomers in combination to conventional soft acrylic monomers to produce partially bio-based PSAs.[17]

These reports show that block copolymer PSAs in which the petroleum-based monomers are partially substituted give interesting mechanical and adhesion properties. However, a close look to the synthetic methods used reveals that these materials are produced in harmful solvent, e.g. toxic DMF.[9, 16, 18] In addition, the sustainability and scalability of the process are compromised by the purification step used after the formation of the first block. Consequently, there is a need to go further in the synthesis of PSAs, by designing a process that promotes the use of renewable resources and that has a lower environmental impact.

Therefore, this chapter aims at demonstrating the feasibility of synthesizing whole bio-sourced triblock PSAs by an environmentally friendly and waterborne process without the need of intermediate purification steps. The synthetic method is

based on RAFT miniemulsion polymerization of terpene-based monomers and it is summarized in Scheme 4.1. The article is organized as follows. First, it is demonstrated that the RAFT polymerization of terpene-based monomers can be achieved in miniemulsion. Then, bio-sourced hard-soft-hard or soft-hard-soft triblock copolymers that can be utilized as waterborne adhesives are synthesized. Tetrahydrogeraniol acrylate (THGA) is employed herein as the "soft" monomer. This monomer has emerged as a robust substitute for BA and/or 2-EHA in the design of thermoplastic elastomers and UV-cured acrylic PSAs.[19-21] Cyclademol acrylate (CDMA) is introduced as a "hard" monomer, to serve as a substitute to the petroleum-based hard monomers such as styrene and methyl methacrylate. Those terpene-based monomers are later polymerized by RAFT polymerization in miniemulsion to achieve hard-soft-hard and soft-hard-soft triblock copolymers. The adhesion properties of the triblock bio-based PSAs are then measured and compared with those of a partially bio-based triblock copolymer prepared with THGA and styrene.

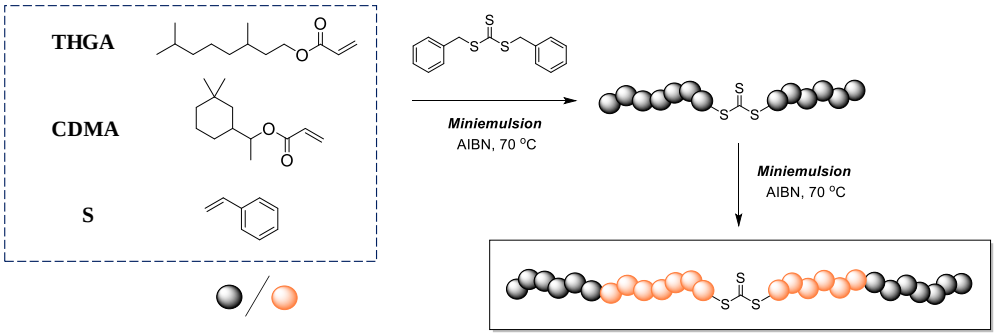

Scheme 4.1. Reaction scheme to yield functional triblock copolymer based on terpene.

4.2. Experimental

4.2.1. Materials

The materials are given in Appendix **I**

4.2.2. Synthesis procedures

4.2.2.1. Preparation of the homopolymer dispersion by RAFT miniemulsion polymerization

Preparation of the miniemulsion

Miniemulsion polymerization is a versatile method that allows the synthesis of a broad range of waterborne dispersions. [22-24] Typically, the organic phase consisted of an homogeneous mixture of monomer (THGA or CDMA, 10 to 25 g), RAFT agent (DBTTC, calculated by targeting a certain DPn = $[M]_0/[DBTTC]_0$) and co-stabilizer (stearyl acrylate at a concentration of 5 *wt.*% based-on-monomer, b-o-m)). The aqueous phase consisted of a surfactant (Dowfax 2A1 at a concentration of 3 *wt.*% b-o-m) solution in deionized water (amount calculated to reach 10-25 *wt.*% solids content). It was found that 3 *wt.*% b-o-m of surfactant and 5 *wt.*% b-o-m of co-stabilizer were necessary to prevent droplets coalescence and Ostwald ripening, as evidenced by light backscattering (Figure 4.1).[22] After mixing the two phases and stirring for 30 minutes, the pre-emulsion was sonicated at 80 % output and 0.8 duty cycle for 10 minutes, in an ice bath to avoid overheating and under magnetic stirring, yielding a stable miniemulsion. The resulting mean droplet sizes for each polymerization are summarized in Table 4.2.

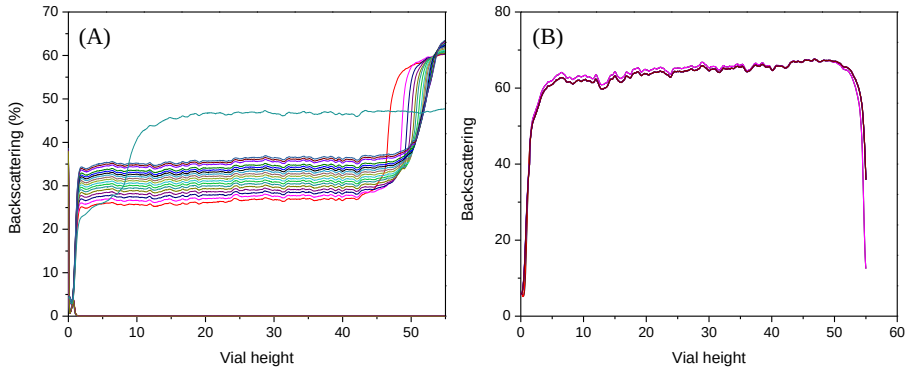

Figure 4.1. Stability of the THGA dispersion at 60 ˚C. The scans were conducted every 30 min for 5 h with 20 *wt*% solids content. (A) entry 1; 2 *wt.*% surfactant and 4 *wt.*% co-stabilizer. (B) entry 2; 3 *wt.*% surfactant and 5 *wt.*% co-stabilizer based on terpene acrylate.

RAFT miniemulsion polymerization

The miniemulsion was placed into a 250 mL round-bottom flask (RBF) equipped with a rubber seal and a magnetic stirring bar and subsequently deoxygenated with purging nitrogen for 30 minutes. The polymerization was carried out by placing the mixture in an oil bath at 70 °C for 7 hours under stirring. In this work, three different initiators were used (AIBN, KPS and THBP/AsAc, with a ratio $[DBTTC]_0/[I_2]_0 = 10$). AIBN was dissolved directly into the organic phase prior to the miniemulsification. In contrast, KPS (dissolved in water) was added as a single shot to the reaction mixture at

70°C. When the redox initiating couple was utilized, the reductant (AsAc) was added as a single shot to the reaction after miniemulsification and the TBHP was subsequently fed into the reaction mixture for 30 minutes. The various reaction conditions are summarized in Table 4.1.

Table 4.1. Recipes for synthesis the poly(THGA) by RAFT miniemulsion polymerization

Entry[a]	Organic phase					Aqueous phase	
	THGA (g)	**Initiator type**	**Initiator (mg)**	**Stearyl acrylate (g)**	**DBTTC (g)**	**Water (g)**	**Dowfax 2A1 (g)[c]**
1	10	KPS	25	0.4	0.270	40	0.44
2	10	KPS	25	0.5	0.270	40	0.66
3	10	TBHB/AscA	15	0.5	0.270	40	0.66
4	10	AIBN	15	0.5	0.270	40	0.66
5	10	AIBN	3	0.5	0.055	40	0.66
6	10	AIBN	2.2	0.5	0.039	40	0.66
7	10	AIBN	1.8	0.5	0.030	40	0.66
8	10	AIBN	10.5	0.5	-	40	0.66

[a] 20 *wt* % solids content. For entry 8, a free radical polymerization was conducted (e.g. in the absence of RAFT agent) with 0.1 *wt.*% initiator b-o-m. [c] 45 *wt.*% active content.

4.2.2.2. Synthesis of poly(THGA)-*b*-poly(CDMMA)-*b*-poly(THGA) soft/hard/soft triblock copolymers

A poly(THGA) seed latex with 10 *wt*% solids ($[M]_0/[DBTTC]_0$ = 262, $[DBTTC]_0/[I_2]_0$ = 10) was first prepared via RAFT miniemulsion polymerization as described above. The reaction was stopped at 95 % monomer conversion, yielding a polymer with M_n = 51,000 g.mol^{-1} and $Đ$ = 1.2. The poly(THGA) seed latex (40 g) was charged into a 250 mL RBF equipped with rubber seals and magnetic stirring bar before deoxygenation by purging nitrogen for 30 min. Subsequently, a mixture of CDMA monomer (3.99 g, 18.9 mmol, $[M]_0$/[macro RAFT agent]$_0$ = 241), AIBN ($[DBTTC]_0/[I_2]_0$ = 11) and acetone (10 *wt.*% b-o-m) was added to the reaction as a single shot and stirred for 30 min. Acetone was added to facilitate the incorporation of CDMA and AIBN to the poly(THGA) particles. Acetone presents the advantage of having benign toxicity and easily removable as shown in the industrial production of polyurethane dispersions.[25] The reaction mixture was then placed in an oil bath at 70°C and left to polymerize for 8 h (by this point all the acetone was removed). After polymerization, the reaction was cooled to room temperature.

4.2.2.3. Synthesis of poly(CDMMA)-*b*-poly(THGA)-*b*-poly(CDMMA) hard/soft/hard triblock copolymers

Poly(CDMMA) seed latex (10 wt% solids content) was prepared *via* RAFT miniemulsion polymerization. The organic phase consisted of a homogeneous mixture of CDMMA (10 g, 4.75×10^{-2} mol), initiator (16 mg, 9.74×10^{-5} mol, $[CTA]/[I_2]$ = 10), DBTTC (0.29 g, 9.74×10^{-5} mol, [M]/[CTA] = 48) and stearyl acrylate (0.5 g, 5 wt.% based-on-monomer, utilized as as a co-stabilizer) . The aqueous phase consisted of a mixture of Dowfax 2A1 (0.66 g, 3 *wt*.% b-o-m) dispersed in deionised water. The preparation of the miniemulsion was similar as describe above. The miniemulsion (particle size 186 nm) was transferred into a round bottle flask sealed with silicone rubber and the mixture was deoxygenated by purging nitrogen for 30 min. Then, the miniemulsion was placed in an oil bath at 70°C and the polymerization was carried out for 7 h under stirring. The reaction was stopped at 97 % conversion with the $\overline{M}_n$ = 13,000 $g.mol^{-1}$ with $Đ$ = 1.10. Then, the poly(CDMA) (10 *wt*% solid content) seed latex (20 g, 1.96×10^{-4} mol) was charged into the reactor equipped with the rubber seal and magnetic stirring bar, and deoxygenated with nitrogen for 30 min. Subsequently, the mixture of THGA (5.10 g, $[M]_0/[\text{macro RAFT agent}]_0$ = 156), AIBN (3.2 mg, $[DBTTC]_0/[I_2]$ = 8) and acetone (10 *wt*.% b-o-m) was added to the reactor and stirred

for 30 min. The reactor was then placed in an oil bath at 70°C and the polymerization was carried out for 8 h. After the polymerization, the reaction was cooled to room temperature.

4.2.2.4. Synthesis of poly(THGA)-*b*-poly(S)-*b*-poly(THGA) soft/hard/soft triblock copolymers

A poly(THGA) seed latex 10 wt% solids ($[M]_0/[DBTTC]_0$ = 251, $[DBTTC]_0/[I_2]_0$ = 10,) was first prepared *via* RAFT miniemulsion polymerization as described above. The reaction was stopped at 97 % monomer conversion, yielding a polymer with M_n = 50 000 g.mol^{-1} and $Đ$ = 1.28. The poly(THGA) seed latex (40 g) was charged to the reactor and purged with nitrogen for 30 min. Subsequently, the mixture of styrene (4.16 g, $[M]_0$/[macro RAFT agent]$_0$ = 500), AIBN (1.3 mg, $[CTA]_0/[I_2]_0$ = 9) and acetone (10 *wt*.% b-o-m) was added to the reactor and stirred for 30 min. The reactor was then placed in an oil bath at 70°C and allow to polymerize for 8 h. After polymerization, the reaction was cooled to room temperature.

4.2.3. Characterization

The monomer conversion was calculated using equation 1, the information is given in Appendix **I**.

The theoretical molar masses were calculated using equation 2, the information is given in Appendix **I**.

4.3. Results and discussion

4.3.1. Miniemulsion homopolymerization of THGA

4.3.1.1. The effect of type of initiator

We first investigated the RAFT homopolymerization of THGA in miniemulsion (Scheme 4.1) ($DP_n = [M]_0/[DBTTC]_0 = 50$, at 70 ºC). Once a stable miniemulsion was reached (see experimental section), we looked at the most efficient way to initiate polymerization. Hence, three types of initiators were tested, which directly impact the concentration of initiating radical in the monomer droplets. Upon decomposition, the hydrophobic initiator azobisisobutyronitrile (AIBN) initiates polymerization inside the

droplets, whilst the hydrophilic potassium persulfate (KPS) generates radicals in the aqueous phase. A redox couple tert-butyl hydroperoxide/ascorbic acid (TBHP/AscA) was also tested. This redox couple yields hydrophobic radicals in the aqueous phase that are readily incorporated into the monomer droplets,[26] and it has shown great potential in RAFT polymerization in solution and in free radical polymerization in dispersed media.[27, 28] In Figure 4.2A, it becomes clear that the more hydrophobic initiators yielded higher monomer conversions (> 90 %). Conversely, only 60 % monomer conversion could be achieved with KPS in 6 hours. This arises from the relative difference in hydrophobicity between initiating radicals and monomers. THGA is highly hydrophobic and hence its concentration in the aqueous phase was low. As a consequence the sulfate radicals generated from KPS did not find enough monomer to propagate and as they are too hydrophilic to directly enter into the monomer droplets, they underwent severe termination in the aqueous phase. This resulted in an inneficient initiation of the droplets. The use of the TBHP/AscA redox couple allowed for a rapid polymerization (> 90 % conversion in 1 hour), due to the fast generation of radicals upon the feeding of the oxidant (TBHP). Despite the advantages that the use of this efficient redox couple can provide, we decided to utilize AIBN as an hydrophobic initiator for further reactions, due to the simplicity of the reaction set-up.

Figure 4.2B highlights the evolution of the particle size during the polymerization with the different initiators. For AIBN the values of the particle sizes remained relatively constant with increasing monomer conversions and monomodal size distributions were obtained. Pleasingly, good control can still be achieved, as evidenced in Figure 4.2C by the linear evolution of molar mass with increasing conversion. The reason is that as the miniemulsion droplets were mostly composed by THGA, the monomer concentration was high $[M]_0 \sim 3.6$ mol.L^{-1} and as shown in Chapter 3 and this is key to reduce the negative effect of side reactions such as intramolecular chain transfer to polymer (also referred to as backbitting).[21, 29] Backbitting is typical in the polymerization of acrylates and leads to the formation of mid-chain radicals (MCRs), which after β-scission yields new radicals and macromonomers,[30, 31] which affect the values of M_n at high monomer conversions (due to the creation of new chains).[32, 33] It should be noted that the dispersity values observed herein ($Đ < 1.2$, Figure 4.2D) are comparable to that of the RAFT polymerization of THGA in solution (Chapter 3 and reference 21).

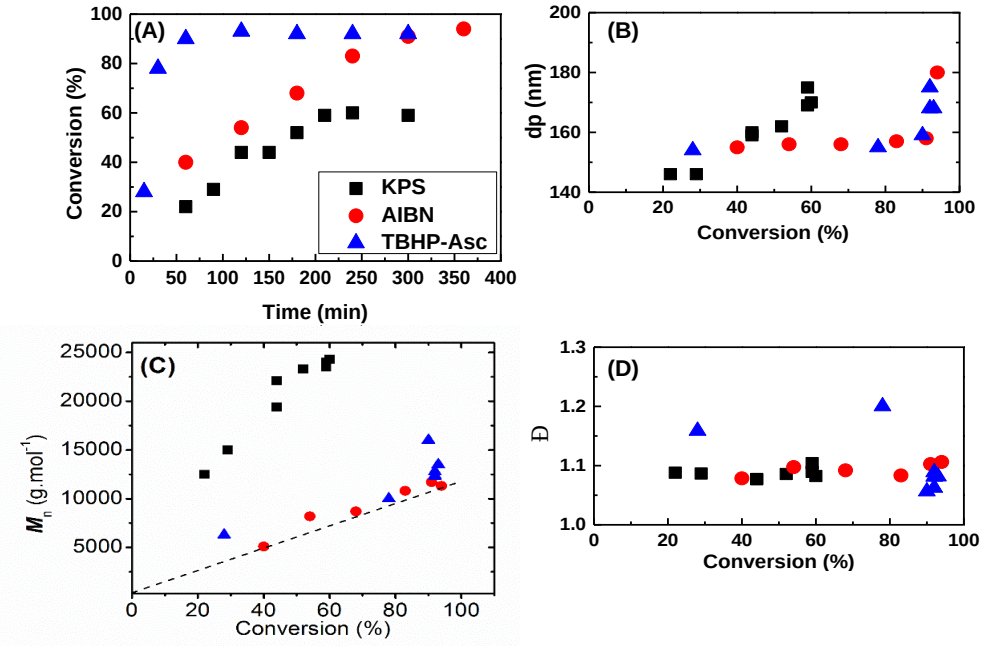

Figure 4.2. Kinetic of the RAFT miniemulsion polymerization of poly(THGA) with different initiators at 70°C, DP_n = 50, $[CTA]_0/[I_2]_0$ = 10. (Squares) KPS; (Circles) AIBN and (Up triangles) TBHP/Asc. (A) Conversion plot as a function of time. (B) Evolution of the particle size as a function of time. (C) Evolution of the measured molar masses as a function of monomer conversion. (D) Evolution of dispersity values as a function of monomer conversion.

4.3.1.2. The effect of targeted degree of polymerization

The good level of control attained at relatively low molar masses (DP_n = 50, M_n = 9,400 g.mol^{-1}) encourages us to push the polymerization system further, by targeting different degrees of polymerization (250, 350 and 450). In all cases, high monomer

conversions (> 90% conversion) were reached after 6 hours, as detailed in Table 4.2 and Figure 4.3A. A lower rate of polymerization can be observed in Figure 4.3A when a DP_n of 50 was targeted. In comparison, the rate of polymerization for higher targeted DP_n was close to that of the free radical polymerization. A similar behavior has been previously observed when the RAFT polymerization of THGA was conducted in solution (Chapter 3 and reference 21). That phenomenon was attributed to a rate retardation due to the RAFT process.[34-36] Finally, it should be noted that the overall rate of polymerizations in miniemulsion at 70 ºC are comparable to that of polymerization in solution at 80 ºC,[21] likely as a result of a compartmentalization effect.[24, 37]

In Figure 4.3B, the droplet/particle size increased as a function of targeted DP_n, which may be the result of an enhanced stabilization at high concentration of the hydrophobic RAFT agent that is highly hydrophobic and may behave as a co-stabilizer.[38] In Figure 4.3C, it can be observed that good control over the RAFT process can be achieved. Thus, the values of observed molar masses increased linearly as a function of increasing monomer conversion, for all targeted DP_ns. Moreover, the observed values of molar masses were close to theory as depicted in Table 4.2, thus suggesting a minimum presence of side reactions. Finally, the polymers were obtained with relatively low dispersity values ($Đ$ < 1.3, Figure 4.3D).

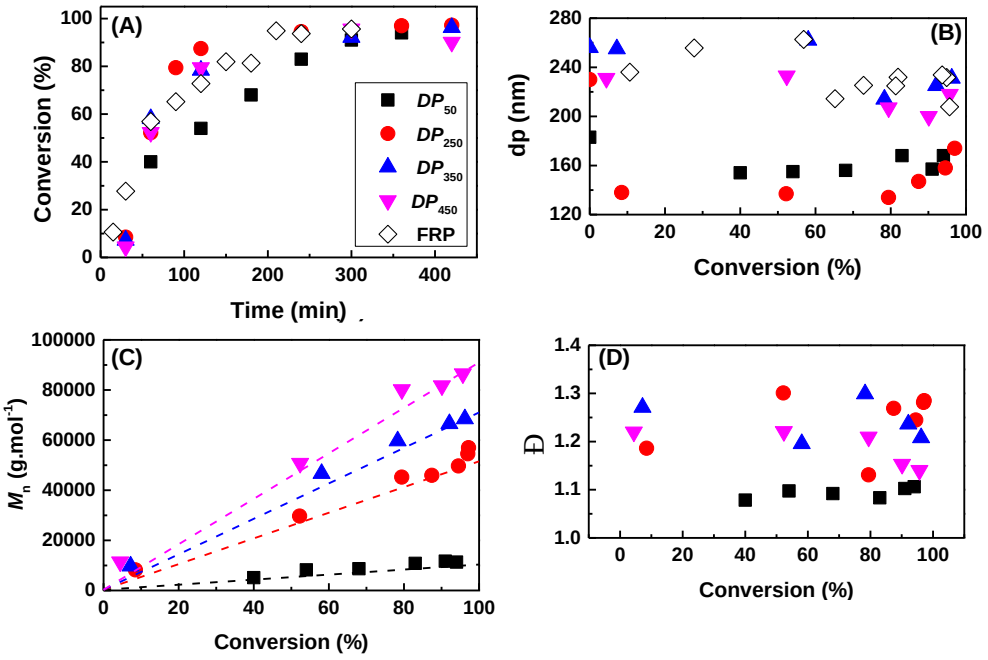

Figure 4.3. The kinetic plot of the poly(THGA) by RAFT miniemulsion polymerization at 70°C for 7 h with AIBN as an initiator at different targeted DP_ns; DP 50 (Squares), DP 250 (Cycles), DP 350 (Up triangles), and DP 450 (Down triangles). (A) Conversion plot as a function of time. (B) Evolution of the particle size as a function of conversion. (C) Evolution of the molar mass as a function of conversion. (D) Dispersity values as a function of conversion.

Table 4.2. Conversion, molar masses and dispersity values of poly(THGA) by RAFT miniemulsion polymerization.

Entry[a]	$[M]_0/[CTA]_0$	$[CTA]0/[I_2]_0$	Time (min)	Conv. (%)	dp (nm)	Np/L latex ($\times 10^{16}$)	$M_{n,th}$[b] (g.mol^{-1})	$M_{n,exp}$[c] (g.mol^{-1})	$Đ$
2	50	10	300	59	170	7.7	6,400	24,000	1.10
3	50	10	180	92	170	7.7	9,790	12,800	1.06
4	50	10	360	94	180	6.5	10,000	11,300	1.10
5	250	10	360	97	175	7.1	50,400	49,700	1.28
6	350	10	420	96	230	3.1	69,500	68,500	1.20
7	450	10	300	96	220	3.6	84,200	82,000	1.15
8*	n/a	n/a	300	96	208	4.2	-	154,000	1.9

[a] Entry 2 conducted with KPS as initiator, Entry 3 conducted with TBHP/Asc as an initiator and AIBN for entries 4-7. For entry 8, a free radical polymerization was conducted (e.g. in the absence of RAFT agent) with 0.1 *wt.*% AIBN b-o-m. [b] The theoretical molar masses were calculated as $M_n^{Th} = M_{CTA} + \frac{[M]_0 \times p \times M_M}{[CTA]_0 + 2 \times f \times [I]_0 \times (1 - e^{-k_D t}) \times (1 - \frac{f_C}{2})}$, where $[M]_0$, $[CTA]_0$, $[I]_0$ are the initial concentrations of monomer, chain transfer agent (CTA) and initiator respectively; M_M, M_{CTA} the molar masses (in g.mol^{-1}) of the monomer and CTA respectively and p the monomer conversion at a time t (in seconds); f the initiator initiation efficiency f = 0.5 and assuming termination by combination only (f_C = 1) and $k_D^{AIBN} = 4.47 \times 10^{15} \times e^{-Ea/RT}$ (s^{-1}).[39, 40] [c] Extracted from SEC-MALS analysis using the measured *dn/dc* value for poly(THGA) (*dn/dc* = 0.0678 mL.g^{-1}).

4.3.1.3. Triblock copolymers

The focus of this chapter is to demonstrate the possibility of synthesizing complete bio-sourced terpene-based triblock copolymers to yield waterborne adhesives without the need of any intermediate purification step. Hence, it was of upmost importance to check that such triblock could be synthesized. Upon formation of a macro-RAFT agent in miniemulsion, one can exploit the effect of compartmentalization and enhanced *"livingness"* of the process (*i.e.* the number of polymer chains able to re-initiate polymerization) to produce block copolymers upon addition of the second monomer.[13, 41] More specifically, the "soft" phase was composed of poly(THGA) (T_g ~ -46 ºC), whilst the "hard" phase consisted of poly(CDMA) (T_g ~ 88 ºC). Two types of structures were targeted, namely soft-hard-soft and hard-soft-hard triblocks. The triblock copolymers prepared are given in Table 4.3. It should be noted that for the sake of comparison, a triblock soft-hard-soft copolymer using styrene as hard block was also synthesized, with comparable weight percentages of soft and hard phases.

Table 4.3. Preparation of terpene-based hard-soft-hard and soft-hard-soft triblock copolymers by RAFT miniemulsion polymerization.

Copolymer	M_n macro-RAFT th [a] (g.mol^{-1})	M_n macro-RAFT exp [b] (g.mol^{-1})	Conv. (%)	M_n triblock th [a] (g.mol^{-1})	M_n triblock exp [b] (g.mol^{-1})	Đ	dp (nm)	Coagulation (wt.%)
PTHGA-b-PCDMA-b-PTHGA	51,400	51,000	96	98,500	105,500	1.6	265	n/a
PCDMA-b-PTHGA-b-PCDMA	9,700	13,000	95	43,200	45,400	1.5	255	n/a
PTHGA-b-PS-b-PTHGA	52300	50000	96	98400	120,000	2.64	310	n/a

[a] The theoretical molar masses were calculated as detailed in Table 2. [b] Extracted from SEC-MALS analysis using the measured *dn/dc* values for poly(THGA) (*dn/dc* = 0.0678 mL.g^{-1}) and poly(CDMA) (*dn/dc* = 0.0997 mL.g^{-1}). The *dn/dc* of the triblock copolymers were determined using eq (1)

The first PTHGA block was synthesized by RAFT miniemulsion polymerization at 70 ºC (DP_n = 262; $[DBTTC]_0/[I_2]_0$ = 10) reaching 95 % conversion in 8 hours. This yielded a macro-RAFT agent with M_n = 51,000 g.mol^{-1}) and low dispersity value ($Đ$ = 1.2, Figure 4.4A). Subsequently, the *"livingness"* of this "soft" block was tested *via* the addition of CDMA and initiator ([CDMA]/[macro-RAFT] = 241 and $[Macro\text{-}RAFT]_0/[I_2]_0$ = 10). A small amount of acetone was also added (10 *wt.*% b-o-m) with the monomer to promote the diffusion of the monomer through the aqueous phase into the polymer particle. Acetone was selected for its good miscibility, benign toxicity and facile removal by the end of the polymerization (*bp* = 56 ºC). It should be stressed that in the absence of solvent, the chain extension was not successful, with low monomer conversions attained (< 60 %, data not shown) and no apparent change in molar mass. A PTHGA-*b*-PCDMA-*b*-PTHGA triblock was obtained with 96 % monomer conversion of the second block after 8 hours of polymerization. This is confirmed by SEC in Figure 4.4A, with the molar mass distributions shifting towards higher masses upon chain extension. The PTHGA-*b*-PCDMA-*b*-PTHGA triblock reached a molar mass of M_n = 105,500 g.mol^{-1} and the dispersity value remained relatively low ($Đ$ ~ 1.6). The slight increase in dispersity value upon chain extension may be due to the presence of residual dead chains.

In Figure 4.4B, a phase separation can be observed in AFM for the PTHGA-*b*-PCDMA-*b*-PTHGA triblock copolymer, with the bright domains corresponding to the "hard" phase (54 *wt.*% of PCDMA) and the dark domains corresponding to the "soft" phase (46 *wt.*% of PTHGA). The triblock configuration is further evidenced through rheological measurement, with the appearance of two major glass transition temperatures (T_g) in Figure 4.4C. Details of the values of T_gs and G', G'' cross over can be found in Table 4.4.

Table 4.4. Rheological properties of the triblock copolymers.

Triblock copolymer	**Soft phase (*wt.*%)**[a]	**Hard phase (*wt.*%)**[a]	**T_gs (ºC)**[b]	**G' / G'' cross over (ºC)**
PTHGA-*b*-PCDMA-*b*-PTHGA	46	54	-42; 91	n/a
PCDMA-*b*-PTHGA-*b*-PCDMA	66	34	-33; 93	62
PTHGA-*b*-PS-*b*-PTHGA	43	57	-32; 19; 120	-37

[a] extracted from ^{1}H NMR. [b] extracted from the local maxima of tan(δ).

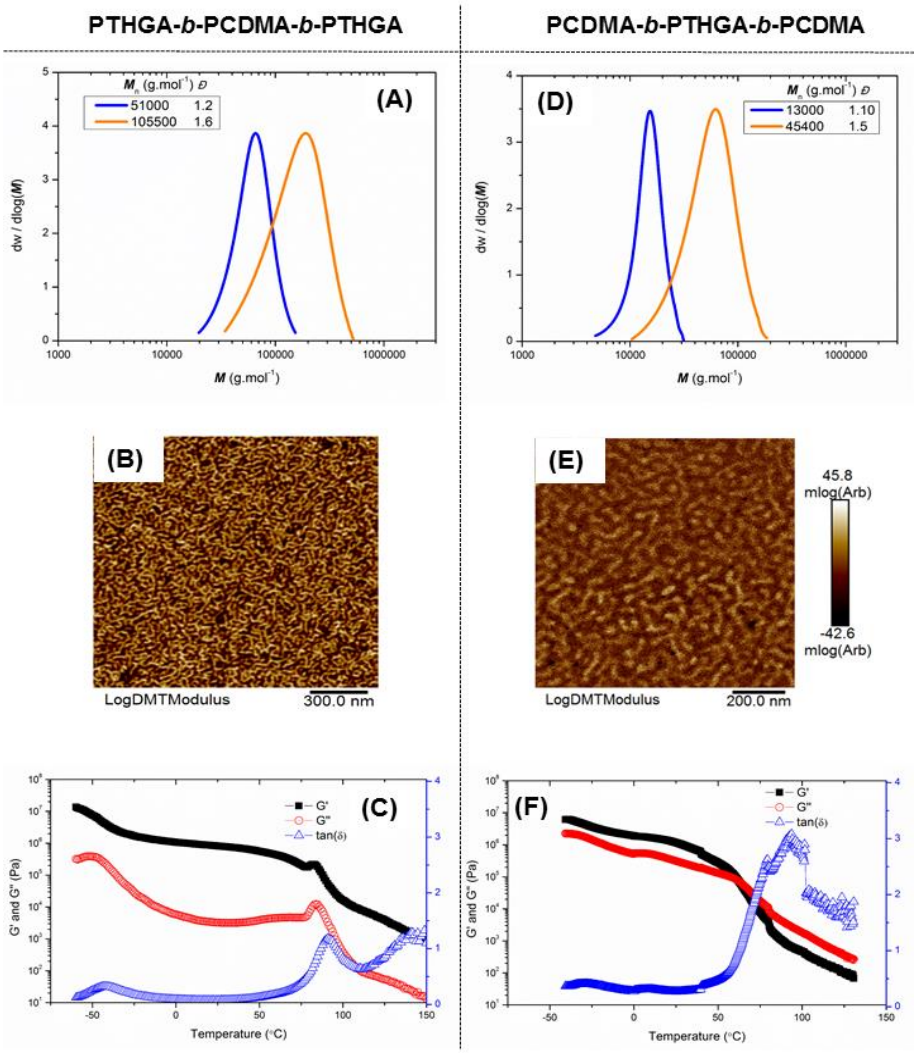

Figure 4.4. (A) and **(D)** SEC-MALS; **(B)** and **(E)** AFM (PeakForce QNM mode); **(C)** and **(F)** Rheological behavior for PTHGA-*b*-PCDMA-*b*-PTHGA and PCDMA-*b*-PTHGA-*b*-PCDMA.

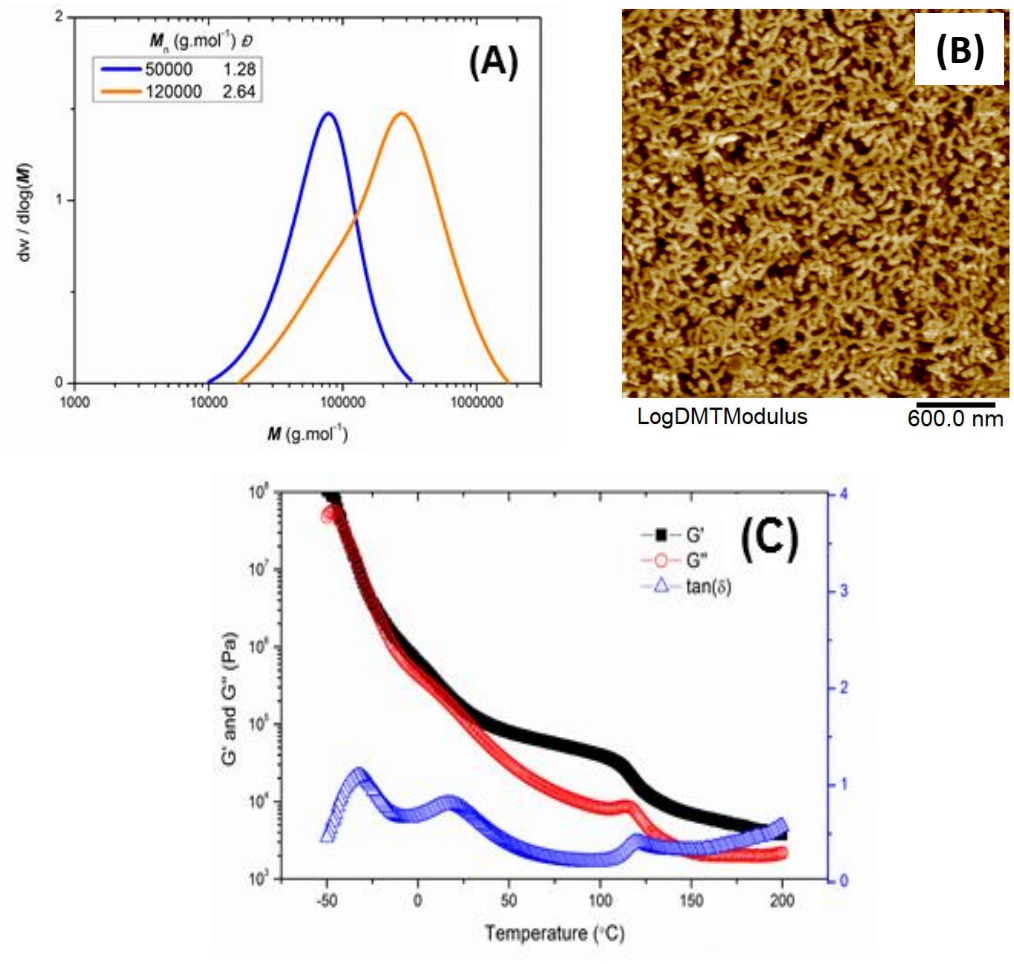

Figure 4.5. (A) SEC-MALS of PTHGA-*b*-PS-*b*-PTHGA. **(B)** AFM (PeakForce QNM mode) of PTHGA-*b*-PS-*b*-PTHGA. **(C)** Rheological behavior of PTHGA-*b*-PS-*b*-PTHGA with constant strain.

Regarding the hard-soft-hard triblock copolymer, a PCDMA macro-RAFT agent was prepared first (DP_n = 48; $[DBTTC]_0/[I_2]_0$ = 10, M_n = 13,000 g.mol^{-1}), reaching 97 % conversion after 8 hours of polymerization. After addition of the THGA and initiator (DP_n = 156; $[Macro\text{-}RAFT]_0/[I_2]_0$ = 8) and 8 hours of second-stage polymerization, a PCDMA-*b*-PTHGA-*b*-PCDMA of M_n = 45,400 g.mol^{-1} ($Đ$ ~ 1.5, Figure 4.4D) was obtained, with a high monomer conversion of 95 %. The morphology of the phase separating hard-soft-hard copolymer is observed in AFM (Figure 4.4E). This is confirmed by rheological analysis, showing the appearance of two major T_gs at –33 ºC and 93 ºC, for PTHGA and PCDMA blocks, respectively. The organization (and relative weight percentage) of the two blocks changes the rheological behavior of the copolymer, as evidenced by the evolutions of G' and G'' in Figure 4.4F. In addition, the difference in weight fraction of the hard and soft phases, in combination with the hard-soft-hard and soft-hard-soft configuration changed the G', G'' cross over (Table 4.4), which will impact the mechanical properties of the final adhesive.[12, 42]

4.3.1.4. Adhesive properties of triblock copolymers

The adhesive properties of the waterborne triblock copolymer were determined. It is worth to point out that no attempt to optimize the adhesive properties of these PSAs was carried out as the main goal of this work is to demonstrate that the synthesis of these bio-sourced materials under industrially implementable conditions was possible. In order to determine the adhesive properties, the dispersions were casted onto a PET substrate. Upon careful drying, a transparent and homogeneous polymer film was obtained (Figure 4.6).

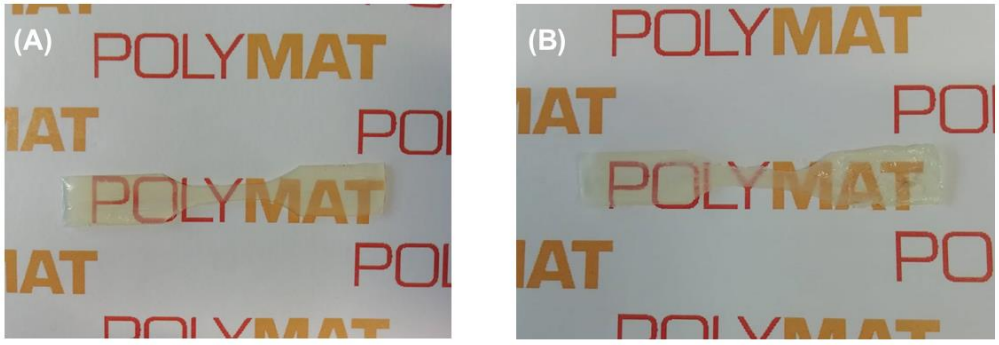

Figure 4.6. Films casted at 23 ºC and 55 % humidity. (A) PTHGA-*b*-PCDMA-*b*-PTHGA. (B) PCDMA-*b*-PTHGA-*b*-PCDMA.

Table 4.5. Adhesion properties of triblock copolymers

Triblock copolymer	Peel resistance (N/25 mm)	WA (J/mm^2)	Shear resistance (min)	Type of failure
PTHGA-*b*-PCDMA-*b*-PTHGA	5.98 ± 0.86	64 ± 6	25	Cohesion
PCDMA-*b*-PTHGA-*b*-PCDMA	1.53 ± 0.09	60 ± 10	3	Cohesion
PTHGA-*b*-PS-*b*-PTHGA	1.32 ± 0.04	34 ± 3	3.05	Cohesion

Peel strength (180º peel), tack and shear resistance were determined as described in the experimental section and the values summarized in Table 4.5. This table shows that modification of the bio-sourced PSA structure (soft-hard-soft vs. hard-soft-hard) and length of the blocks led to widely different adhesive properties. A cohesive failure is typical for PSAs based on triblock copolymers, due to the absence of crosslinking points that increase the cohesive strength of the adhesive.[9, 12, 16]

In order to compare the performance of the fully bio-sourced PSAs, a soft-hard-soft PSA having similar structure and molecular weights, but using styrene instead CDMA was synthesized. The adhesives properties of this PSA are also given in Table

4.5. It can be seen that the bio-sourced PSA had better peel and shear resistances. It must be stressed that this result does not mean that the bio-resourced PSAs have a superior performance, because none of the PSA formulations was optimized. Besides, changes in the chain length strongly affect adhesion.[10] It might be the case herein that for varying block lengths, the non-fully bio-sourced PSAs outperformed the bio-based ones. Nevertheless, the key aspect of these results is that bio-sourced PSAs synthesized by a sustainable and industrially implementable process can compete in performance with regular PSAs. Finally, it should be stated that the adhesive properties could be improved further, by playing with the percentages of soft and hard phases and the presence of additives (e.g. tackifiers and/or plasticizers)[10].

4.4. Conclusions

In conclusion, the investigations conducted herein show that through the synthesis of terpene-based triblock copolymers it is possible to obtain waterborne pressure-sensitive adhesives in an industrially scalable manner with minimal environmental impact. The copolymers are synthesized by RAFT miniemulsion polymerization, as a more sustainable alternative to existing synthetic strategies relying on solvent-borne or bulk processes. The process is readily scalable as no intermediate purification step of the first block is needed. In addition, the yielded hard-soft-hard or soft-hard-soft triblock copolymers structures solely consist of terpene derivatives namely poly(tetrahydrogeraniol acrylate) and poly(cyclademol acrylate), thus maximizing the use of renewable resources. The phase-separating copolymers show interesting rheological behaviors, with the organization of the blocks (*e.g.* hard-soft-hard and soft-hard-soft) and their relative weight percentages influencing the values of T_gs, G' and G''. Finally, the resulting formulations show good mechanical properties and adhesives performances, which are comparable to that of a partially petroleum-based system. It is our hope that the relative ease of monomer synthesis and polymerization in aqueous dispersed media presented herein will serve as a building

stone for the development and industrialization of more sustainable pressure-sensitive adhesives.

4.5. References

(1). Pulidindi, K.; Chakraborty, S., Pressure Sensitive Adhesives Market Size By Technology (Water Based, Solvent Based, Hot-Melt, UV-Cured), By Product (Rubber-Based, Acrylic, Silicone), By Application (Tapes, Labels, Graphics, Films & Laminates), By End-User (Food & Beverage, Packaging, Electronics & Laminates, Medical & Healthcare, Building & Construction, Automotive & Transportation), Industry Analysis Report, Regional Outlook (U.S., Canada, Germany, UK, France, Spain, Italy, Russia, China, India, Japan, Australia, Indonesia, Malaysia, South Korea, Brazil, Mexico, South Africa, Saudi Arabia, UAE, Kuwait), Growth Potential, Price Trends, Competitive Market Share & Forecast, 2018 – 2024. https://www.gminsights.com/industry-analysis/pressure-sensitive-adhesives-market, (accessed July 2019), 2018.

(2). Heinrich, L. A. Future opportunities for bio-based adhesives – advantages beyond renewability. *Green Chemistry* **2019,** 21, 1866-1888.

(3). Vendamme, R.; Schüwer, N.; Eevers, W. Recent synthetic approaches and emerging bio-inspired strategies for the development of sustainable pressure-sensitive adhesives derived from renewable building blocks. *Journal of Applied Polymer Science* **2014,** 131,

(4). Hillmyer, M. A.; Tolman, W. B. Aliphatic Polyester Block Polymers: Renewable, Degradable, and Sustainable. *Accounts of Chemical Research* **2014,** 47, 2390-2396.

(5). Ozturk, G. I.; Pasquale, A. J.; Long, T. E. Melt Synthesis and Characterization of Aliphatic Low-Tg Polyesters as Pressure Sensitive Adhesives. *The Journal of Adhesion* **2010,** 86, 395-408.

(6). Wanamaker, C. L.; O'Leary, L. E.; Lynd, N. A.; Hillmyer, M. A.; Tolman, W. B. Renewable-Resource Thermoplastic Elastomers Based on Polylactide and Polymenthide. *Biomacromolecules* **2007,** 8, 3634-3640.

(7). Shin, J.; Martello, M. T.; Shrestha, M.; Wissinger, J. E.; Tolman, W. B.; Hillmyer, M. A. Pressure-Sensitive Adhesives from Renewable Triblock Copolymers. *Macromolecules* **2011,** 44, 87-94.

(8). Ding, K.; John, A.; Shin, J.; Lee, Y.; Quinn, T.; Tolman, W. B.; Hillmyer, M. A. High-Performance Pressure-Sensitive Adhesives from Renewable Triblock Copolymers. *Biomacromolecules* **2015,** 16, 2537-2539.

(9). Gallagher, J. J.; Hillmyer, M. A.; Reineke, T. M. Acrylic Triblock Copolymers Incorporating Isosorbide for Pressure Sensitive Adhesives. *ACS Sustainable Chemistry & Engineering* **2016,** 4, 3379-3387.

(10). Benedek, I., *Pressure-sensitive adhesives and applications*. CRC Press: 2004.

(11). Badía, A.; Movellan, J.; Barandiaran, M. J.; Leiza, J. R. High Biobased Content Latexes for Development of Sustainable Pressure Sensitive Adhesives. *Industrial & Engineering Chemistry Research* **2018,** 57, 14509-14516.

(12). Boutillier, J.-M.; Disson, J.-P.; Havel, M.; Inoubli, R.; Magnet, S., Self-assembling acrylic block copolymers for enhanced adhesives properties. Adhesives & Sealants Industry Magazine, 2013

(13). Jennings, J.; He, G.; Howdle, S. M.; Zetterlund, P. B. Block copolymer synthesis by controlled/living radical polymerisation in heterogeneous systems. *Chemical Society reviews* **2016,** 45, 5055-5084.

(14). Creton, C. Block Copolymers for Adhesive Applications. *Macromolecular Engineering* **2011**, 1731-1751.

(15). Holmberg, A. L.; Reno, K. H.; Wool, R. P.; Epps, I. I. I. T. H. Biobased building blocks for the rational design of renewable block polymers. *Soft Matter* **2014,** 10, 7405-7424.

(16). Nasiri, M.; Saxon, D. J.; Reineke, T. M. Enhanced Mechanical and Adhesion Properties in Sustainable Triblock Copolymers via Non-covalent Interactions. *Macromolecules* **2018,** 51, 2456-2465.

(17). Wang, S.; Shuai, L.; Saha, B.; Vlachos, D. G.; Epps, T. H. From Tree to Tape: Direct Synthesis of Pressure Sensitive Adhesives from Depolymerized Raw Lignocellulosic Biomass. *ACS Cent. Sci.* **2018,** 4, 701-708.

(18). Wang, S.; Shuai, L.; Saha, B.; Vlachos, D. G.; Epps, T. H. From Tree to Tape: Direct Synthesis of Pressure Sensitive Adhesives from Depolymerized Raw Lignocellulosic Biomass. *ACS Central Science* **2018,** 4, 701-708.

(19). Baek, S.-S.; Hwang, S.-H. Preparation of biomass-based transparent pressure sensitive adhesives for optically clear adhesive and their adhesion performance. *European Polymer Journal* **2017,** 92, 97-104.

(20). Baek, S.-S.; Jang, S.-H.; Hwang, S.-H. Construction and adhesion performance of biomass tetrahydro-geraniol-based sustainable/transparent pressure sensitive adhesives. *Journal of Industrial and Engineering Chemistry* **2017,** 53, 429-434.

(21). Noppalit, S.; Simula, A.; Ballard, N.; Callies, X.; Asua, J. M.; Billon, L. Renewable Terpene Derivative as a Biosourced Elastomeric Building Block in the Design of Functional Acrylic Copolymers. *Biomacromolecules* **2019,** 20, 2241-2251.

(22). Asua, J. M. Miniemulsion polymerization. *Progress in Polymer Science* **2002,** 27, 1283-1346.

(23). Asua, J. M. Challenges for industrialization of miniemulsion polymerization. *Progress in Polymer Science* **2014,** 39, 1797-1826.

(24). Zetterlund, P. B.; Kagawa, Y.; Okubo, M. Controlled/Living Radical Polymerization in Dispersed Systems. *Chemical Reviews* **2008,** 108, 3747-3794.

(25). Dieterich, D. Aqueous emulsions, dispersions and solutions of polyurethanes; synthesis and properties. *Progress in Organic Coatings* **1981,** 9, 281-340.

(26). Ilundain, P.; Alvarez, D.; Da Cunha, L.; Salazar, R.; Barandiaran, M. J.; Asua, J. M. Knowledge-based choice of the initiator type for monomer removal by postpolymerization. *Journal of Polymer Science Part A: Polymer Chemistry* **2002,** 40, 4245-4249.

(27). Martin, L.; Gody, G.; Perrier, S. Preparation of complex multiblock copolymers via aqueous RAFT polymerization at room temperature. *Polymer Chemistry* **2015,** 6, 4875-4886.

(28). Moad, G.; Solomon, D. H., 3 - Initiation. In *The Chemistry of Radical Polymerization (Second Edition)*, Solomon, G. M. H., Ed. Elsevier Science Ltd: Amsterdam, 2005; pp 49-166.

(29). Ballard, N.; Rusconi, S.; Akhmatskaya, E.; Sokolovski, D.; de la Cal, J. C.; Asua, J. M. Impact of Competitive Processes on Controlled Radical Polymerization. *Macromolecules* **2014,** 47, 6580-6590.

(30). Ballard, N.; Asua, J. M. Radical polymerization of acrylic monomers: An overview. *Progress in Polymer Science* **2018,** 79, 40-60.

(31). Ahmad, N. M.; Charleux, B.; Farcet, C.; Ferguson, C. J.; Gaynor, S. G.; Hawkett, B. S.; Heatley, F.; Klumperman, B.; Konkolewicz, D.; Lovell, P. A.; Matyjaszewski, K.; Venkatesh, R. Chain Transfer to Polymer and Branching in Controlled Radical Polymerizations of n-Butyl Acrylate. *Macromolecular Rapid Communications* **2009,** 30, 2002-2021.

(32). Guillaneuf, Y.; Gigmes, D.; Junkers, T. Investigation of the End Group Fidelity at High Conversion during Nitroxide-Mediated Acrylate Polymerizations. *Macromolecules* **2012,** 45, 5371-5378.

(33). Veloso, A.; Garcia, W.; Agirre, A.; Ballard, N.; Ruiperez, F.; de la Cal, J. C.; Asua, J. M. Determining the effect of side reactions on product distributions in RAFT polymerization by MALDI-TOF MS. *Polymer Chemistry* **2015,** 6, 5437-5450.

(34). Coote, M. L. Ab Initio Study of the Addition−Fragmentation Equilibrium in RAFT Polymerization: When Is Polymerization Retarded? *Macromolecules* **2004,** 37, 5023-5031.

(35). Ting, S. R. S.; Davis, T. P.; Zetterlund, P. B. Retardation in RAFT Polymerization: Does Cross-Termination Occur with Short Radicals Only? *Macromolecules* **2011,** 44, 4187-4193.

(36). Moad, G. Mechanism and Kinetics of Dithiobenzoate-Mediated RAFT Polymerization – Status of the Dilemma. *Macromolecular Chemistry and Physics* **2017,** 218,

(37). Zetterlund, P. B.; Thickett, S. C.; Perrier, S.; Bourgeat-Lami, E.; Lansalot, M. Controlled/Living Radical Polymerization in Dispersed Systems: An Update. *Chemical Reviews* **2015,** 115, 9745-9800.

(38). Qi, G.; Schork, F. J. On the Stability of Miniemulsions in the Presence of RAFT Agents. *Langmuir* **2006,** 22, 9075-9078.

(39). Moad, G. A Critical Assessment of the Kinetics and Mechanism of Initiation of Radical Polymerization with Commercially Available Dialkyldiazene Initiators. *Progress in Polymer Science* **2019,** 88, 130-188.

(40). Gody, G.; Maschmeyer, T.; Zetterlund, P. B.; Perrier, S. Pushing the Limit of the RAFT Process: Multiblock Copolymers by One-Pot Rapid Multiple Chain Extensions at Full Monomer Conversion. *Macromolecules* **2014,** 47, 3451-3460.

(41). Khan, M.; Guimarães, T. R.; Zhou, D.; Moad, G.; Perrier, S.; Zetterlund, P. B. Exploitation of Compartmentalization in RAFT Miniemulsion Polymerization to Increase the Degree of Livingness. *Journal of Polymer Science Part A: Polymer Chemistry* **2019,** 0,

(42). Ewert, T. R.; Mannion, A. M.; Coughlin, M. L.; Macosko, C. W.; Bates, F. S. Influence of rheology on renewable pressure-sensitive adhesives from a triblock copolymer. *Journal of Rheology* **2017,** 62, 161-170.

Chapter 5. Nitroxide mediated miniemulsion polymerization of using terpene methacrylates*

5.1. Introduction

Most synthetic plastics are derived from fossil fuel and their production increases every year. As a consequence, fossil resources are being exploited faster than they are being replenished, the price of oil and its derived products escalates, and hazardous materials are being released in large quantities into environment.[1-4] Therefore, the environmental concerns and the depletion of petroleum oil have promoted the search for greener plastics using (i) raw materials derived from natural renewable sources and (ii) more environmentally friendly polymerization processes. An answer to the first point is the development of bio-based monomers for the production of various polymer matrices.[5-7] However, achieving the mechanical, thermal, electrical, rheological, and other physical properties required for commercial

*The fruitful discussions with Prof. Costantino Creton on the adhesive properties of the block copolymers synthesized in this chapter are acknowledged.

applications is challenging. Therefore, the use of bio-resources for the synthesis of polymers is subjected to intensive research. This PhD is an attempt to contribute to this field using monomers derived from terpenes that area side product of the local paper including based on the "Landes" pine forest in the South West of France. The synthesis of the monomers is described in Chapter 2 and Chapters 3 and 4 are devoted to the polymerization of the terpene acrylates. An answer to the second point is the polymerization in aqueous dispersed system. This technique has shown several advantages compare to the synthesis in solution, especially in term of the environmentally friendly process, cost and controlling the heat transfer.[8]

Reversible deactivation radical polymerization (RDRP) has been extensively researched during the past decades and several techniques have been developed. The most often used are nitroxide-mediated polymerization (NMP),[9-11] reversible addition-fragmentation chain transfer polymerization (RAFT)[12] and transition metal-mediated radical polymerization (TMM-RDRP that includes atom transfer radical polymerization, ATRP)[13-15]. In spite of the intensive research the industrial implementation has been modest[16, 17] mainly because none of these techniques completely fulfils the requirements for industrial production. RAFT and ATRP are able to polymerize a wide range of polymers, but they present problems of odour (RAFT)

coloring (RAFT and ATRP) and catalyst residues (copper in ATRP). Although extensive efforts have been undertaken in the past decade towards the removal of RAFT agents, post-polymerization modification and reducing copper catalyst content[18, 19] the problem has not been solved yet. Although the polymers produced by NMP are not affected by this problem as they require no or minimal purification, there is no a general nitroxide able to control the polymerization of different monomer families.[20] Basically the nitroxides that control the polymerization of styrene and acrylates (BlocBuilder-SG1[21, 22] and TIPNO[23] fail with methacrylates, whereas those able to control the polymerization of methacrylates (*e.g*. DPAIO and derivatives) are not successful for acrylates and/or styrene. [24, 25]

A hurdle that affects all the RDRP techniques is the cost associated to the control agent. As each polymer chain contains a molecule of the control agent and typically RDRP aims at producing polymers with a relatively low molecular weight (often for their use as additives) the cost due to the control agent is substantial.

Recently, Ballard *et al* have introduced new alkoxyamine (3-(((2-cyanopropan-2-yl)oxy)(cyclohexyl)amino)-2,2-dimethyl-3-phenylpropanenitrile, Dispolreg 007) that can be easily synthesized by a cost-effective process and it is able to mediate the polymerization of methyl methacrylate and styrene[26, 27] and up to some extent that of acrylates[28]. Moreover, this alkoxyamine could be utilized to synthesize the block

copolymer in batch and semicontinuous reactors in both solution and dispersed media.[29-31]

This chapter explores the possibility of synthesizing block copolymers from bio-sourced terpene-based methacrylates by nitroxide mediated miniemulsion polymerization. The formulation is adapted for the application as pressure sensitive adhesives (PSAs). This work complements Chapter 4 as diblock copolymers instead of triblock copolymers are obtained and a more-friendly and economically effective control agent (Dispolreg 007) is used. On the other hand, the requirement of easy scalability by avoiding any intermediate purification step is maintained.

Soft (tetrahydrogeraniol methacrylate monomer, THGMA, T_g = -30 ºC) and hard (cyclademol methacrylate, CDMMA, T_g = 92 ºC) were synthesized in Chapter 2. First, in order to optimize the polymerization, THGMA was polymerized *via* NMP in toluene in the presence of the alkoxyamine Dispolreg 007. The effect of the reaction temperature and the possibility to control different degrees of polymerization were studied. Then, still in toluene (Scheme 5.1), the retention of active chain ends was tested by chain extension with cyclademol methacrylate (CDMMA). The phase separation of the diblock soft-hard copolymer obtained was observed by atomic force microscopy (AFM). After that, miniemulsion NMP of THGMA was studied aiming at obtaining a

broad range of degrees of polymerization (*DP*n = 50, 100, 200, 400, 500). Miniemulsion polymerization was also used to synthesize poly(THGMA)-*b*-poly(CDMMA) diblock copolymers (Scheme 5.1) and their adhesive properties were measured. A poly(THGMA)-*b*-poly(styrene) diblock copolymer was also synthesized in miniemulsion for comparative purposes.

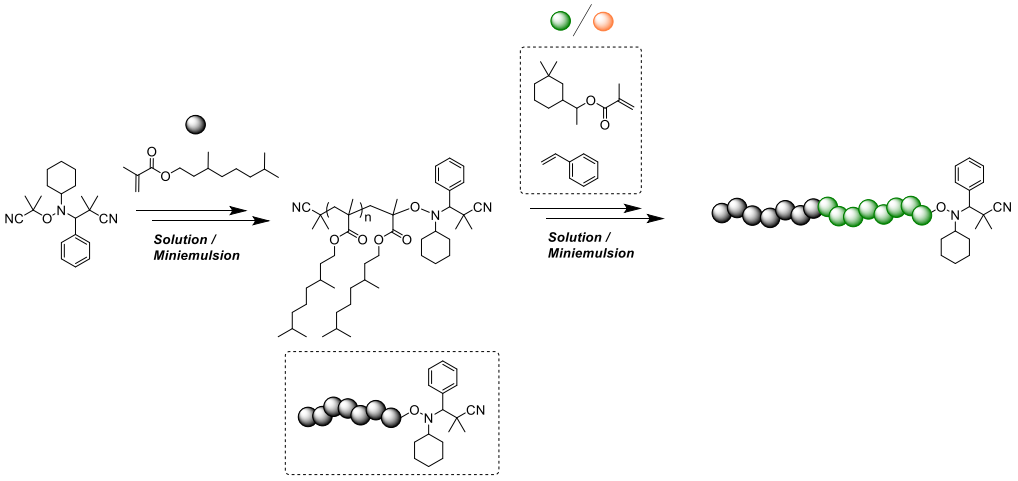

Scheme 5.1. Synthesis of soft/hard diblock copolymers based on terpene methacrylate.

5.2. Experimental

5.2.1. Materials

The materials are given in Appendix **I**

5.2.2. Synthesis procedures

5.2.2.1. NMP of THGMA in toluene

The NMP polymerization of THGMA in toluene was performed using Dispolreg 007. Reactions 1-3 were carried out and different temperatures (90, 95 and 97 ºC) aiming at the same degree of polymerization, *DP*n = 25. Reactions 3-6 were carried out at 97 ºC aiming at different degrees of polymerization. The formulations are given in Table 5.1. Typically, THGMA (2 g, 8.83 x 10^{-3} mol) and toluene (2 g) were placed into a 25 mL RBF equipped with rubber seals and a magnetic stirring bar. Dispolreg 007 was added in order to adjust the $[M]_0/[\text{Dispolreg 007}]_0$ ratio to the target *DP*n (25, 100, 200 and 400). The mixture was deoxygenated for 30 minutes by purging nitrogen and subsequently placed into an oil bath at 97 °C. Polymerization occurred under stirring for 6 hours and samples were carefully withdrawn via a deoxygenated

syringe. Monomer conversion was calculated from ^{1}H NMR by comparison of the vinyl signals and OC$\boldsymbol{H}_2$ signals The polymer solution was quenched by cooling in contact with air, precipitated three times in methanol and dried under vacuum to yield the purified polymer as a white powder.

Table 5.1. Reaction conditions and resulting monomer conversion and molecular weights for synthesis the poly(THGMA) by NMP in toluene.

Entry[a]	$[M]_0$ (mol.L^{-1})	$[\text{Dispolreg 007}]_0$ (mol.L^{-1})	$[M]_0$/ $[\text{Dispolreg 007}]_0$	T (°C)	Conv (%)[a]	$M_{n,th}$[c] (g.mol^{-1})[b]	$M_{n,exp}$ (g.mol^{-1})[c]	Đ
1	1.95	7.73 x 10^{-2}	25	90	84	5 130	11 990	1.20
2	1.95	7.73 x 10^{-2}	25	95	85	5 190	5 010	1.60
3	1.95	7.73 x 10^{-2}	25	97	90	5 500	5 580	1.25
4	1.95	1.93 x 10^{-2}	100	97	86	20 600	20 200	1.30
5	1.95	9.66 x 10^{-3}	200	97	83	38 200	36 400	1.35
6	1.95	4.83 x 10^{-3}	400	97	79	72 000	66 600	1.30

[a] Calculated from ^{1}H NMR. [b] $M_{n,th} = M_{alkoxyamine} + \frac{[M]_0 \times p \times M_M}{[alkoxyamine]_0}$. [c]Extracted from SEC-MALS analysis using the measured dn/dc value for poly(THGMA) (dn/dc = 0.056 mL.g^{-1})

5.2.2.2. Chain extension of Poly(THGMA) to yield a soft/hard diblock copolymers in toluene

A poly(THGMA) macro-initiator ($[M]_0/[\text{Dispolreg 007}]_0$ = 100, $M_{n,th}$ = 23,000 g.mol^{-1}) was first prepared in toluene *via* NMP as described above and the reaction was stopped at 86 % monomer conversion. The mixture was purified by precipitation in methanol to yield a polymer with M_n = 20,600 g.mol^{-1} with $Đ$ = 1.38. The macro-initiator agent was subsequently placed in a 25 mL RBF equipped with rubber seals and a magnetic stirring bar in the presence of styrene (1.93 g, 1.84 x 10^{-2} mol, $[M]_0/[\text{macro initiator agent}]_0$ = 382) and toluene (3 g). The mixture was deoxygenated for 30 minutes purging nitrogen and subsequently placed in an oil bath at 97 °C. Polymerization was carried out under stirring for 8 hours to reach 93 % conversion. The polymer solution was quenched by cooling in contact with air, precipitated three times in methanol and dried under vacuum to yield the purified diblock copolymer (M_n = 55,000 g.mol^{-1}, $Đ$ = 1.50)

5.2.2.3. Synthesis of THGMA in NMP miniemulsion

The formulations used are given in Table 5.2. The organic phase consisted of a homogeneous mixture of THGMA (10.09 g, 4.41 x 10^{-2} mol), Dispolreg 007 (varying

amounts to target different DP_ns, see Table 5.2), and stearyl methacrylate (0.52 g, 5 wt% based-on-monomer, b-o-m) that was utilized as co-stabilizer. The aqueous phase consisted of a mixture of Dowfax 2A1 (45 *wt*% active content) (0.66 g, 3 *wt*% b-o-m) and deionised water. The organic phase was transferred to the aqueous phase and stirred for 30 min to yield a coarse pre-emulsion. Then, the pre-emulsion was sonicated using a Branson 450 sonifier operating at 80% output and 0.8 duty cycle for 10 min in an ice bath under magnetic stirring, thus yielding a stable miniemulsion.

The miniemulsion (droplet diameter in the range of 170 nm) prepared as detailed above was transferred to a round bottom flask sealed with silicone rubber and the mixture was deoxygenated purging nitrogen for 30 min. Then, the miniemulsion was placed in an oil bath at 97°C and the polymerization was carried out under stirring for 8 hours, with samples carefully taken via a deoxygenated syringe. Monomer conversion was calculated by gravimetry.

Table 5.2. Recipes for synthesis the poly(THGMA) by NMP miniemulsion.

Entry[a]	Organic phase			DP_n	Aqueous phase	
	Monomer (g)	Alkoxyamine (g)	Stearyl methacrylate (g)		Water (g)	Dowfax 2A1 (g)
7	10	0.31	0.5	50	40	0.66
8	10	0.15	0.5	100	40	0.66
9	10	0.073	0.5	200	40	0.66
10	10	0.038	0.5	400	40	0.66
11	10	0.03	0.5	500	40	0.66

[a] 20 wt.% solids content.

5.2.2.4. Poly(THGMA)-*b*-poly(CDMMA) diblock copolymers in miniemulsion

The formulations used for the synthesis of poly(THGMA)-*b*-poly(CDMMA) diblock copolymers are summarized in Table 5.3. A poly(THGMA) seed latex 10 wt% solids ($[M]_0/[\text{Dispolreg 007}]_0 = 225$, $M_{n,th} = 50{,}400$ g.mol^{-1}) was first prepared via NMP miniemulsion as described above. The reaction was stopped at 98 % monomer conversion, yielding a polymer with M_n = 50,000 g.mol^{-1} and $Đ$ = 1.13 The poly(THGA) seed latex (25 g) was charged to the reactor equipped with rubber seals and magnetic stirring bar before deoxygenation with purging nitrogen gas for 30 min.

Subsequently, the mixture of CDMMA monomer (3.5 g, $[M]_0/[\text{macro initiator}]_0 = 312$) and acetone (10 *wt*.% b-o-m) was added to the reactor and stirred for 60 min. Acetone was added to facilitate the mass transport of CDMMA to the seed particles. As discussed in Chapter 4, acetone presents the advantage of having benign toxicity and easily removable as shown in the industrial production of polyurethane dispersions.[32] The reactor was then placed in an oil bath at 97°C and allowed to polymerize for 8 hours. After polymerization, the reaction was cooled to room temperature.

5.2.2.5. Poly(THGMA)-*b*-poly(S) diblock copolymers in miniemulsion

The formulations used in these syntheses are given in Table 5.3. A poly(THGMA) seed latex 10 wt% solids ($[M]_0/[\text{Dispolreg 007}]_0 = 225$, $M_{n,th}$ = 50,400 g.mol^{-1}) was first prepared via NMP miniemulsion as described above. The reaction was stopped at 98 % monomer conversion, yielding a polymer with M_n = 50,000 g.mol^{-1} and $Đ$ = 1.13. The poly(THGA) seed latex (25 g) was charged to the reactor equipped with rubber seals and magnetic stirring bar before deoxygenation with purging nitrogen gas for 30 min. Subsequently, the mixture of styrene monomer (3.5 g, $[M]_0/[\text{macro initiator agent}]_0 = 672$) and acetone (10 wt.% b-o-m) was added to the reactor and stirred for 60 min. The reactor was then placed in an oil bath at 97°C and left to

polymerize for 8 hours. After polymerization, the reaction was cooled to room temperature.

Table 5.3. Recipes for synthesis the soft/hard diblock copolymer.

Entry	macro-initiator seed latex (g)	Monomer	Monomer (g)	Acetone (10 *wt*.% b-o-m)
12	25	CDMMA	3.5	0.35
13	25	CDMMA	1.5	0.15
14	25	Styrene	3.5	0.35
15	25	Styrene	1.5	0.15

5.2.3. Characterization

Monomer conversion was calculated from ^{1}H NMR ($CDCl_3$, 400 MHz) and gravimetric for NMP in solution and miniemulsion, respectively, the information is given in Appendix **I**.

The theoretical molar masses were calculated using equation 4, the information is given in Appendix **I**.

5.3. Results and discussion

5.3.1. NMP solution of THGMA

5.3.1.1. The effect of the temperature reaction

The synthesis of tetrahydrogeraniol methacrylate (THGMA) monomer was carried out by incorporation of a methacrylic group. The successful synthesis of the monomer was presented in Chapter 2. The bio-sourced THGMA was polymerized in toluene in the presence of the alkoxyamine Dispolreg 007 (Scheme 5.1). Previous experience in the polymerization of methacrylates using Dispolreg 007 shows that the adequate range of polymerization temperatures is about 90 ºC.[26, 27, 33] Therefore, polymerizations were carried out at 90, 95 and 97 ℃, targeting a degree of polymerization (*DP*n) of 25.

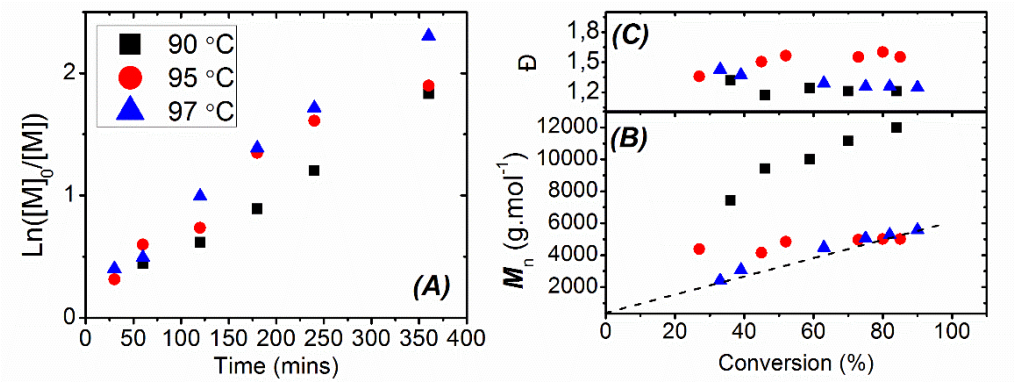

Figure 5.1. Polymerization of THGMA ($[M]_0/[Dispolreg\ 007]_0 = 25$) in toluene, $[M]_0 = 1.95\ mol.L^{-1}$ t at 90 (Squares), 95 (Circles) and 97 ºC (Up triangles). (A) Evolution of $Ln[M]_0/[M]$ as a function of time. (B) Evolution of the measured molar masses as a function of monomer conversion. (C) Evolution of the dispersity values as a function of monomer conversion.

In all cases, high conversion was reached in 6 hours. At 90 ºC, an increase of the polymerization rate over time is evident in Figure 5.1A and the molecular weight was higher than the theoretical one. Both results suggest a slow opening of Dispolreg 007 at that temperature. This problem was solved at 97 ºC, when a linear kinetic plot, good match between the theoretical and the experimental molar masses, and a low value of the dispersity were obtained (at 95 ºC, there was still some deviations of the molar masses in the first part of the reaction). Therefore, 97 ºC were retained for further reactions.

The DSC thermogram of homopoly(THGMA) (M_n = 5,500 g.mol^{-1}) is presented in Figure 5.2, showing low glass transition temperature (T_g) approximately -30 ℃. It should be noted that this T_g is higher than that of tetrahydrogeraniol acrylate (THGA) (T_g = -46 ℃) used in Chapter 4. This is likely due to the presence of the methyl group in the chain backbone of poly(THGMA) resulting in a higher steric hindrance to the segmental rotation, leading to an increase of stiffness chain that results in a higher T_g.[34]

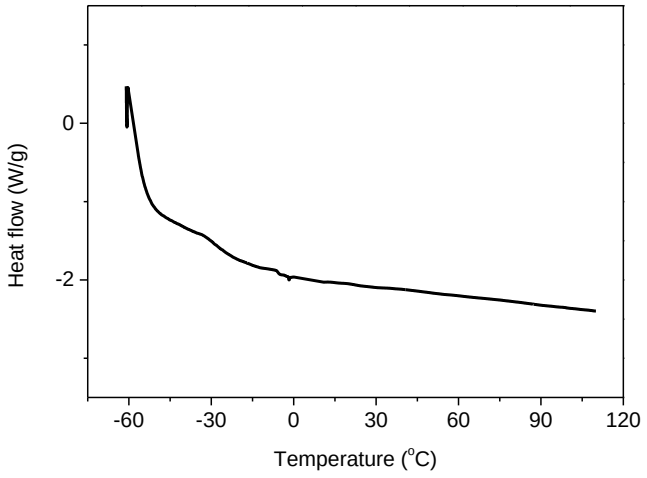

Figure 5.2. DSC thermogram of poly(THGMA) synthesized by NMP.

5.3.1.2. The effect of targeted degree of polymerization

In order to determine the extent of control over the polymerization of the THGMA biobased-monomer, reactions targeting different degrees of polymerization (*DP*n = 25, 100, 200 and 400) were carried out in toluene at 97°C. The reaction conditions, resulting monomer conversions and the molar masses are summarized in Table 5.1 (entries 3 to 6). As expected, the rate of polymerization increased by decreasing the degree of polymerization, due to the higher radical concentration (Figure 5.3A). Figure 5.3B shows that the molecular weights linearly increased with conversion and that relatively low dispersity indexes were obtained when DP_n from 25 to 200 were targeted. On the other hand, at higher targeted DP_n (DP_n = 400), the molar masses slightly deviated from the theoretical line at high monomer conversions. This might be due to the occurrence of the undesired chains such as the termination by disproportionation between the nitroxide and propagating radical and the bimolecular termination of radical species that for methacrylates occurs by disproportionation.[22, 35, 36] All these events yield an unsaturated end group, *i.e.* often called macromonomer, and result in the decrease of molecular weight as well as the broadening of dispersity, which is commonly observed in the polymerization of methyl methacrylate in NMP system.[25, 37-39]

In order to clarify this point, a poly(THGMA) with *DP*n = 400 was synthesized in toluene and the polymerization was stopped at 82 % conversion to yield a polymer with M_n = 70,000 g.mol^{-1} and $Đ$ = 1.50. The presence of macromonomer was checked with ^{1}H NMR. Figure 5.4 shows that the ^{1}H NMR spectrum revealed the vinyl resonances (δ = 6.2 and 5.5 ppm) indicative of unsaturated carbon. It could be confirmed that the disproportionation termination occurred during the course of polymerization. The percentage of macromonomer calculated from the ratio between the areas of the peaks from the macromonomer and OC$\boldsymbol{H}_2$ was 0.09 % at 82 % conversion. This small percentage can cause a decrease of *DP*n from 332 (M_n = 75,200 g.mol^{-1}) to *DP*n 309 (M_n = 70,000 g.mol^{-1}, $Đ$ = 1.50), which is close to the deviation observed in Figure 5.3B. It is worth pointing out that although this confirms the existence of side reactions, it is not possible to determine which of these reactions is the main responsible for the formation of macromonomers. The reason is that all of the side reactions give the same type of macromonomer. In this regard, it should be mentioned that Simula *et al.*[33] have shown that disproportionation between the nitroxide and the radical is the main cause of macromonomer formation at high conversions. Finally, it should be stressed that the amount of macromonomer formed with Dispolreg 007 is lower than those obtained with other NMP control agents.[33, 35, 38]

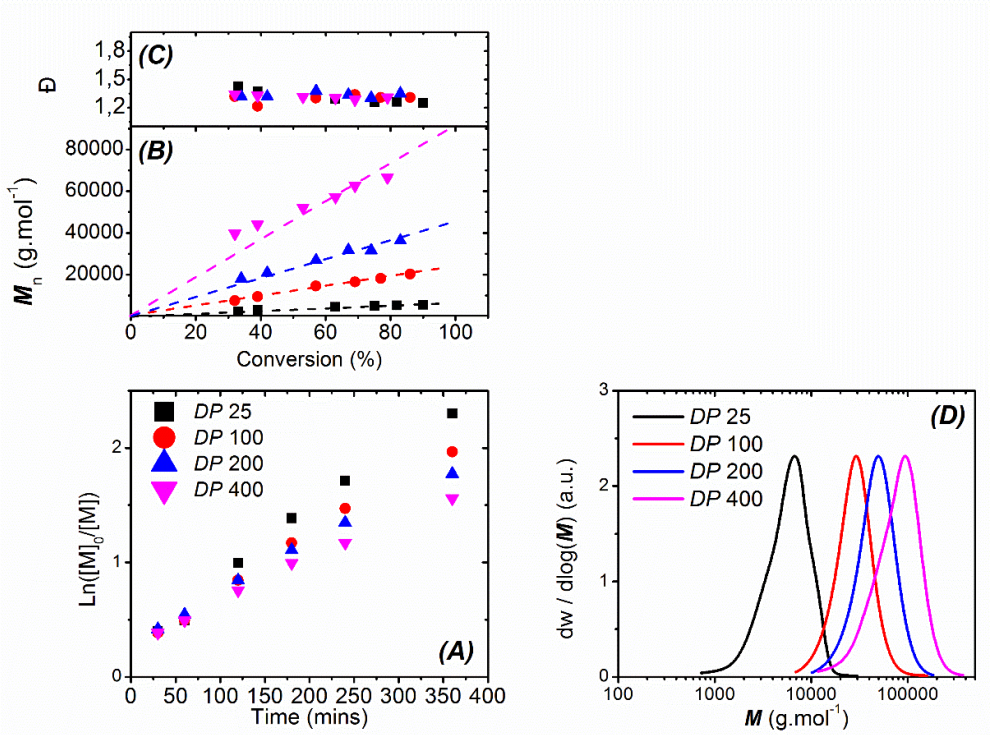

Figure 5.3. Kinetics of the polymerization of THGMA at 97 °C in toluene via NMP at various targeting degree of polymerization (Squares) *DP*n 25; (Circles) *DP*n 100; (Up triangles) *DP*n 200; (Down triangles) *DP*n 400. (A) Evolution of Ln($[M]_0/[M]$) as a function of time. (B) Evolution of the measured molar masses as a function of monomer conversion; the dash lines are a guide for the eye. (C) Evolution of the dispersity values as a function of monomer conversion. (D) Molar mass distributions (from SEC-MALS) of the final sample of poly(THGMA).

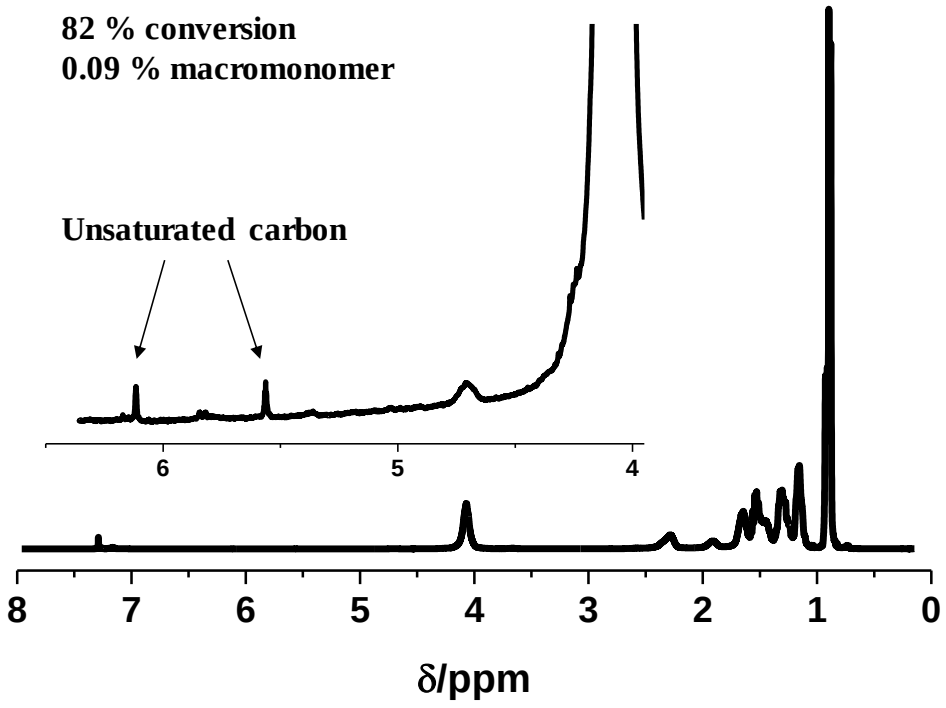

Figure 5.4. ^{1}H NMR ($CDCl_3$, 400 MHz) of poly(THGMA) ($[M]_0/[\text{Dispolreg 007}]_0$ = 400, M_n = 70,000 g.mol^{-1}, $Đ$ = 1.50 at 82 % conversion) prepared by NMP in toluene at 97 °C.

5.3.1.3. Diblock copolymers

One of the most attractive aspects of the RDRP is the ability to synthesize block copolymers. In order to test the versatility of the Dispolreg 007 to form block copolymers, styrene was used to form a soft/hard diblock copolymer. To this end, a

poly(THGMA) was prepared in toluene via NMP (90 % conversion, M_n = 20,600 g.mol^{-1} with $Đ$ 1.30). Subsequently, styrene was added to the mixture as a single shot and polymerized at 97 °C for 8 hours. The success of the chain extension is shown in Figure 5.5A, where it can be seen that the MMD of the copolymer shifted toward higher molar masses (98 % conversion, M_n = 55,000 g.mol^{-1}) with a relatively low dispersity. Herein, the soft/hard diblock copolymer contained 41 *wt*.% of poly(THGMA), and 59 *wt*.% of poly(S).

Figure 5.5B presents the AFM image of the copolymer. It can be seen that the diblock copolymer clearly showed a two-phase lamellae morphology (the bright domains correspond to poly(styrene) and the dark ones to poly(THGMA)). In agreement with the theoretical predictions that when the fractions of both polymers are similar, a lamellae structure is formed.[40]

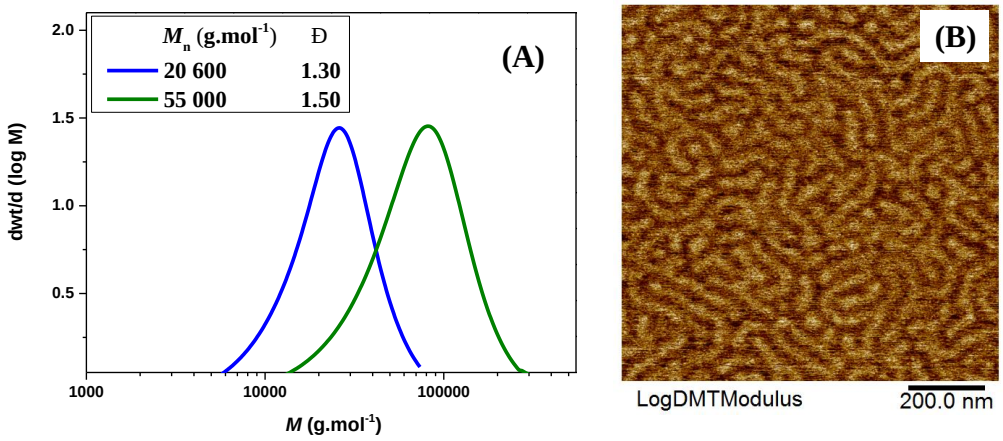

Figure 5.5. (A) SEC traces of the chain extension of a poly(THGMA) macro-initiator agent with styrene in toluene at 97 °C for 8 hours. (B) AFM picture of poly(THGMA)-*b*-poly(S) soft/hard diblock copolymer (log DMT modulus with scale bar = 200 nm). The molecular weight was extracted from SEC-MALS analysis using the measured dn/dc value for poly(THGMA) (dn/dc = 0.056 mL.g^{-1}) and poly(styrene) (*dn/dc* = 0.187 mL.g^{-1}).

5.3.2. NMP miniemulsion of THGMA

5.3.2.1. The effect of targeted degree of polymerization

Once it was checked that the NMP of THGMA could be carried out under controlled conditions by using Dispolreg 007, the NMP of THGMA in miniemulsion was addressed. DP_n*s* ranging from 50 to 500 were tested to evaluate the degree of control of the system. As observed when the THGMA was polymerized in NMP

solution, polymerization rate increased when lower *DP*n was targeted due to higher radical concentration (Figure 5.6A). Figure 5.6B shows that the particle size was constant all along the polymerization, indicating the efficient droplet nucleation and the good colloidal stability of the system. The evolution of molecular weights increased linearly with the conversion and approached to the theoretical lines with relatively low dispersity values (*Đ*~1.25) as shown in Figure 5.6C and Table 5.4. Pleasingly, at high targeted *DP*n (*DP*n 400 and 500), the molecular weights were still close to the predicted line, which differs from the results observed in the polymerization of THGMA in toluene. This could be attributed to the effect of the compartmentalization, which can decrease the rate of termination between propagating radicals due to the segregation of the propagating radicals in the different particles.[41] However, this would imply that bimolecular radical termination is the main side reaction and Simula *et al*.[33] have shown that this is not the case and that the main reason is the disproportionation between a propagating and nitroxide radicals. A more likely reason for the lower prominence of the nitroxide-propagating radical disproprotionation is the fast recombination of the propagation radical and the nitroxide resulting from the activation of the macroalkoxyamine in the confined environment of the polymer particle. This recombination will decrease the concentration of free and nitroxide radicals and therefore the disproportionation is less likely. It has been suggested that in the case of

radical polymerization where various reactions are competing (*e.g.* propagation, transfer to polymer, disproportionation), the reaction of higher rate (*e.g.* reversible deactivation in RDRP) could suppress the reaction of slower rate (*e.g.* chain transfer to polymer).[42]

Table 5.4. Conversion, molar masses and dispersity values of poly(THGMA) by NMP miniemulsion.

Entry	$[M]_0$/[Dispolreg 007]$_0$	Conv.[a] (%)	dp (nm)	$M_{n,th}$[b] (g.mol^{-1})	$M_{n,exp}$[c] (g.mol^{-1})	$Đ$
7	50	97	167	11 340	11 000	1.24
8	100	90	170	21 220	24 480	1.26
9	200	93	178	43 570	42 430	1.28
10	400	90	170	80 970	81 720	1.37
11	500	78	170	89 390	93 390	1.31

[a] Calculated by gravimetry. [b] $M_{n,th} = M_{alkoxyamine} + \frac{[M]_0 \times p \times M_M}{[alkoxyamine]_0}$. [c]Extracted from SEC-MALS analysis using the measured dn/dc value for poly(THGMA) (dn/dc = 0.056 mL.g^{-1})

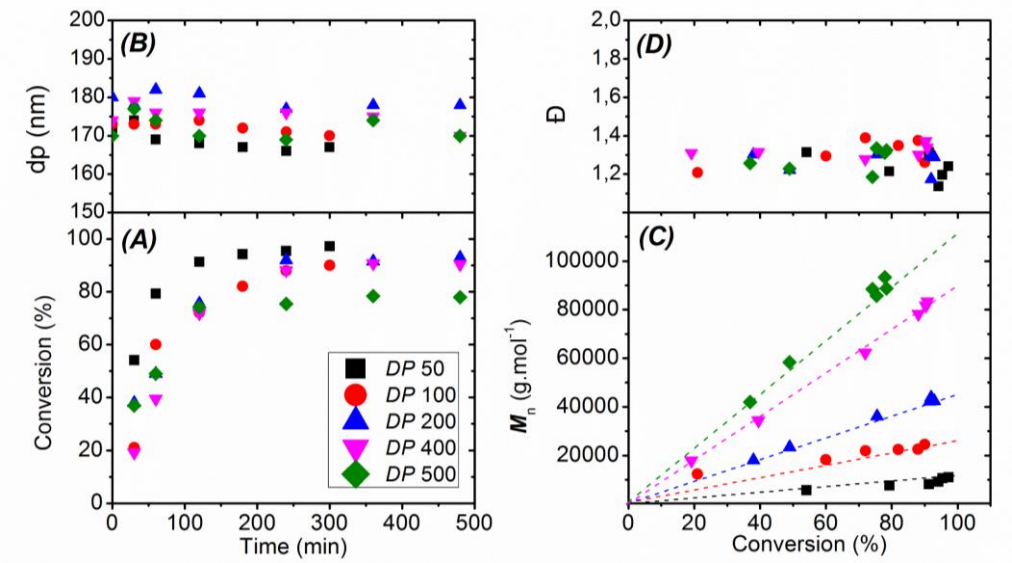

Figure 5.6. Kinetics of the polymerization of THGMA at 97 °C in NMP miniemulsion at various targeted degree of polymerization (Squares) *DP*n 50; (Circles) *DP*n 100; (Up triangles) *DP*n 200; (Down triangles) *DP*n 400 and (Diamond) *DP*n 500. (A) Evolution of the Ln($[M]_0/[M]$) as a function of time. (B) Evolution of the particle size as a function of time. (C) Evolution of the measured molar masses as a function of monomer conversion; the dash lines are a guide for the eye. (D) Evolution of the dispersity values as a function of monomer conversion.

5.3.2.2. Diblock copolymers

The successful polymerization of THGMA via NMP in aqueous media being achieved, the synthesis of waterborne adhesive based on full terpene soft/hard diblock

copolymers was targeted. THGMA (T_g = -30 ℃) and CDMMA (T_g = 92 ℃) were used for the soft and hard segments, respectively.

A macro-initiator of poly(THGMA) was synthesized using Dispolreg 007 in nitroxide mediated miniemulsion polymerization ($[M]_0/[\text{Dispolreg 007}]_0$ = 225), the reaction was stopped at 98 % conversion with M_n = 50,000 g.mol^{-1} and $Đ$ = 1.13. Subsequently, a mixture of CDMMA (3.5 g, $[M]_0/[\text{macro-initiator}]_0$ = 312) and acetone (10 wt% based on monomer) was added to the poly(THGMA) latex and polymerized at 97 ℃ for 8 hours. In this way, the full terpene soft/hard diblock copolymers of poly(THGMA)$_{50000}$-*b*-poly(CDMMA)$_{74000}$ and poly(THGMA)$_{50000}$-b-poly(CDMMA)$_{27000}$) were synthesized. The block copolymers prepared are summarized in Table 5.5. It should be highlighted that the synthesis of the diblock copolymers in miniemulsion was carried out without using any intermediate purification. This is necessary for industrial implementation.

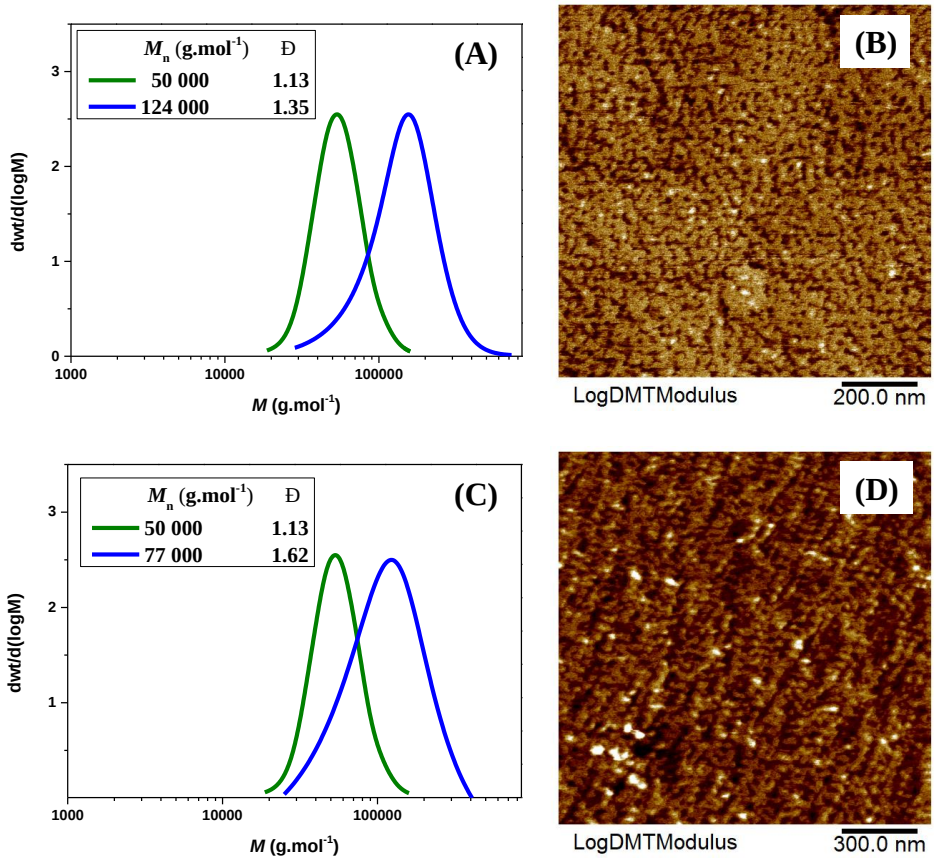

Figure 5.7. ***(A)*** SEC traces and ***(B)*** AFM picture of a poly(THGMA)$_{50000}$-*b*-poly(CDMMA)$_{74000}$ soft/hard diblock copolymer via chain extension of poly(THGMA) macro-initiator agent with CDMMA. ***(C)*** SEC traces and ***(D)*** AFM picture of a poly(THGMA)$_{50000}$-*b*-poly(CDMMA)$_{27000}$ soft/hard diblock copolymer via chain extension of poly(THGMA) macro-initiator agent with CDMMA. The molecular weights were extracted from SEC-MALS analysis using the measured dn/dc value for poly(THGMA) (dn/dc = 0.056 mL.g^{-1}) and poly(CDMMA) (*dn/dc* = 0. 0.089 mL.g^{-1}).

The success of the chain extension of poly(THGMA) macroinitiator with CDMMA is evidenced in Figure 5.7. SEC analyses show a shift toward to higher molar masses (97 % conversion, M_n = 124,000 g.mol^{-1} for poly(THGMA)$_{50000}$-*b*-poly(CDMMA)$_{74000}$ and 89 % conversion, M_n = 77,000 g.mol^{-1} for (poly(THGMA)$_{50000}$-*b*-poly(CDMMA)$_{27000}$. A monomodal distribution is obtained for the diblock copolymers with relatively low dispersity values. Subsequently, the phase-separated morphology of poly(THGMA)-*b*-poly(CDMMA) diblock copolymer was analyzed via AFM. Figures 5.7B and D show two-phase morphologies between soft and hard segments, which consist of the dark and bright domain relative to poly(THGMA) and poly(CDMMA), respectively. Theoretically, as a result of relative percentage of each domain (Table 5.5) a lamellae structure should be obtained for poly(THGMA) -*b*-poly(CDMMA) diblock coplymers. However, a relatively limited segregation between soft and hard phases is observed resulting in a mixed phase transition. This may be due to the presence of some dispersity in both molecular weights and chain composition, thus limiting the segregation of the soft and hard phases into one defined transition.[43, 44]

Table 5.5. Preparation of terpene-based soft/hard copolymers.

Entry	macro-initiator th [a] (g.mol^{-1})	macro-initiator exp [b] (g.mol^{-1})	Conv. (%)	M_n diblock th [a] (g.mol^{-1})	M_n diblock exp [b] (g.mol^{-1})	$Đ$	dp (nm)	Coagulation (*wt.*%)	Soft polymer (*wt.*%)	Hard polymer (*wt.*%)	T_g (°C)	T_g (°C)
12	50 400	50 000	97	117 900	124 000	1.35	228	n/a	48	52	-25	90
13	50 400	50 000	89	76 700	77 000	1.62	275	n/a	59	41	-29	90
14	50 400	50 000	95	118 900	127 000	1.30	205	n/a	36	64	-30	89
15	50 400	50 000	97	79 100	79 400	1.68	247	n/a	63	37	-31	94

[a] $M_{n,th} = M_{alkoxyamine} + \frac{[M]_0 \times p \times M_M}{[alkoxyamine]_0}$. [b] Extracted from SEC-MALS analysis using the measured *dn/dc* values for poly(THGMA) (*dn/dc* = 0.0568 mL.g^{-1}), poly(CDMMA) (*dn/dc* = 0.0897 mL.g^{-1}) and poly(styrene) (*dn/dc* = 0.187 mL.g^{-1}). [c] Calculated from gravimetic

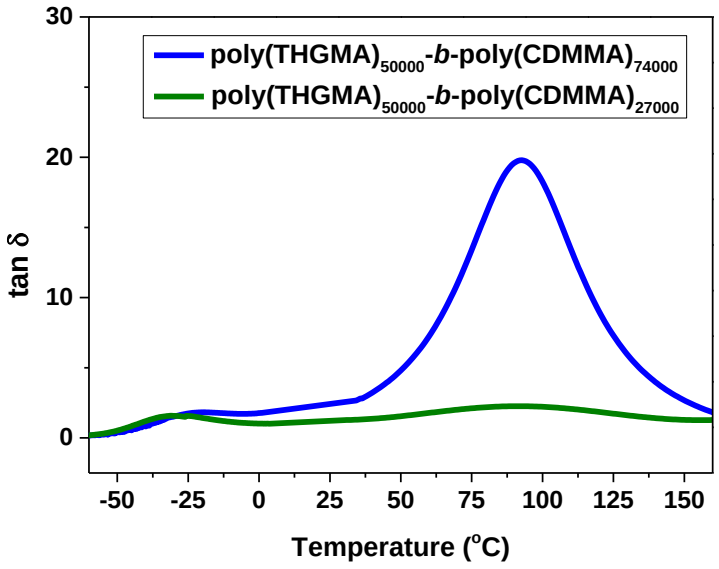

Figure 5.8. *Tan δ* as a function of the temperature of the poly(THGMA)-*b*-poly(CDMMA) soft/hard diblock copolymer. The rheology of the block copolymers was performed using parallel plate geometry with constant strain on a rotational rheometer (TA ARES). Mechanical spectroscopy experiment was performed at frequency 0.1 rad/s over the temperature from 160 to -60 ˚C.

In addition, the phase-separated of soft/hard diblock copolymer was further investigated with rheological measurements. Figure 5.8 shows that the poly(THGMA)-*b*-poly(CDMMA) diblock copolymer, presented two distinct glass transition temperatures. The low temperature (-25 ℃ to -29 ℃) corresponds to the poly(THGMA) phase and the high one is related to poly(CDMMA). The T_gs of the diblock copolymers are summarized in Table 5.5.

Soft/hard diblock copolymers of similar molecular weights to those of THGMA/CDMMA, but using styrene instead CDMMA were synthesized to compare the adhesive properties. Poly(THGMA) (10 wt% solids content) was prepared via NMP miniemulsion using Dispolreg 007. The reaction was stopped at 98 % conversion obtaining a polymer with M_n = 50,000 g.mol^{-1} and $Đ$ = 1.13. Subsequently, without any purification step, styrene (3.5 g, $[M]_0/[\text{macro initiator}]_0$ = 672 and 1.5 g $[M]_0/[\text{macro initiator}]_0$ = 288) mixed with the acetone (10 wt% based on monomer) was added to the (THGMA) latex and polymerized at 97 °C for 8 hours. After polymerization, soft/hard diblock copolymers (poly(THGMA)$_{50000}$-*b*-poly(S)$_{77000}$ and poly(THGMA)$_{50000}$-*b*-poly(S)$_{29400}$) were obtained. In Figure 5.9, SEC evidences the success of the chain extension as in both cases the MWD is shifted to higher molar masses after chain extension with styrene (95 % conversion, M_n = 127,000 g.mo^{-1} and 97 % conversion, M_n = 79,400 g.mol^{-1})). A monomodal distribution was obtained for the diblock copolymers with a slight increase in dispersity. The broadening of the molecular weight distribution that was also observed for the poly(THGMA)-*b*-poly(CDMMA) diblock copolymers (Figure 5.7) might be due to the small fraction of dead chains formed during the synthesis of the macro-initiator.

Figures 5.9 B and D present the AFM images of the morphology of the copolymer. It can be seen that well-organized of the lamellae and gyriod structures were obtained for poly(THGMA)$_{50000}$-*b*-poly(styrene)$_{77000}$ and poly(THGMA)$_{50000}$-*b*-poly(styrene)$_{29400}$, respectively, which differs from the poly(THGMA)-*b*-poly(CDMMA) diblock copolymers under the same conditions (same targeted molecular weight). This could be due to the effect of interaction parameter (Flory-Huggins interaction parameter, χ) between poly(THGMA) and poly(CDMMA) or poly(S), which affects the block copolymer segregation.[45, 46] It can be seen that at high value interaction parameters (THGMA vs S) led to strong segregation. On the other hand, lower value interaction parameters (THGMA vs CDMMA) led to weaker segregation (Figure 5.7B and D).

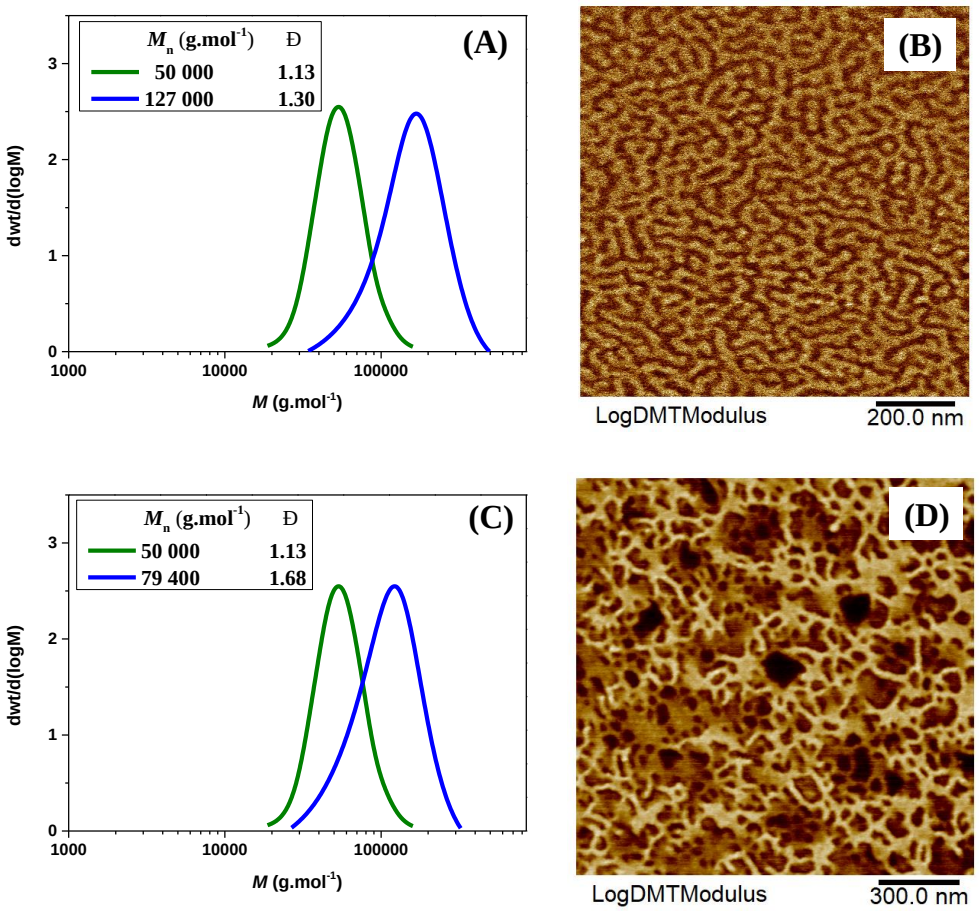

Figure 5.9. (A) SEC traces and (B) AFM picture of a poly(THGMA)$_{50000}$-*b*-poly(styrene)$_{77000}$ AB diblock copolymer via chain extension of poly(THGMA) macro-initiator agent with styrene. (C) SEC traces and (D) AFM picture of a poly(THGMA)$_{50000}$-*b*-poly(styrene)$_{29400}$ AB diblock copolymer via chain extension of poly(THGMA) macro-initiator agent with styrene.

5.3.2.3. Adhesive properties of diblock copolymers

The adhesive properties (work of adhesion from probe-tack, 180º peel strength and shear resistance) of the block copolymers were investigated. The results are summarized in Table 5.6 and the probe-tack curves are given in Figures 5.10A and 5.11A. It can be seen that for both classes of block copolymers, the work of adhesion and the shear resistance increased and peel resistance decreased when the length of the hard block (CDMMA or S) decreased. This is an unexpected result because, usually, work of adhesion and shear resistance show opposite trends.[47] Peel resistance can align with both the work of adhesion and shear. In order to shed light on these findings, linear rheology measurements were carried out and they are included in Figures 5.10 and 5.11.

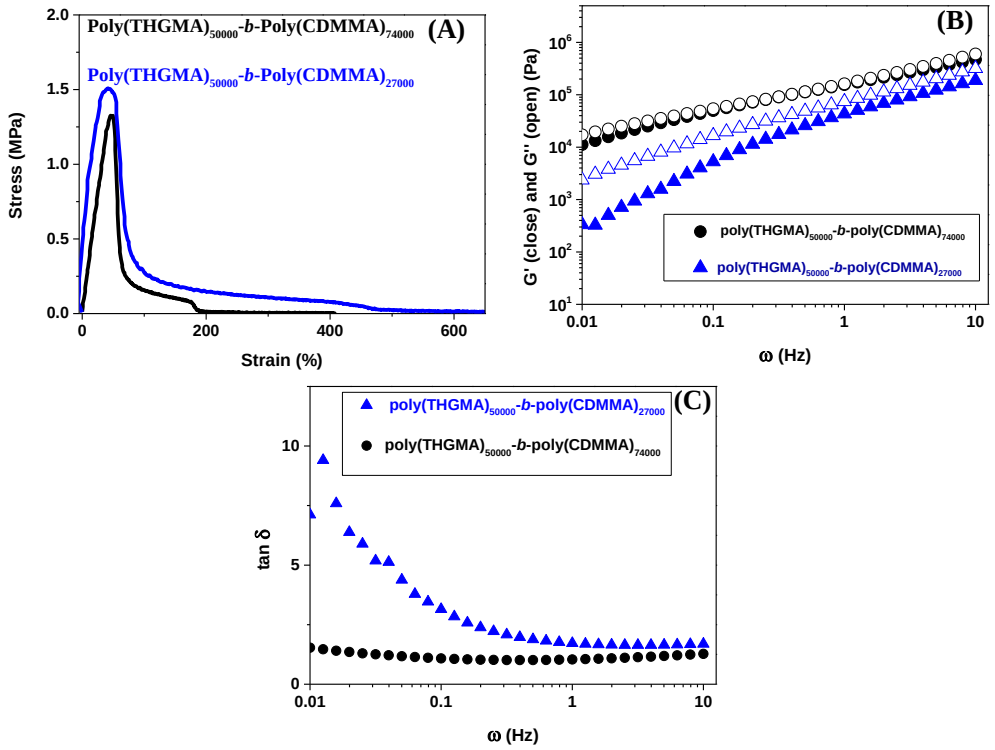

Figure 5.10. Evolution of adhesive properties for poly(THGMA)-*b*-poly(CDMMA) soft/hard diblock copolymer. (A) Stress-strain curve of the probe-tack test. (B) G' and G'' as a function of frequency at room temperature. (C) tan δ as a function of frequency at room temperature.

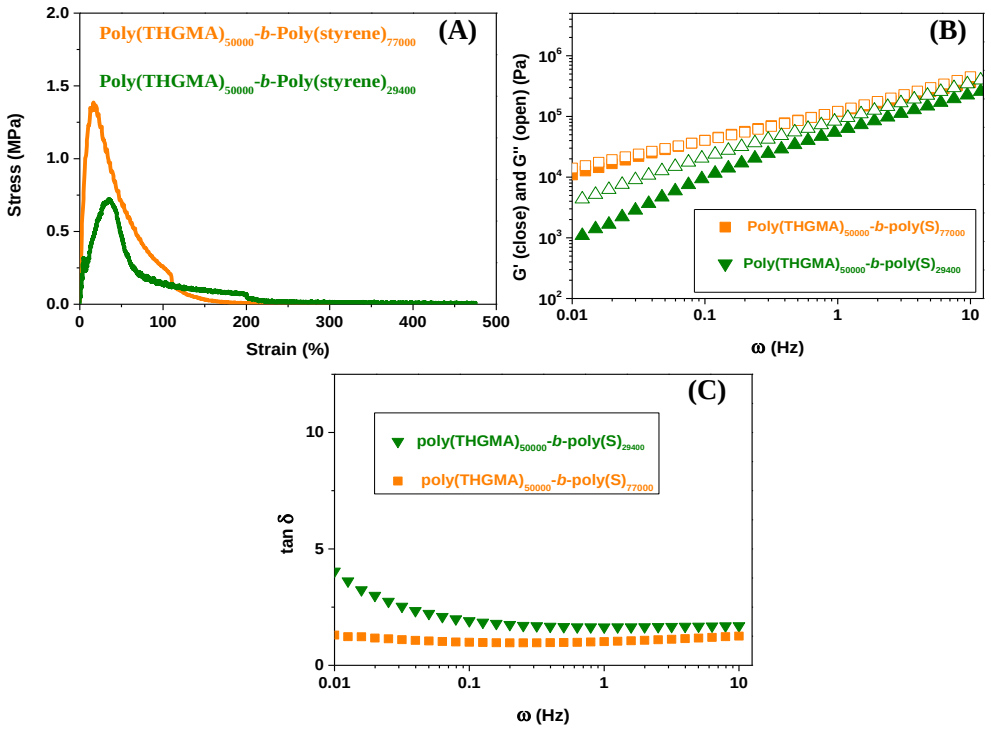

Figure 5.11. Evolution of adhesive properties for poly(THGMA)-*b*-poly(S) soft/hard diblock copolymer. (A) Stress-strain curve of the probe-tack test. (B) G' and G'' as a function of frequency at room temperature. (C) tan δ as a function of frequency at room temperature.

They show the expected result, for the two types of block copolymers, both G' and G'' increased with the content of hard polymer. However, although they may

justify the results for work of adhesion and peel, this does not justify the results obtained in the shear tests.

A point in the adhesive tests that is remarkable is the adhesive failure observed in the shear tests. Considering that the molecular weight of the block copolymers is relatively low (at least if they are compared with the common acrylic PSAs) and that the linear rheology shows a liquid behavior at low frequencies, one would expect a cohesive failure as it was observed in Chapter 4 for the tri-block copolymers. The adhesive failure suggests the presence of a weak interface. This weak interface could be formed by relatively shorter and softer chains that preferentially migrate to the interface.

In the discussion on the synthesis of the block copolymers, it was commented that the increase of dispersity observed during chain extension was due to terminations occurring during both the synthesis of the macro-initiator or during chain extension. In both cases, the dead polymer chains will have shorter lengths and will be softer than the average block copolymer. Migration of these chains to the film-substrate interface will lead to the formation of weak boundary. Migration is expected to be stronger for less compatible polymers.[48] In this regard, the compatibility between a THGMA-rich or even pure polymer chains and the block copolymers will be less when the fraction

of hard monomer (CDMMA or St) increased, namely that more migration is expected for THGMA/CDMMA = 50,000/74,000 than for THGMA/CDMMA = 50,000/27,000 and for THGMA/St = 50,000/77,000 than for THGMA/St = 50,000/29,400.

This may justify the results of the adhesive tests because increase of the hard monomer content will result in a decrease of the work of adhesion and an increase in the peel resistance that agree with the rheological measurements. In parallel, the increase in the hard monomer content enhanced the migration of the short and soft polymer chains to form a weak boundary layer that lowered the shear resistance through an adhesive failure. This weak layer may take some time to form and therefore it was more evident in the low frequency shear test.

Table 5.6 also shows that the fully bio-sourced PSAs compared well with the PSAs containing S, which opens the possibility to substitute petrol-based monomers by bio-sourced ones.

Table 5.6. Adhesion properties of soft/hard diblock copolymers.

Block copolymer	Work of adhesion (J/m^2)	Peel (N/25mm)	Shear resistance (min)	Type of failure
Poly(THGMA)$_{50000}$-*b*-poly(CDMMA)$_{74000}$	85±5.6	13± 0.2	25± 0.7	Adhesion
Poly(THGMA)$_{50000}$-*b*-poly(CDMMA)$_{27000}$	132±11	9 ± 1.4	35± 1.5	Adhesion
Poly(THGMA)$_{50000}$-*b*-poly(S)$_{77000}$	65±6.7	24 ± 2.3	18± 2.5	Adhesion
Poly(THGMA)$_{50000}$-*b*-poly(S)$_{29400}$	96±11	17± 0.3	25± 3.2	Adhesion

Comparison with the acrylates-based tri-block copolymers obtained in Chapter 4 shows that the methacrylate-based block copolymers presented better adhesive properties. However, as no attempt to optimize the PSAs was done and no formulated adhesives were used, no conclusions about the final performance of these PSAs can be made.

5.4. Conclusions

This chapter presents the synthesis of block copolymers from bio-sourced terpene-based methacrylates by nitroxide mediated polymerization and their use as pressure sensitive adhesives. First, the ability of an alkoxyamine recently developed in our lab (Dispolreg 007) to control the polymerization of tetrahydrogeraniol methacrylate (THGMA) in solution of toluene was investigated. Good control over the polymerization was obtained up to *DP*n 200. At higher targeted *DP*n, formation of macromonomer was observed, which led to a reduced molar mass compared to the targeted value. When the process was carried out in miniemulsion, excellent control over the polymerization of THGMA could be achieved up to *DP*n 500 and narrow molecular weight distributions at high conversion were obtained. The improvement was attributed to the fast recombination of the radical and the nitroxide in the confined environment of the polymer particle. Terpene-based soft/hard diblock copolymers were synthesized starting with a THGMA macroradical with varying the molecular weight of hard polymer (CDMMA). Diblock THGMA-S copolymers were also synthesized for comparison purposes. SEC showed a successful chain extension in all cases, although the increase in dispersity indicated the presence of a small fraction of dead chains. Well-defined phase-separation between soft and hard polymers were observed.

The adhesive properties of the diblock copolymers were evaluated with probe tack, peel strength and shear resistance. It was found that migration of the short polymer chains could affect the shear resistance. The adhesive performance of the fully bio-sourced PSAs was comparable to the partially petroleum-based styrene systems and better than that found for the acrylates-based triblock copolymers in Chapter 4.

5.5. References

(1). Gandini, A. The irruption of polymers from renewable resources on the scene of macromolecular science and technology. *Green Chem.* **2011,** 13, 1061-1083.

(2). Ragauskas, A. J.; Williams, C. K.; Davison, B. H.; Britovsek, G.; Cairney, J.; Eckert, C. A.; Jr, W. J. F.; Hallett, J. P.; Leak, D. J.; Liotta, C. L.; Mielenz, J. R.; Murphy, R.; Templer, R.; Tschaplinski, T. The Path Forward for Biofuels and Biomaterials. *Science* **2006,** 311, 484-489.

(3). Huber, G. W.; Iborra, S.; Corma, A. Synthesis of Transportation Fuels from Biomass: Chemistry, Catalysts, and Engineering. *Chem. Rev.* **2006,** 106, 4044-4098.

(4). Okada, M. Chemical syntheses of biodegradable polymers. *Prog. Polym. Sci.* **2002,** 27, 87-133.

(5). Holmberg, A. L.; Reno, K. H.; Wool, R. P.; Thomas H. Epps, I. Biobased building blocks for the rational design of renewable block polymers. *Soft Matter* **2014,** 10, 7405-7424.

(6). Llevot, A.; Grau, E.; Carlotti, S.; Grelier, S.; Cramail, H. From Lignin-derived Aromatic Compounds to Novel Biobased Polymers. *Macromol. Rapid Commun.* **2016,** 37, 9-28.

(7). Gallagher, J. J.; Hillmyer, M. A.; Reineke, T. M. Isosorbide-based Polymethacrylates. *ACS Sustainable Chem. Eng.* **2015,** 3, 662-667.

(8). Asua, J. M. Challenges for industrialization of miniemulsion polymerization. *Prog. Polym. Sci.* **2014,** 39, 1797-1826.

(9). Solomon, D. H.; Rizzardo, E.; Cacioli, P. Polymerization process and polymers produced thereby. 1986.

(10). Hawker, C. J.; Bosman, A. W.; Harth, E. New Polymer Synthesis by Nitroxide Mediated Living Radical Polymerizations. *Chem. Rev.* **2001,** 101, 3661-3688.

(11). Nicolas, J.; Guillaneuf, Y.; Lefay, C.; Bertin, D.; Gigmes, D.; Charleux, B. Nitroxide-mediated polymerization. *Prog. Polym. Sci.* **2013,** 38, 63-235.

(12). Moad, G.; Rizzardo, E.; Thang, S. H. Living Radical Polymerization by the RAFT Process – A Third Update. *Aust. J. Chem.* **2012,** 65, 985-1076.

(13). Ouchi, M.; Terashima, T.; Sawamoto, M. Transition Metal-Catalyzed Living Radical Polymerization: Toward Perfection in Catalysis and Precision Polymer Synthesis. *Chem. Rev.* **2009,** 109, 4963-5050.

(14). Matyjaszewski, K. Atom Transfer Radical Polymerization (ATRP): Current Status and Future Perspectives. *Macromolecules* **2012,** 45, 4015-4039.

(15). Anastasaki, A.; Nikolaou, V.; Nurumbetov, G.; Wilson, P.; Kempe, K.; Quinn, J. F.; Davis, T. P.; Whittaker, M. R.; Haddleton, D. M. Cu(0)-Mediated Living Radical Polymerization: A Versatile Tool for Materials Synthesis. *Chem. Rev.* **2016,** 116, 835-877.

(16). Destarac, M. Controlled Radical Polymerization: Industrial Stakes, Obstacles and Achievements. *Macromol. React. Eng.* **2010,** 4, 165-179.

(17). Destarac, M. Industrial development of reversible-deactivation radical polymerization: is the induction period over? *Polym. Chem.* **2018,** 9, 4947-4967.

(18). Willcock, H.; O'Reilly, R. K. End group removal and modification of RAFT polymers. *Polym. Chem.* **2010,** 1, 149-157.

(19). Tsarevsky, N. V.; Matyjaszewski, K. "Green" Atom Transfer Radical Polymerization: From Process Design to Preparation of Well-Defined Environmentally Friendly Polymeric Materials. *Chem. Rev.* **2007,** 107, 2270-2299.

(20). Simula, A.; Ballard, N.; Asua, J. M., Nitroxide Mediated Polymerization. In *In Nitroxides Synthesis, Properties and Applications*, Gigmes, D., Ed. 2019.

(21). Harrisson, S.; Couvreur, P.; Nicolas, J. SG1 Nitroxide-Mediated Polymerization of Isoprene: Alkoxyamine Structure/Control Relationship and α,ω–Chain-End Functionalization. *Macromolecules* **2011,** 44, 9230-9238.

(22). Dire, C.; Belleney, J.; Nicolas, J.; Bertin, D.; Magnet, S.; Charleux, B. β-Hydrogen transfer from poly(methyl methacrylate) propagating radicals to the nitroxide SG1: Analysis of the chain-end and determination of the rate constant. *J. Polym. Sci. A Polym. Chem.* **2008,** 46, 6333-6345.

(23). Benoit, D.; Chaplinski, V.; Braslau, R.; Hawker, C. J. Development of a Universal Alkoxyamine for "Living" Free Radical Polymerizations. *J. Am. Chem. Soc.* **1999,** 121, 3904-3920.

(24). Guillaneuf, Y.; Gigmes, D.; Marque, S. R. A.; Astolfi, P.; Greci, L.; Tordo, P.; Bertin, D. First Effective Nitroxide-Mediated Polymerization of Methyl Methacrylate. *Macromolecules* **2007,** 40, 3108-3114.

(25). Greene, A. C.; Grubbs, R. B. Nitroxide-Mediated Polymerization of Methyl Methacrylate and Styrene with New Alkoxyamines from 4-Nitrophenyl 2-Methylpropionat-2-yl Radicals. *Macromolecules* **2010,** 43, 10320-10325.

(26). Ballard, N.; Aguirre, M.; Simula, A.; Agirre, A.; Leiza, J. R.; Asua, J. M.; Es, S. v. New Class of Alkoxyamines for Efficient Controlled Homopolymerization of Methacrylates. *ACS Macro Lett.* **2016,** 5, 1019-1022.

(27). Simula, A.; Aguirre, M.; Ballard, N.; Veloso, A.; Leiza, J. R.; Es, S. v.; Asua, J. M. Novel alkoxyamines for the successful controlled polymerization of styrene and methacrylates. *Polym. Chem.* **2017,** 8, 1728-1736.

(28). Simula, A.; Ballard, N.; Aguirre, M.; Leiza, J. R.; Es, S. v.; M.Asua, J. Nitroxide mediated copolymerization of acrylates, methacrylates and styrene: The importance of side reactions in the polymerization of acrylates. *Eur. Polym. J.* **2019,** 110, 319-329.

(29). Ballard, N.; Aguirre, M.; Simula, A.; Leiza, J. R.; Es, S. v.; Asua, J. M. High solids content nitroxide mediated miniemulsion polymerization of n-butyl methacrylate. *Polym. Chem.* **2017,** 8, 1628-1635.

(30). Ballard, N.; Aguirre, M.; Simula, A.; Leiza, J. R.; Es, S. v.; M.Asua, J. Nitroxide mediated suspension polymerization of methacrylic monomers. *Chem Eng J* **2017,** 316, 655-662.

(31). Ballard, N.; Simula, A.; Aguirre, M.; Leiza, J. R.; Es, S. v.; M.Asua, J. Synthesis of poly(methyl methacrylate) and block copolymers by semi-batch nitroxide mediated polymerization. *Polym. Chem.* **2016,** 7, 6964-6972.

(32). Dieterich, D. Aqueous emulsions, dispersions and solutions of polyurethanes; synthesis and properties. *Progress in Organic Coatings* **1981,** 9, 281-340.

(33). Simula, A.; Ruipérez, F.; Ballard, N.; Leiza, J. R.; Es, S. v.; Asua, J. M. Why can Dispolreg 007 control the nitroxide mediated polymerization of methacrylates? *Polym. Chem.* **2019,** 10, 106-113.

(34). Gilbert, M., Chapter 4 - Relation of Structure to Thermal and Mechanical Properties. In *Brydson's Plastics Materials (Eighth Edition)*, Gilbert, M., Ed. Butterworth-Heinemann: 2017; pp 59-73.

(35). Mchale, R.; Aldabbagh, F.; Zetterlund, P. B. The role of excess nitroxide in the SG1 (N-tert-butyl-N-[1-diethylphosphono-(2,2-dimethylpropyl)] nitroxide)-mediated polymerization of methyl methacrylate. *J. Polym. Sci. A Polym. Chem.* **2007,** 45, 2194-2203.

(36). Ananchenko, G. S.; Souaille, M.; Fischer, H.; Mercier, C. L.; Tordo, P. Decomposition of model alkoxyamines in simple and polymerizing systems. II. Diastereomeric N-(2-methylpropyl)-N-(1-diethyl-phosphono-2,2-dimethyl-propyl)-aminoxyl-based compounds. *J. Polym. Sci. A Polym. Chem.* **2002,** 40, 3264-3283.

(37). Guillaneuf, Y.; Gigmes, D.; Marque, S. R. A.; Tordo, P.; Bertin, D. Nitroxide-Mediated Polymerization of Methyl Methacrylate Using an SG1-Based Alkoxyamine: How the Penultimate Effect Could Lead to Uncontrolled and Unliving Polymerization. *Macromol. Chem. Phys.* **2006,** 207, 1278-1288.

(38). Souaille, M.; Fischer, H. Living Free Radical Polymerizations Mediated by the Reversible Combination of Transient Propagating and Persistent Nitroxide Radicals. The Role of Hydroxylamine and Alkene Formation. *Macromolecules* **2001,** 34, 2830-2838.

(39). Burguière, C.; Dourges, M.-A.; Charleux, B.; Vairon, J.-P. Synthesis and Characterization of ω-Unsaturated Poly(styrene-b-n-butyl methacrylate) Block Copolymers Using TEMPO-Mediated Controlled Radical Polymerization. *Macromolecules* **1999,** 32, 3883-3890.

(40). Tseng, Y.-C.; Darling, S. B. Block Copolymer Nanostructures for Technology. *Polymers* **2010,** 2, 470-489.

(41). Maehata, H.; Buragina, C.; Cunningham, M.; Keoshkerian, B. Compartmentalization in TEMPO-Mediated Styrene Miniemulsion Polymerization. *Macromolecules* **2007,** 40, 7126-7131.

(42). Ballard, N.; Rusconi, S.; Akhmatskaya, E.; Sokolovski, D.; Cal, J. C. d. l.; Asua, J. M. Impact of Competitive Processes on Controlled Radical Polymerization. *Macromolecules* **2014,** 47, 6580-6590.

(43). Jullian, N.; Rubatat, L.; Gerard, P.; Peyrelasse, J.; Derail, C. Structure and rheology of di- and triblock copolymers of polystyrene and poly(n-butyl acrylate). *J. Rheol.* **2011,** 55, 379-400.

(44). Matsen, M. W. Polydispersity-induced macrophase separation in diblock copolymer melts. *Phys. Rev. Lett.* **2007,** 99, 148304.

(45). Gu, X.; Gunkel, I.; Russell, T. P. Pattern transfer using block copolymers. *Philos Trans A Math Phys Eng Sci.* **2013,** 371, 20120306.

(46). Sinturel, C.; Bates, F. S.; Hillmyer, M. A. High χ–Low N Block Polymers: How Far Can We Go? *ACS Macro Lett.* **2015,** 4, 1044-1050.

(47). Ebnesajjad, S.; Landrock, A. H., Chapter 5 - Characteristics of Adhesive Materials. In *Adhesives Technology Handbook (Third Edition)*, Ebnesajjad, S., Landrock, A. H., Eds. William Andrew Publishing: Boston, 2015; pp 84-159.

(48). Goikoetxea, M.; Reyes, Y.; Alarcón, C. M. d. l. H.; Minari, R. J.; Beristain, I.; Paulis, M.; Barandiaran, M. J.; Keddie, J. L.; M.Asua, J. Transformation of waterborne hybrid polymer particles into films: Morphology development and modeling. *Polymer* **2012,** 53, 1098-1108.

Chapter 6. Conclusions

This PhD thesis aims at contributing to the reduction of the petroleum dependence by producing polymers using monomer obtained from bio-sourced terpenes. The terpenes are side products of the local paper industry created around the "Landes" pine forest in the South West of France. Tetrahydrogeraniol (THG) and Cyclademol (CDM) were chosen as terpene derivatives to prepare (meth)acrylic monomers that can replace its petroleum-based homologues *n*-butyl acrylate, 2-ethylhexyl acrylate, methyl methacrylate and styrene. A synthetic method for the efficient production of several terpene-containing (meth)acrylates (tetrahydrogeraniol acrylate (THGA), tetrahydroheranoiol methacrylate (THGMA), cyclademol acrylate (CDMA) and cyclademol methacrylate (CDMMA)) was developed. These monomers were polymerized in bulk, solution and aqueous dispersed systems by free radical polymerization, RAFT polymerization and nitroxide mediated polymerization (NMP).

THGA was first polymerized in toluene and bulk *via* free-radical polymerization, achieving high conversions and molecular weights up to 278 kg·mol^{-1}. The synthesized poly(THGA) showed a relatively low T_g (−46 °C), making it useful as a replacement for low T_g acrylic monomers, such as the widely used *n*-butyl acrylate. RAFT polymerization of THGA in toluene ($[M]_0$ = 3.6 mol.L^{-1}, $[CTA]_0/[I_2]_0$ = 10) led to polymers with degrees of polymerization (*DP*n) from 25 to 500 and narrow molecular weight distributions ($Đ \approx 1.2$) even at high conversions. At lower monomer concentrations ($[M]_0$ = 1.8 mol.L^{-1}of the control was not that good due to the intramolecular chain transfer to polymer that was demonstrated by detection of branching (arising from the propagation of midchain radicals) and terminal double bonds (arising from β-scission of midchain radicals). Solution polymerization was also used for the successful synthesis of poly(THGA)-*b*-poly(styrene)-*b*-poly(THGA) soft/hard/soft and poly(styrene)-*b*-poly(THGA)-*b*-poly(styrene) hard/soft/hard triblock copolymers, demonstrating its potential as a component of thermoplastic elastomers. The morphology of the triblock copolymers observed *via* atomic force microscopy (AFM) revealed the phase separation between the soft and hard segments (poly(THGA) and poly(styrene), respectively). The phase-separation of the triblock copolymers was further confirmed by rheological measurements, where two distinct glass transition temperatures were observed.

However, the synthetic route used is not sustainable as the polymerizations were carried out in solution, namely with an extensive use of solvent. The seek for a more sustainable synthetic method prompted us to polymerize the new monomers in aqueous dispersed media, which is more environmentally friendly. Due to the fact that the bio-sourced monomers synthesized in this work as well as the control agents used are rather hydrophobic, miniemulsion polymerization was utilized in order to avoid the the need of mass transport through the aqueous phase, which is characteristic of emulsion polymerization. As in polymerization in dispersed media the type of initiator strongly affects the polymerization, three different initiators were tested: the oil-soluble AIBN that produces radicals in the polymer particles, the water-soluble potassium persulfate that forms highly hydrophilic radicals in the aqueous phase, and the redox couple (TBHP/AscA) that forms hydrophobic radicals in the aqueous phase. It was found that high conversion was achieved when the polymerization was conducted with the initiators yielding hydrophobic radicals (AIBN and TBHP/AscA). Good control over the RAFT polymerization was achieved, an stable dispersions of poly(THGA) with degrees of polymerization ranging from 50 to 450, relatively low polydispersity values and high conversions were obtained. Terpene-based triblock copolymers were then synthesized by RAFT miniemulsion polymerization. Both hard-soft-hard and soft-hard-soft triblock copolymers were prepared using poly(THGA) as soft segment and

poly(CDMMA) as hard one. These triblocks consist only of terpene derivatives, thus maximizing the use of renewable resources. An important characteristic of the process developed is its scalability as no intermediate purification step after the synthesis of the first block is needed. The nano-phase segregation of the copolymers was observed by AFM and rheological measurements. Finally, the formulations using fully bio-based monomers shown good adhesive performance, in comparison to triblock copolymers partially based on styrene.

Block copolymers from bio-sourced terpene-based methacrylates were also successfully synthesized by nitroxide mediated polymerization using the alkoxyamine Dispolreg 007. The NMP of THGMA was first carried out in toluene with good control over the polymerization for degrees of polymerization up to *DP*n = 200. At higher targeted *DP*n, evidence of the macromonomer was observed leading to a reduced molar mass compared to the predicted value. When the process was carried out in miniemulsion, excellent control over the polymerization of THGMA could be achieved up to *DP*n 500 and narrow molecular weight distributions at high conversion were obtained. The improvement was attributed to the fast recombination of the radical and the nitroxide in the confined environment of the polymer particles. Terpene-based soft/hard diblock copolymers were successfully synthesized starting with a THGMA

macroradical, varying the molecular weight of hard polymer (CDMMA). Diblock THGMA-St copolymers were also synthesized for comparison purposes. Well-defined phase-separation between soft and hard polymers was observed. The adhesive properties of the diblock copolymers were evaluated with probe tack, peel strength and shear resistance measurements. It was found that migration of the short polymer chains could affect the shear resistance. The adhesive performance was comparable to the partially petroleum-based styrene system and better than that found for the acrylate-based triblock copolymers.

Resumen y Conclusiones

Esta tesis de doctorado tiene como objetivo contribuir a la reducción de la dependencia del petróleo mediante la producción de polímeros utilizando monómeros obtenidos de terpenos de origen biológico. Los terpenos son subproductos de la industria papelera local creada alrededor del bosque de pinos "Las Landas". El tetrahidrogeraniol (THG) y el cicladamol (CDM) se eligieron como derivados de terpeno para preparar monómeros (met)acrílicos que pueden reemplazar a sus homólogos a base de petróleo (acrilato de n-butilo, acrilato de 2-etilhexilo, metacrilato de metilo y estireno). Se desarrolló un método sintético para la producción eficiente de varios (met)acrilatos que contienen terpeno (acrilato de tetrahidrogeraniol (THGA), metacrilato de tetrahidroheranoiol (THGMA), acrilato de cicladamol (CDMA) y metacrilato de cicladamol (CDMMA). Estos monómeros se polimerizaron en masa, en solución y en sistemas dispersos acuosos mediante polimerización por radicales libres, polimerización RAFT y polimerización mediada por nitróxido (NMP).

El THGA se polimerizó primero en tolueno y en masa mediante polimerización por radicales libres, logrando altas conversiones y pesos moleculares de hasta 278 $kg \cdot mol^{-1}$. El poli(THGA) sintetizado mostró una *T*g relativamente baja (-46 °C), por lo que es útil como sustituto de los monómeros acrílicos de baja *T*g, como el acrilato de n-butilo ampliamente utilizado. La polimerización RAFT de THGA en tolueno ($[M]_0$ = 3.6 $mol.L^{-1}$, $[CTA]_0$ / $[I_2]_0$ = 10) condujo a polímeros con grados de polimerización (*DP*n) de 25 a 500 y distribuciones de peso molecular estrechas ($Đ \approx 1.2$) incluso a altas conversiones. A concentraciones de monómero más bajas ($[M]_0$ = 1.8 $mol.L^{-1}$) el control no fue tan bueno debido a la transferencia de cadena intramolecular al polímero que se demostró mediante la detección de ramificación (que surge de la propagación de radicales de cadena media) y dobles enlaces terminales (que surgen de la escisión β de radicales de cadena media). La polimerización en solución también se usó para la síntesis exitosa de copolímeros tribloque blando/duro/blando de poli (THGA)-b-poli(estireno)-b-poli(THGA) y tribloque duro/blando/duro poli (estireno)-b-poli(THGA)-b-poli(estireno), demostrando su potencial como componente de elastómeros termoplásticos. La morfología de los copolímeros tribloque observada mediante microscopía de fuerza atómica (AFM) reveló la separación de fases entre los segmentos blandos y duros (poli(THGA) y poli(estireno), respectivamente). La separación de fases de los copolímeros tribloque se confirmó adicionalmente mediante

mediciones reológicas, donde se observaron dos temperaturas de transición vítrea distintas.

Sin embargo, la ruta sintética utilizada no es sostenible ya que las polimerizaciones se llevaron a cabo en solución, es decir, con un uso extenso de disolvente. La búsqueda de un método sintético más sostenible nos llevó a polimerizar los nuevos monómeros en medios dispersos acuosos, que son más ecológicos. Debido al hecho de que los monómeros de origen biológico sintetizados en este trabajo, así como los agentes de control utilizados, son bastante hidrófobos, se utilizó la polimerización en miniemulsión para evitar la necesidad de transporte de masa a través de la fase acuosa, que es característica de la polimerización en emulsión. Como en la polimerización en medio disperso el tipo de iniciador afecta fuertemente la polimerización, se probaron tres iniciadores diferentes: el AIBN soluble en la fase orgánica que produce radicales en las partículas de polímero, el persulfato de potasio, soluble en agua que forma radicales altamente hidrófilos en la fase acuosa, y el par redox (TBHP/AscA) que forma radicales hidrófobos en la fase acuosa. Se encontró que se logró una alta conversión cuando la polimerización se realizó con los iniciadores produciendo radicales hidrófobos (AIBN y TBHP/AscA). Se logró un buen control sobre la polimerización RAFT, se obtuvieron dispersiones estables de poli (THGA) con

grados de polimerización que varían de 50 a 450, valores de polidispersidad relativamente bajos y altas conversiones. Los copolímeros tribloque a base de terpeno también se sintetizaron mediante polimerización en miniemulsión RAFT. Tanto los copolímeros de tres bloques duro-blando-duros y blando-duro-blando se prepararon usando poli (THGA) como segmento blando y poli (CDMMA) como duro. Estos tribloques consisten solo en derivados de terpenos, maximizando así el uso de recursos renovables. Una característica importante del proceso desarrollado es su escalabilidad, ya que no se necesita una etapa de purificación intermedia después de la síntesis del primer bloque. La segregación de nanofase de los copolímeros se observó mediante AFM y mediciones reológicas. Finalmente, las formulaciones que utilizan monómeros totalmente biológicos mostraron un buen comportamiento adhesivo, en comparación con los copolímeros tribloque parcialmente basados en estireno.

Los copolímeros de bloque de metacrilatos basados en terpeno de origen biológico se sintetizaron con éxito mediante polimerización mediada por nitróxido (NMP) usando la alcoxiamina Dispolreg 007. La NMP de THGMA se realizó primero en tolueno con un buen control sobre la polimerización para grados de polimerización de hasta DPn = 200. En DPn objetivos más altos, se observó evidencia del macromonómero que conduce a una masa molar reducida en comparación con el valor

predicho. Cuando el proceso se llevó a cabo en miniemulsión, se pudo lograr un control excelente sobre la polimerización de THGMA hasta *DP*n 500 y se obtuvieron distribuciones de peso molecular estrechas a alta conversión. La mejora se atribuyó a la rápida recombinación del radical y el nitróxido en el ambiente confinado de las partículas de polímero. Los copolímeros dibloque blando/duro a base de terpeno se sintetizaron con éxito comenzando con un macroradical THGMA, variando el peso molecular del polímero duro (CDMMA). Los copolímeros dibloque THGMA-S también se sintetizaron con fines comparativos. Se observó una separación de fases bien definida entre polímeros blandos y duros. Las propiedades adhesivas de los copolímeros dibloque se evaluaron con medidas de pegajosidad de sonda, resistencia al desprendimiento y resistencia a la cizalla. Se descubrió que la migración de las cadenas cortas de polímero afectaba la resistencia al corte. El comportamiento adhesivo fue comparable al sistema de estireno parcialmente a base de petróleo y mejor que el encontrado para los copolímeros tribloque a base de acrilato.

Conclusions

Cette thèse a pour objectif de contribuer à la réduction de la dépendance au pétrole en produisant des polymères à partir de monomères obtenus à base de terpènes biosourcés. Les terpènes sont des produits dérivés de l'industrie papetière locale créée autour de la pinède landaise. Le tétrahydrogeraniol (THG) et le cyclademol (CDM) ont été choisis comme dérivés terpéniques pour préparer des monomères (méth)acryliques pouvant remplacer leurs homologues à base de pétrole: l'acrylate de *n*-butyle, l'acrylate de 2-éthylhexyle, le méthacrylate de méthyle et le styrène. Une méthode de synthèse pour la production efficace de plusieurs (méth)acrylates contenant des terpènes (acrylate de tétrahydrogéraniol (THGA), méthacrylate de tétrahydrohéranol (THGMA), acrylate de cycladérol (CDMA) et méthacrylate de cycladérol (CDMMA)) a été mise au point. Ces monomères ont été polymérisés en masse, en solution et dans

des systèmes dispersés aqueux par polymérisation radicalaire, polymérisation RAFT et polymérisation à l'aide de nitroxyde (NMP).

Le THGA a d'abord été polymérisé dans le toluène et en masse par polymérisation radicalaire, permettant des conversions élevées et des poids moléculaires allant jusqu'à 278 kg.mol $^{-1}$. Le poly (THGA) synthétisé présentait une T_g relativement basse (-46 °C), ce qui le rend utile pour le remplacement des monomères acryliques à faible T_g, tel que l'acrylate de *n*-butyle largement utilisé. La polymérisation RAFT de THGA dans le toluène ($[M]_0$ = 3.6 mol.L^{-1}, $[CTA]_0/[I_2]_0$ = 10) a conduit à des polymères avec des degrés de polymérisation (DP_n) de 25 à 500 et des distributions de masse moléculaire étroites (1.2) même à des conversions élevées. À des concentrations plus faibles en monomères ($[M]_0$ = 1.8 mol.L^{-1}) le contrôle n'était pas très bon en raison du transfert intramoléculaire au sein du polymère démontré par la détection de ramifications (résultant de la propagation de radicaux en milieu de chaîne) et de doubles liaisons terminales (résultant de la β-scission des radicaux en milieu de chaîne). La polymérisation en solution a également été utilisée pour la synthèse réussie de copolymères triblocs poly(THGA)-*b*-poly(styrène)-*b*-poly(THGA) souple/dur/souple et de poly(styrène)-*b*-poly(THGA)-*b*-poly(styrène) dur/souple/dur, démontrant leur potentiel en tant que composant d'élastomères thermoplastiques. La

morphologie des copolymères triblocs observée par microscopie à force atomique (AFM) a révélé la séparation de phase entre les segments souples et durs (poly(THGA) et poly(styrène), respectivement). La séparation de phase des copolymères triblocs a été confirmée par des mesures rhéologiques, où deux températures de transition vitreuse distinctes ont été observées.

Cependant, la voie de synthèse utilisée n'est pas durable car les polymérisations ont été réalisées en solution, notamment avec une utilisation excessive de solvant. La recherche d'une méthode de synthèse plus durable nous a incitée à polymériser les nouveaux monomères en milieu aqueux dispersé, plus respectueux de l'environnement. Du fait que les monomères biosourcés synthétisés dans ce travail ainsi que les agents de contrôle utilisés soient plutôt hydrophobes, une polymérisation en miniémulsion a été utilisée afin d'éviter le besoin de transport de masse à travers la phase aqueuse, caractéristique de la polymérisation en émulsion. Etant donné que dans la polymérisation en milieu dispersé le type d'amorceur influe fortement sur la polymérisation, trois amorceurs différents ont été testés: l'AIBN, soluble dans la phase organique, qui produit des radicaux dans les particules de polymère, le persulfate de potassium, soluble dans l'eau, qui forme des radicaux hautement hydrophiles dans la phase aqueuse, et le couple rédox (TBHP/AscA) qui forme des radicaux hydrophobes

dans la phase aqueuse. Il s'est avéré qu'une conversion élevée était obtenue lorsque la polymérisation était conduite avec les amorceurs produisant des radicaux hydrophobes (AIBN et TBHP/AscA). Un bon contrôle de la polymérisation RAFT a été obtenu, des dispersions stables de poly(THGA) avec des degrés de polymérisation allant de 50 à 450, des valeurs de polydispersité relativement basses et des conversions élevées ont été obtenus. Des copolymères triblocs à base de terpènes ont également été synthétisés par polymérisation RAFT en miniémulsion. Les deux copolymères triblocs dur/souple/dur et souple/dur/souple ont été préparés en utilisant du poly(THGA) en tant que segment souple et du poly(CDMMA) en tant que segment dur. Ces triblocs sont uniquement constitués de dérivés terpéniques, maximisant ainsi l'utilisation de ressources renouvelables. Une caractéristique importante du procédé mis au point est sa capacité a être employé à plus grande échelle, car aucune étape de purification intermédiaire après la synthèse du premier bloc n'est nécessaire. La ségrégation de phase des copolymères à l'échelle nanométrique a été observée par AFM et par mesures rhéologiques. Enfin, les formulations utilisant des monomères entièrement biosourcés ont montré de bonnes performances adhésives par rapport aux copolymères triblocs partiellement à base de styrène.

Les copolymères de méthacrylates à base de terpènes biosourcés ont été synthétisés avec succès par polymérisation radicalaire contrôlée par les nitroxydes en utilisant l'alcoxyamine Dispolreg 007. La NMP de THGMA a tout d'abord été réalisée dans le toluène avec un bon contrôle de la polymérisation pour des degrés de polymérisation jusqu'à DP_n = 200. A plus hauts DP_n, la présence de macromonomère a été observée conduisant à une masse molaire plus faible que la valeur prédite. Lorsque le procédé a été effectué en mini-émulsion, il était possible d'obtenir un excellent contrôle de la polymérisation du THGMA jusqu'à DP_n 500 et d'obtenir des distributions de masses moléculaires étroites à conversion élevée. L 'amélioration a été attribuée à la recombinaison rapide du radical et du nitroxyde dans l'environnement confiné des particules de polymère. Des copolymères diblocs souple/dur à base de terpènes ont été synthétisés avec succès depuis un macroradical THGMA, en faisant varier le poids moléculaire du polymère dur (CDMMA). Les copolymères diblocs THGMA-St ont également été synthétisés afin de pouvoir comparer les deux types de copolymères. Une séparation de phase bien définie a été observée entre les polymères souple et dur. Les propriétés adhésives des copolymères diblocs ont été évaluées avec des mesures d'adhésivité, de résistance au pelage et de résistance au cisaillement. Il a été constaté que la migration des courtes chaînes de polymère affectait la résistance au cisaillement. Les performances adhésives étaient comparables à celles du système

partiellement à base de styrène provenant de ressource pétrolière et meilleures que celles présentées pour les copolymères triblocs à base d'acrylate.

Appendix I

I.1. Materials

Styrene (S, 99.8 %, Quimidroga), Fluorescein o-acrylate (95 %, Sigma-Aldrich), acryloyl chloride (96 %, Sigma-Aldrich), dichloromethane (99.8%, Sigma-Aldrich), toluene (99 %, Sigma-Aldrich), 2,2`-azobis(2-methylproprionitrile) (AIBN, 98 %, Sigma-Aldrich) were used as received without further purification unless otherwise stated. Acrylic acid (AA, 99 %, Sigma-Aldrich), methacrylic acid (MA, 99 %, Sigma-Aldrich), potassium persulfate (KPS, ≥ 99%, Sigma Aldrich), tert-butyl hydroperoxide (TBHP, 70 *wt.*% aqueous solution, Sigma Aldrich), ascorbic acid (AsAc, ≥ 99%, Acros), stearyl acrylate (97%, Sigma Aldrich), styrene (St, 99.8%, Quimidroga), Dowfax 2A1 (alkyl diphenyloxide disulfonate, 45 *wt.*% active content, Dow Chemical), 2-methyltetrahydrofuran (MeTHF, 99 %, Sigma-Aldrich), propylphosphonic anhydride solution (50 *wt.*% in ethyl acetate) (T3P®, Sigma Aldrich) and triethylamine (99 %, Sigma-Aldrich) were used as received without further purification, unless otherwise stated. Tetrahydrogeraniol (THG, 95 %) and cyclademol (CDM, 95 %) were kindly supplied by Dérivés Résiniques Terpéniques (DRT, France), 3-(((2-Cyanopropan-2-yl)oxy)(cyclohexyl)amino)-2,2-dimethyl-3-

phenylpropanenitrile or Dispolreg 007 was synthesized according to a previously published procedure[1] and S,S´-dibenzyl trithiocarbonate (DBTTC, 97 %) was kindly supplied by Arkema and used as received without further purification.

I.2. Monomer conversion

Solution polymerization

Monomer conversion was calculated from ^{1}H NMR ($CDCl_3$, 400 MHz) by comparison of the vinyl signals (***H***C=C***H***$_2$, δ = 5.77; 6.23; 6.40 ppm) to the combined OC***H***$_2$- signals of both monomer and polymer (δ = 4.23-4.04 ppm, 3H).

Miniemulsion polymerization

The monomer conversion in dispersed media was calculated by gravimetric. The samples withdraw from the rector (1 ml of latex) at each time interval were placed in an aluminium cup contained of 1 wt% of hydroquinone water solution and dried in an oven (60 ℃) for overnight.

I.3. Theoretical molar masses

RAFT polymerization at 80 °C

The theoretical molar masses (for Chapter 3) were calculated using equations 1 and 2 using k_D $^{AIBN@65\ °C}$ = 1.9254×10^{-5} s^{-1}, the activation energy of AIBN E_a = 132 $kJ.mol^{-1}$, R = 8.314 $J.mol^{-1}.K^{-1}$, *f* the initiator initiation efficiency *f* = 0.5 and assuming termination by combination only (f_C = 1).

$$k_D^{AIBN\ @\ 80\ C} = k_D^{AIBN\ @\ 65\ C} \times e^{\frac{-Ea}{R}\left(\frac{1}{353}-\frac{1}{338}\right)} = 1.42 \times 10^{-4}\ s^{-1} \qquad (1)$$

$$M_n^{Th} = M_{CTA} + \frac{[M]_0 \times p \times M_M}{[CTA]_0 + 2 \times f \times [I]_0 \times \left(1-e^{-k_D t}\right) \times \left(1-\frac{f_C}{2}\right)} \qquad (2)$$

Where $[M]_0$, $[CTA]_0$, $[I]_0$ are the initial concentrations of monomer, chain transfer agent (CTA) and initiator respectively; M_M, M_{CTA} the molar masses (in $g.mol^{-1}$) of the monomer and CTA respectively and *p* the monomer conversion at a time *t* (in seconds).

RAFT polymerization at 70 ℃

The theoretical molar masses (for chapter 4) were calculated as

$$M_n^{Th} = M_{CTA} + \frac{[M]_0 \times p \times M_M}{[CTA]_0 + 2 \times f \times [I]_0 \times \left(1 - e^{-k_D t}\right) \times \left(1 - \frac{f_C}{2}\right)}, \quad (3)$$

where $[M]_0$, $[CTA]_0$, $[I]_0$ are the initial concentrations of monomer, chain transfer agent (CTA) and initiator respectively; M_M, M_{CTA} the molar masses (in g.mol^{-1}) of the monomer and CTA respectively and p the monomer conversion at a time t (in seconds); f the initiator initiation efficiency f = 0.5 and assuming termination by combination only (f_C = 1) and $k_D^{AIBN} = 4.47 \times 10^{15} \times e^{-Ea/RT}\ (s^{-1})$.[2, 3]

NMP at 97 ℃

The theoretical molar masses (for chapter 5) were calculated as

$$M_{n,th} = M_{alkoxyamine} + \frac{[M]_0 \times p \times M_M}{[alkoxyamine]_0}. \quad (4)$$

Where $[M]_0$ is the initial concentrations of monomer; $M_{alkozyamine}$, M_M the molar masses (in g.mol^{-1}) of the alkoxyamine and monomer, respectively and *p* the monomer conversion

I.3. Branching and macromonomer fractions

The branching fraction is calculated as % Branching =100 × ∫ $\boldsymbol{C}_q$ / (∫ $\boldsymbol{C}_q$ + ∫ $\boldsymbol{C}H_t$). The methyl group was used instead of the tertiary carbon in the backbone.

The macromonomer fraction was calculated by ^{1}H-NMR from the ratio of the sum of the integral from hydrogens from the macromonomer at shifts of δ = 6.13 and δ = 5.57 ppm to the OC$\boldsymbol{H}_2$ δ = 4.25 ppm peak. The *β*-scission content is calculated as % *β*-scission = 100 × ∫ $\boldsymbol{H}_2$C=C / ∫ OC$\boldsymbol{H}_2$.

I.4. Miniemulsion stability

The miniemulsion stability was investigated by studying the evolution of the backscattered light the Turbiscan LAb^{expert} equipment. The reading head of this device consists of pulsed near infrared light source (λ = 880 nm) and two synchronous detectors. The transmission detector receives the light flux transmitted through the

sample, while the backscattering detector measures the back scattering light. The detection head scans the entire length of the sample (55 nm) acquiring transmission and backscattering data every 40 μm. A representation of the equipment is presented in Figure I.1. The curve that are obtained provide the transmitted and backscattered light flux in percentage relative to standards (suspension of monodisperse spheres and silicon oil) as a function of sample height (in mm).This technique allows very early visualization of creaming, sedimentation and coalescence/flocculation. Creaming takes place when the dispersed has a lower density than the continuous phase. It can be easily detected because the backscattering flux decrease at the bottom of the sample and increases at the top due to the increase in the dispersed phase concentration. Sedimentation rakes place when the density of the disperse phase is greater than the continuous one. In this case, the back scattering increases at the bottom of the sample due to an increase in the sample concentration. Coalescence/flocculation leads to the fusion of interfaces increasing the droplet size. The particle size variation leads to a variation (usually a decrease) of the backscattering over the whole height of the sample.

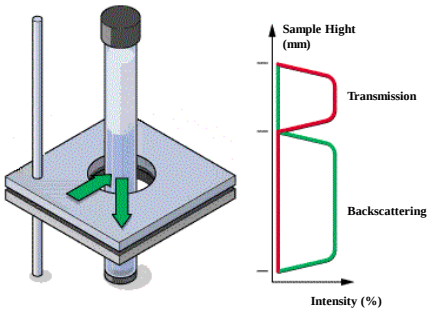

Figure I.1 Representation of the Turbiscan Lab^{expert} detection principle.

I.4. Dynamic light scattering (DLS)

Particle size was measured by Dynamic Light Scattering (DLS) using a Malvern Zetasizer Nano ZS. The equipment determines the particle size by measuring the rate of fluctuations in light intensity scattered by particles as they diffuse trough a fluid. Samples were prepared by diluting a fraction of the latex with deionized water. The analyses were carried out at 25ºC and each run consist in 1 minute of temperature equilibration followed by 3 size measurement per sample. An average is given as a final value.

I.5. Molecular weight and molecular weight distribution

Size Exclusion Chromatography Multiangle Light Scattering (SEC-MALS) traces were obtained on a set up consisting of a pump (LC-20A, Shimadzu), an autosampler (Sil-20AHT), a differential refractometer (Optilab Rex, Wyatt), a light scattering detector (Dawn Heleos II, Wyatt), a viscosimeter (Viscoton, Wyatt) and three columns in series (Styragel HR2, HR4 and HR6 with pore sizes ranging from 102 to 106 Å). Chromatograms were obtained in THF (HPLC grade) at 35 °C using a flow rate of 1 $mL.min^{-1}$. The absolute molecular weights were extracted considering MALS and Refractive Index (RI) signals using a measured value of dn/dc for poly(THGA) dn/dc = 0.0678 $mL.g^{-1}$, dn/dc for poly(THGMA) = 0.056 $mL.g^{-1}$, dn/dc for poly(CDMA) = 0.0997 $mL.g^{-1}$, dn/dc for poly(CDMMA) = 0.0897 $mL.g^{-1}$ and dn/dc for poly(styrene) = 0.187 $mL.g^{-1}$. All samples were passed through 0.45 µm nylon filter before analysis. The absolute molar masses were calculated from the MALS/RI data using the Debye plot (with the 1st order Zimm formalism).

I.6. Nuclear Magnetic Spectroscopy (NMR)

NMR spectra were recorded at 25 °C in $CDCl_3$ at concentration of 350 $mg.mL^{-1}$ on a DPX-400 or a DPX-500 Spectrometer. 1D ^1H spectra were acquired by use of 32K

data points, which were zero-filled to 64K data points prior to Fourier transformation. 1D ^{13}C spectra were recorded at a ^{13}C Larmor frequency of 125.77 MHz. The spectra were recorded using 20,000 transients. Quantitative ^{13}C spectrum were recorded using single pulse excitation, using 5.5 μs 90˚ pulse, inverse gated waltz16 decoupling to avoid NOE effects, and relaxation delay of 5 s. Apodization was achieved using an exponential window function equivalent to a line width of 5 Hz. DOSY(diffusion ordered spectroscopy) were recorded using pulse sequence dstebpgp3s.

I.7. Atomic Force Microscopy (AFM)

Atomic force microscopy (AFM) was performed on Multimode 8 Atomic Force Microscope a (Bruker) and recorded in PeakForce QNM mode. The polymer film was obtained by spin coating of a diluted polymer solution (3 wt.% in toluene) onto a silicon wafer.

I.8. Rheological measurement

Samples for the rheological experiment were prepared as follow; the latex was deposited in the silicone molds and dried at room temperature. The volume of latex was calculated to give the required final film thickness which depending on the latex solid

content. Then, the dried sample was cut to the desired dimension. The linear viscoelastic of the block copolymers was performed using parallel plate geometry with constant strain on a rotational rheometer (AR2000, TA Instrument). Mechanical spectroscopy experiment was performed at frequency 0.1 rad/s over the temperature from 150 to -60 ˚C. Frequency sweeps (0.001 -10 Hz) with applied strain 1 to 5 %, the characterization was performed at room temperature.

I.9. References

(1). Ballard, N.; Aguirre, M.; Simula, A.; Agirre, A.; Leiza, J. R.; Asua, J. M.; Es, S. v. New Class of Alkoxyamines for Efficient Controlled Homopolymerization of Methacrylates. *ACS Macro Lett.* **2016,** 5, 1019-1022.

(2). Moad, G. A Critical Assessment of the Kinetics and Mechanism of Initiation of Radical Polymerization with Commercially Available Dialkyldiazene Initiators. *Progress in Polymer Science* **2019,** 88, 130-188.

(3). Gody, G.; Maschmeyer, T.; Zetterlund, P. B.; Perrier, S. Pushing the Limit of the RAFT Process: Multiblock Copolymers by One-Pot Rapid Multiple Chain Extensions at Full Monomer Conversion. *Macromolecules* **2014,** 47, 3451-3460.

Appendix II

II.1. Adhesion

The science of adhesion is the study of the interactions between two solid surfaces, the energy needed to separate both surface and of the deformation mechanism occurring during the adhesion test.[1] Peel adhesion, shear resistance and tack are the basic properties that have to be optimized for the PSA material. Peel is the characterized by measuring the force required to remove a PSA from the substrate and shear resistance is defined by the resistance of the adhesive to failure in the direction parallel to the interface. Tack is the capacity to stick instantaneously to a substrate by simple contact. A high tack requires a high level of molecular mobility at the interface at frequencies of the order of sticking time. Peel requires a highly dissipative behavior at high shear rates. There two properties are optimal for a very viscous liquid. However, good resistance to shear over long times requires a good resistance to creep and is optimal for elastic solid. Hence, viscoelastic materials are needed for a good compromise in properties between tack, peel and resistance to shear.

More specially, PSAs are typically composed of high molecular weight entangled polymer chains, with a T_g below the application temperature and the Young's modulus of the polymer at 1 Hz should be below 0.1 MPa (known as the Dahlquist criterion) in order to form a good contact even with rough surface.

II.1.1. Peel test

In this work, the adhesive film were tested on a TA.HD Plus Texture Analyzer (Texture Technologies, Hamilton, MA) using 180° (Figure II.2.). The adhesive films were prepared by casting the latex over a flame-treated polyethylene terephthalate (PET) sheet (29 μm thick) using a gap applicator with reservoir. A gap of 200 μm was used in order to obtain films of approximately 70-80 μm thickness. Films were dried at 23 °C and 55% humidity for 12 h, protected from dust. The sample were covered by silicon paper and finally cut with the standard dimensions (2.5 cm x 14 cm). Subsequently, the sample was applied to the standard stainless steel panel and pressing a 2 kg of roller to make the contact, the roller was passed for 4 times. The sample was clamped to the upper jaw of the instrument (Figure II.2.). The adhesion value was the average peel force obtained during the peel force.

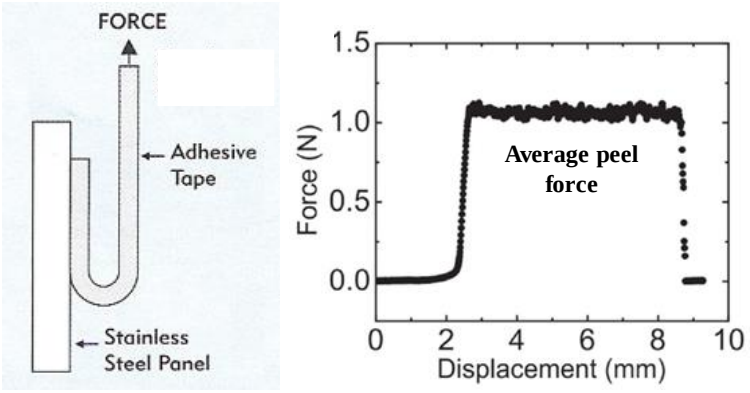

Figure II.2. Schematic of a probe tack test.

II.1.2. Shear resistance

The shear strength is the internal or cohesive strength of adhesive. Generally, it measures the holding power test and it is determined as the time require for standard strip of PSA to fall from a test panel after application of a load. The adhesive films were prepared by casting the latex over a flame-treated polyethylene terephthalate (PET) sheet (29 μm thick) using a gap applicator with reservoir. A gap of 200 μm was

used in order to obtain films of approximately 70-80 μm thickness. Films were dried at 23 °C and 55% humidity for 12 h, protected from dust. The sample were covered by silicon paper and finally cut with the standard dimensions (2.5 cm x 8 cm). In this work, the adhesive film were tested on a TA.HD Plus Texture Analyzer (Texture Technologies, Hamilton, MA). Subsequently, the sample was placed on the stainless steel and the rest was placed in the triangular subjection where the load was placed afterwards. The sample was tested in the oven at room temperature. When the failure of the adhesive occurred, the standard weights fall into a weight detector which stopped the counter of the corresponding sample. The oven was connected to a computer where the time of failure was recorded.

II.1.2. Probe tack

The probe tack test consist in putting the surface of the solid probe into contact with a thin adhesive layer coated on a rigid substrate and measuring the force required to detach it from the adhesive. In this work, the adhesive film were tested on a TA.HD Plus Texture Analyzer (Texture Technologies, Hamilton, MA). Figure II.3 shows a typical probe tack test. First, a flat-ended probe comes in contact with adhesive film cast on the glass substrate. After contact in controlled pressure at controlled time, the

probe is pulled back from the film. During the test, the forced required to debon the probe and its displacement d(t) are recorded. From this data, the stress/strain curve are plotted.

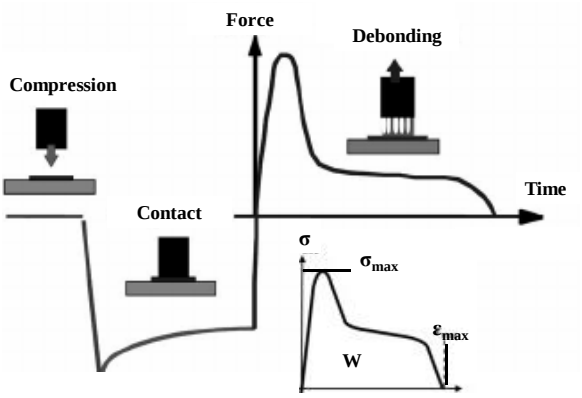

Figure II.1. Schematic of a probe tack test.

Four types of stress-strain curves have been observed for the adhesive polymer.[2-4] The first type of curve (Figure II.3A) is characterized by sharp maximum at rather low strains and a very small area under the stress-strain curves. At the other extreme (Figure II.3C) is the case of highly viscous liquid. The adhesive joint breaks by cohesive fracture within the adhesive and the debonding process is governed by viscous flow. This typical liquid-like debonding, also call cohesive debonding, where some residues of adhesive are on the probe at the end of the test. In between these two case,

stress-strain curves are characterized by maximum in the stress followed by pronounced shoulder (Figure II.3B-1). The curve finally ends up by decrease in the force to zero. Detachment in that case occurs at the interface between the probe and the adhesive layer. Such a debonding is call adhesive debonding (no residual on the probe at the end of the test). Figure II.3B-2 is observed when the material strain-hardens just before the final detachment. In that case a slight increase in the stress is observed and a second peak is observed.

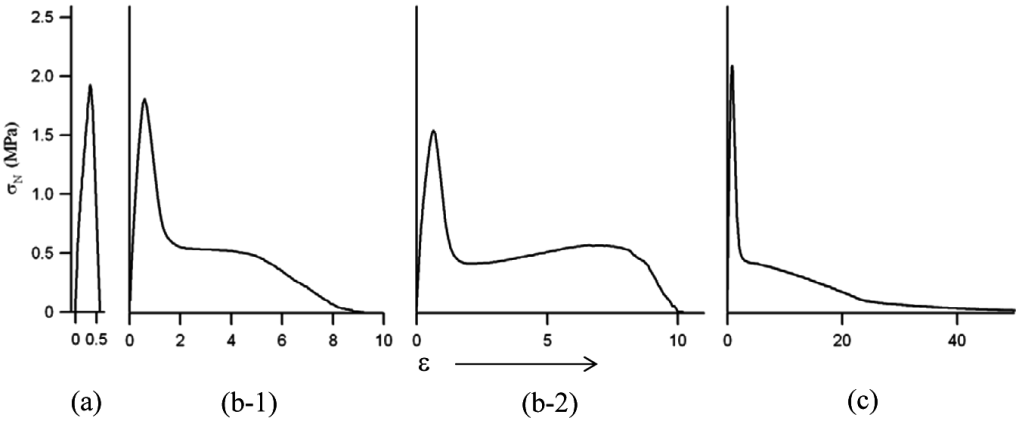

Figure II.2. Different stress-strain tack curves. (a) brittle failure; (B) adhesive debonding; with hardening in the case of b-2; (c) cohesive debonding liquid-like behavior.

II.2. References

(1). Creton, C. Pressure-Sensitive Adhesives: An Introductory Course. *MRS Bulletin* **2011,** 28, 434-439.

(2). Deplace, F.; Carelli, C.; Mariot, S.; Retsos, H.; Chateauminois, A.; Ouzineb, K.; Creton, C. Fine Tuning the Adhesive Properties of a Soft Nanostructured Adhesive with Rheological Measurements. *The Journal of Adhesion* **2009,** 85, 18-54.

(3). Shull, K. R.; Creton, C. Deformation behavior of thin, compliant layers under tensile loading conditions. *J. Polym. Sci. B Polym. Phys.* **2004,** 42, 4023-4043.

(4). Lakrout, H.; Sergot, P.; Creton, C. Direct Observation of Cavitation and Fibrillation in a Probe Tack Experiment on Model Acrylic Pressure-Sensitive-Adhesives. *The Journal of Adhesion* **1999,** 69, 307-359.

Abbreviations and Acronyms

AA	Acrylic acid
AFM	Atomic force microscopy
AIBN	2,2`-azobis(2-methylproprionitrile
AsAc	ascorbic acid
CDM	Cyclademol
CDMA	Cyclademol acrylate
CDMMA	Cyclademol methacrylate
DBTTC	S,S´-dibenzyl trithiocarbonate
DCM	Dichloromethane
Dispolreg 007	Cyanopropan-2-yl)oxy)(cyclohexyl)amino)-2,2-dimethyl-3-phenylpropanenitrile
DP	Degree of polymerization

f	The initiator initiation efficiency
KPS	potassium persulfate
LAM	Less activated monomer
MA	Methacrylic acid
MAM	More activated monomer
MMD	Molar mass distribution
Mn	Number average molecular weight
Mw	Weight average molecular weight
MWD	Molecular weight distribution
NCR	Mid-chain radical
NMP	Nitroxide-Mediated Polymerization
NMR	Nuclear magnetic resonance
PS	Poly(styrene)
PSAs	Pressure sensitive adhesives
RDRP	Reversible deactivation radical polymerization

RAFT	Reversible addition-fragmentation chain transfer polymerization
S	Styrene
SEC	Size exclusion chromatography
Tg	Glass transition
TBHP	tert-butyl hydroperoxide
THG	Tetrahydrogeraniol
THGA	Tetrahydrogeraniol acrylate
THGMA	Tetrahydrogeraniol methacrylate